TURUN YLIOPISTO

Field- and geochemical assessment of Rytkynkylä volcanic rock formation on the Raahe-Ladoga Shear Complex

Matias Hirsimäki

Geology (bedrock)
Master's thesis
Laajuus: 30 op

Supervisor:
Esa Heilimo

18.6.2026
Turku

Pro gradu -tutkielma

Pääaine: Geologia
Tekijä: Matias Hirsimäki
Otsikko: Kenttä- ja geokemiallinen kartoitus Rytkynkylän vulkaanisesta muodostumasta Raahe-Laatokka hiertokompleksilla
Ohjaaja: Esa Heilimo
Sivumäärä: 69 sivua + liitteet 37 sivua
Päivämäärä: 18.6.2026

Ylivieskan ja Pyhäjärven kuntia ympäröivä seutu on Suomessa kaivosteollisuuden kannalta tärkeä alue. Tällä alueella on suuria vulkaanisissa muodostumissa esiintyviä kaivoksia, kuten Pyhäsalmen ja Vihannin kaivokset, sekä lukuisia pienikokoisia kaivoksia ja malmipotentiaalinsa kannalta kiinnostavia kohteita. Tästä huolimatta alueella on muodostumia, joille ei ole tehty merkittäviä tutkimuksia eikä niiden merkitystä seudun geologisessa kontekstissa tunneta hyvin. Rytkynkylän muodostuma on hyvä esimerkki alueen vähemmän tutkituista vulkaanisista muodostumista, joka sijaitsee yhden Suomen tärkemimmän rakenteellisen elementin, Raahe-Laatokka-hiertokompleksin päällä. Tämä tutkimus luo geologisen kuvauksen Rytkynkylän muodostumasta ja sen alkuperäisestä synty-ympäristöstä sekä vertaa Rytkynkylän muodostumaa Pyhäsalmen ja Ylivieskan vulkaanisiin ryhmiin. Menetelminä tutkimuksessa hyödynnetään geologista kartoitusta, petrografisia kuvauksia ja geokemiallisia analyyseja.

Rytkynkylän muodostuman kivet ovat mafis-intermediäärisiä amfiboliporfyriittejä, joista suurin osa on kalkkialkaalisia muutamaa tholeiittista poikkeusta lukuun ottamatta. Tutkittujen kivien SiO_2-pitoisuus vaihtelee välillä 45 – 65 wt. %. Kaikki Rytkynkylän muodostuman kivet muodostavat mafis-intermediäärisen jatkumon ilman bimodaalisuuteen viittaavia indikaattoreita ja osoittavat LILE-rikastumista, sillä Ba-pitoisuudet vaihtelevat välillä 215 – 1336 ppm ja Sr-pitoisuudet välillä 125 – 651 ppm.

Rytkynkylän muodostuma muistuttaa Ylivieska-ryhmää eli Svekofennisen päävaiheen vulkaanisia kiviä, sillä molempien kivet koostuvat mafis-intermediäärisistä sekä tholeiittisista – kalkkialkaalisista kivistä. Kivillä on myös samankaltainen kehityshistoria, ja ovat molemmat kokeneet fraktioitunutta kiteytymistä. Rytkynkylän muodostuman korkeat LILE-pitoisuudet ja tholeiittiset piirteet vastaavat pitkälti Ylivieska-ryhmän arvoja, mikä viittaa subduktioon liittyvään kalkkialkaaliseen saarikaariympäristöön tai saarikaaren takaosa-altaan repeämisympäristöön. Tähän verrattuna Pyhäsalmi-ryhmä eroaa huomattavasti selvän bimodaalisuutensa vuoksi. Tulokset osoittavat, että Rytkynkylä-muodostuma edustaa mafis-intermediääristä vulkaanista amfiboliporfyriittimuodostumaa ja kuuluu osaksi Ylivieska-ryhmää.

Avainsanat: Rytkynkylän muodostuma, Pyhäsalmi-ryhmä, Ylivieska-ryhmä, Raahe-Laatokka-hiertovyöhyke, Svecofennian orogenia, petrografia, geokemia, vulkaaniset kivet, tholeiittinen, kalkkialkaalinen, bimodaalinen

Master's thesis

Subject: Geology
Author: Matias Hirsimäki
Title: Field- and geochemical assessment of Rytkynkylä volcanic rock formation on the Raahe-Ladoga Shear Complex
Supervisor: Esa Heilimo
Number of pages: 69 pages + attachments 37 pages
Date: 18.6.2026

A region of Central Finland, around Ylivieska and Pyhäjärvi, is a famous brownfield locale with a few large mines eg. Pyhäsalmi and Vihanti, and dozens of smaller scale deposits and potential locations studied for mineralisations, commonly hosted in volcanic rock formations. Despite this, many volcanic formations lack detailed descriptions nor a detailed geological framework. Rytkynkylä formation is one such undescribed volcanic rock unit, locating directly on the Raahe-Ladoga Shear Complex, a major structural feature on the Svecofennian orogen. This study provides a detailed description of the Rytkynkylä formation including its original formation environment and compares it to Pyhäsalmi- and Ylivieska groups. This study's methods utilize field work, petrographical descriptions, and geochemical whole-rock analysis.

The Rytkynkylä formation rocks are mafic to intermediate amphibole porphyrites, of which most are calc-alkaline with some tholeiitic exceptions. SiO_2 of the studied rocks varies between 45 – 65 wt. %, and all the samples form one continuous group with no bimodal indicators. LILE's show enrichment in all analysed samples, with Ba 215 – 1336 ppm, and Sr 125 – 651 ppm.

The Rytkynkylä formation shares large similarities with the Ylivieska group which represents the main phase of the Svecofennian orogeny. Both consist of mafic to intermediate and tholeiitic to calc-alkaline rocks, with similar evolution and fractional crystallization. Rytkynkylä formation's high LILE consentrations correspond to the Ylivieska group's similar values, indicating subduction related calc-alkaline island arc environment with tholeiitic back arc basin volcanism due to tholeiitic rocks being present. The Pyhäsalmi group, however, shows a clear difference due to its evident bimodality. These results provide an understanding that the Rytkynkylä formation is mafic-intermediate volcanic amphibole porphyrite unit, and a part of the Ylivieska group.

Key words: Rytkynkylä formation, Pyhäsalmi group, Ylivieska group, Raahe-Ladoga Shear Complex, Svecofennian orogeny, petrography, geochemistry, volcanic rocks, tholeiitic, calc-alkalic, bimodal

Table of contents

1 Introduction

The Raahe-Ladoga Shear Complex (RLSC) is one of the most important ore potential brownfield regions in Finland with multiple VMS-type deposits eg. the Vihanti- and the Pyhäsalmi mine, which are located in volcanic rock groups of the same names. These groups represent the Savo belt (Figure 1) (Luukas 2018). These two historical deposits produced a total of ca. 90 Mt of ore during their lifetimes with Zn, Cu, Pb, Ag and Au as the most common commodities. In addition to these large deposits, multiple smaller satellite VMS and orogenic gold deposits are located around the Vihanti-Pyhäsalmi region, primarily hosted in volcanic rock formations (Geological survey of Finland 2026). Located SW of the RLSC in Central Finland, the Ylivieska group consists of volcanic- and sedimentary Paleoproterozoic supracrustal rocks and is a part of the Pohjanmaa belt (Figure 1) (Kousa 2008). The Ylivieska group region has its own history in mining eg. Jouhineva for Co and Au, and Ängesneva for Au and Cu (Geological survey of Finland 2026). However, the exploration and mining has been in a remarkably smaller scale compared to either the Vihanti- or the Pyhäsalmi groups. The Ylivieska group volcanic rock formations are also less studied compared to the Vihanti- and Pyhäsalmi groups, stemming from research flow onto known ore potential areas. The border between the Vihanti-Pyhäsalmi- and the Ylivieska groups mostly follows the RLSC, which is generally regarded as the divide between the oldest and younger Paleoproterozoic supracrustal rocks. However, the line blurs close to and on the RLSC due to the complexity of the large-scale shearing, faulting, alterations and younger cross-cutting plutonic rocks. Thus, recognizing and categorizing volcanic rocks as belonging to Vihanti-, Pyhäsalmi- or Ylivieska groups in this complex area becomes a challenge.

The Rytkynkylä formation (RF) is a volcanic rock formation located geographically inside the Vihanti-Pyhäsalmi region (Figure 1). The RF is also located directly on the RLSC by one of the main shear zones and thus lies exactly on the border between the Pyhäsalmi- and Ylivieska groups. Due to this, without a study of the RF's geology and geochemistry, it is challenging to know whether the RF belongs to the Pyhäsalmi- or the Ylivieska group. In detail, additional studies and data from both Pyhäsalmi- and Ylivieska groups is required for any real conclusions regarding RF's real lithostratigraphic group. Hence, the aim of this study is to gather and analyse the RF's volcanic rocks, compare the RF's data to both Pyhäsalmi- and Ylivieska groups data, and find out which group the RF belongs to.

2 Geological context

2.1 The Fennoscandian Shield

Fennoscandia is a crustal segment located in the NW part of the East European Craton with two other crustal segments, Volgo-Uralia and Sarmatia (Gorbatschev & Bogdanova 1993). Fennoscandia consists of Lapland-Kola-, Karelian-, Svecofennian-, Norrbotten-, Sveconorwegian- and Caledonide provinces, where all but the last are also a part of the Fennoscandian Shield, an old crystalline region inside the Fennoscandian crustal segment (Figure 1) (Nironen 2017). All of Finland is a part of the Fennoscandian Shield but can be divided into regions belonging into the Lapland-Kola-, Karelian- and Svecofennian provinces. The Lapland-Kola- and Karelian provinces formed during the Archean ca. 3.5 – 2.5 Ga, whilst the Svecofennian region formed during the Paleoproterozoic ca. 2.5 – 1.6 Ga, and the Mesoproterozoic 1.6 – 1.0 Ga (Lahtinen 2012).

The Svecofennian province in Central Finland is most notably characterized by the Central Finland Granitoid Complex (CFGC), the Pohjanmaa Belt, and various sedimentary and volcanic rock units along the RLSC. The CFGC is a large geological unit composed nearly completely of ca. 1.89 – 1.87 Ga synkinematic igneous rocks, more specifically granodiorites, granites and some mafic igneous rocks (Heilimo et al. 2023). The CFGC covers most of the Central Finland and is bordered by the RLSC in the North. The Pohjanmaa Belt is a large geological unit on the Western side of the CFGC, defined by supracrustal sedimentary rocks that are mainly composed of metamorphosed turbiditic greywackes, mudstones and volcanic rocks (Kähkönen 2005).

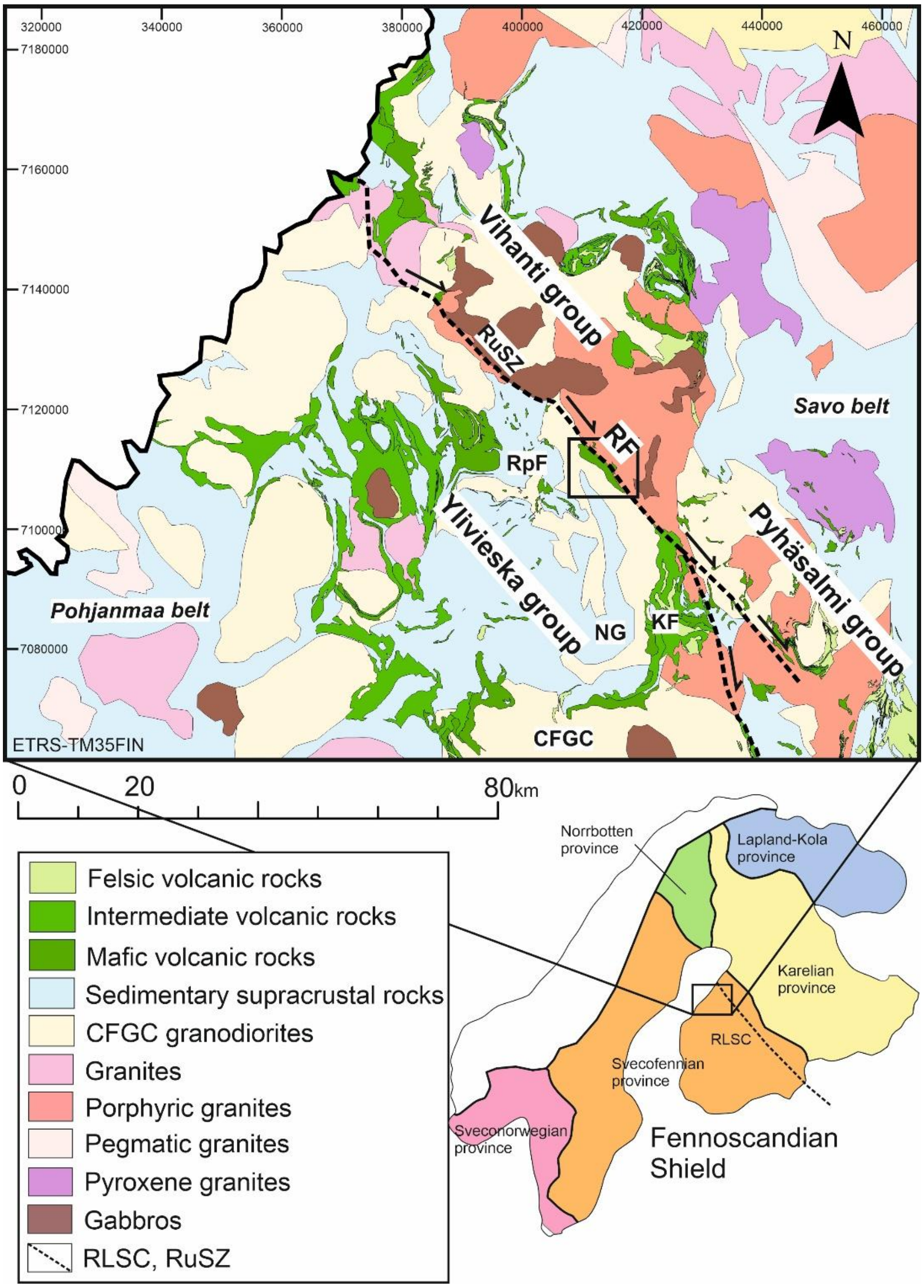

Figure 1. Geological map of the region surrounding the Rytkynkylä formation. RF = Rytkynkylä formation, RLSC = Raahe-Ladoga Shear Complex, RuSZ = Ruhaperä Shear Zone, CFGC = Central Finland Granitoid Complex, NG = Nivala group, RpF = Rauhaperä formation, KF = Kuusaa formation. Modified after Geological survey of Finland (2026). Index map is a geological map of the Fennoscandian Shield, modified after Gorbatschev & Bogdanova (1993).

2.2 Early evolution of the Fennoscandian Shield

The earliest stages of the Fennoscandian Shield’s evolution occurred ca. 2.83 – 2.75 Ga with the formation of the Archean Karelian province through accretion of various terranes which further collided in an orogeny ca. 2.73 – 2.68 Ga (Hölttä et al. 2012). The Archean Karelian province experienced extensional rifting ca. 2.5 – 2.1 Ga which resulted in large amounts of layered mafic intrusions, felsic intrusions, and intermediate-felsic volcanism in the present-day Lapland-Kola- and Karelian province (Lahtinen 2015; Ahtonen et al. 2007; Vuollo & Huhma 2005). This large-scale extension was likely the result of mantle plume upwelling (Hanski & Huhma 2005). The early convergence of the Fennoscandian shield ca. 1.95 Ga occurred when the Lapland-Kola- and Karelian provinces collided resulting in the Lapland-Kola orogeny (Daly et al. 2006).

When considering the Svecofennian orogeny there are two models under consideration, the continuous subduction model (Gorbatchev & Bogdanova 1993; Bogdanova et al. 2015; Hermansson et al. 2008; Saalmann et al. 2009) and the several microcontinent collisions model (Nironen 1997; Lahtinen et al. 2005; Nironen 2017). This study will consider an updated continuous subduction model after Mikkola et al. (2018), which provides evidence on misconceptions about the microcontinent collision model.

The Svecofennian orogeny was preluded ca. 1.93 – 1.92 Ga by an active NW-SE trending continental margin where subduction and sediment deposition from the Karelian province occurred towards the SW forming an island arc environment, the Savo arc, and a depositional basin, the Savo belt (Figure 2a) (Mikkola et al. 2018). In this study, only Savo belt shall be used when referencing to both Savo arc and Savo belt (Mikkola et al. 2018). The Savo belt collided with the Karelian province ca. 1.91 – 1.90 Ga resulting in the end of the primitive volcanism of the Savo belt. This period was also characterized by voluminous sediment deposition, generally turbiditic greywackes, to a passive margin basin to the SW of the Savo belt which also experienced extension and related mafic volcanism (Figure 2b) (Mikkola et al. 2018). Another phase of subduction began ca. 1.89 Ga with a flipped NE direction towards and under the Savo belt, resulting in widespread calc-alkaline volcanism in the Savo belt (Nironen 1997). The 1.89 Ga volcanism is accompanied by calc-alkaline intrusive magmatism which would form the CFGC (Figure 2c). The calc-alkaline magmatism reaches its peak ca. 1.88 – 1.87 Ga when a continental block from the South starts to collide with the Savo belt from SW, rounding the arc and CFGC to the extent seen today. The collision also created transtensional faulting creating pathways for geochemically A-type granites to intrude through ca. 1.88 – 1.86 Ga (Figure 2d) (Nironen et al. 2000). The collision of the Southern continental block is the main phase of the Svecofennian orogeny in Finland as peak deformation is recorded ca. 1.88 – 1.87 Ga (Nironen 2017).

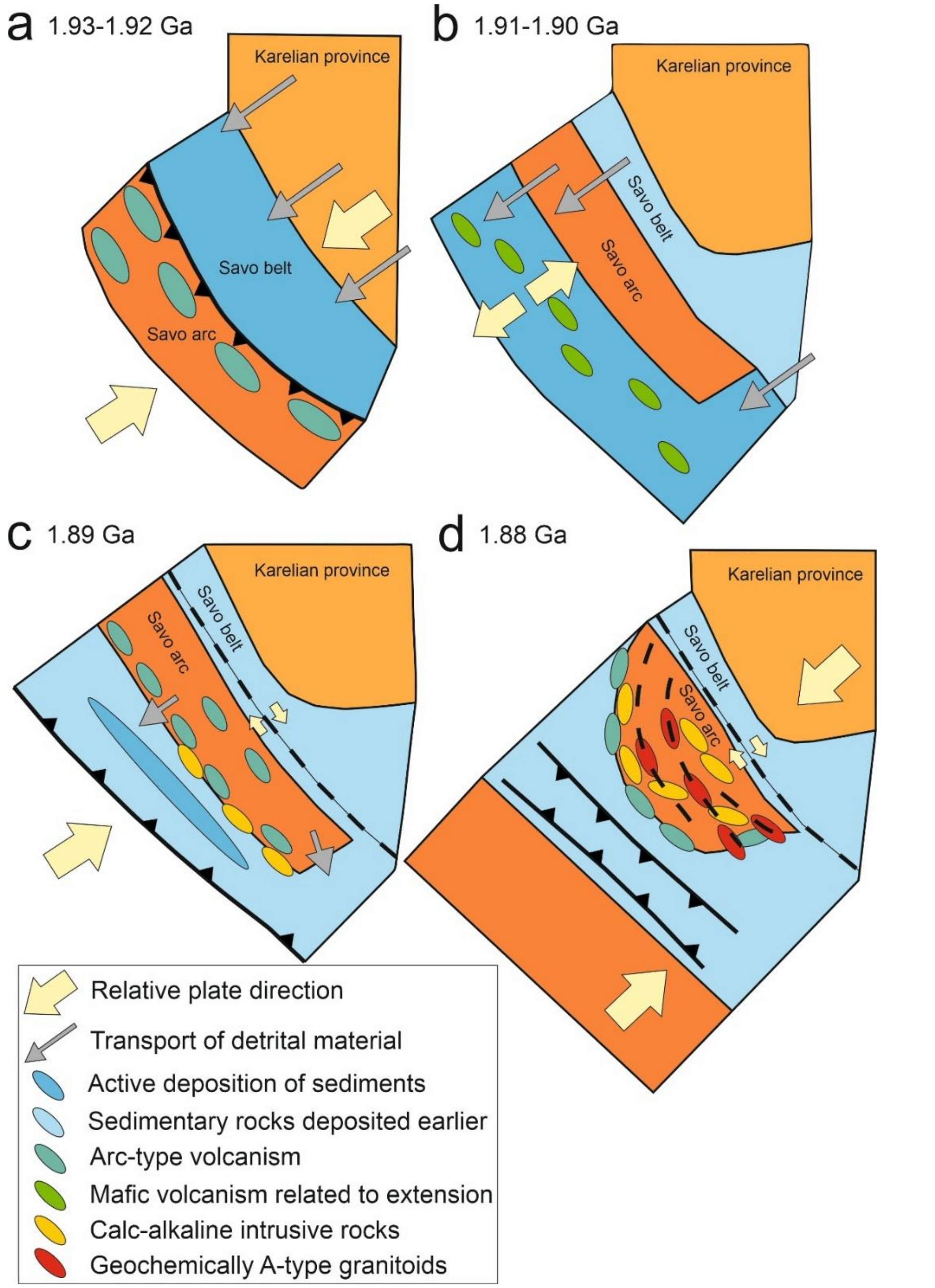

Figure 2. Model for the early evolution of the Fennoscandian shield and Svecofennian orogeny. a) The Savo belt is subducting SW under the Savo arc with large amounts of sediments depositing from the Karelian province on the continental margin. b) The Savo arc collides with the Karelian province ending arc volcanism. Turbiditic graywackes are deposited, and extension related mafic volcanism appears SW of the Savo arc. c) A new subduction zone is subducting NE under the Savo arc. Calc-alkaline intrusive magmatism begins. Dextral shearing begins around the Savo belt. d) CFGC forming magmatism peaks whilst geochemically A-type granitic magma intrudes through transtensional faults caused by the early collision of a continental block from South. Subduction related volcanism continues. Modified after Mikkola et al. (2018).

2.3 Regional geology

The geological setting surrounding the Central Finland region can be divided into the CFGC, Pohjanmaa belt and the Savo belt (Figure 1). Ylivieska group is a part of the larger Pohjanmaa belt consisting of both sedimentary and volcanic supracrustal rocks, whilst Vihanti-Pyhäsalmi group is a volcanic rock unit and a part of the Savo belt (Figure 1). The RLSC, which dominates the region, is a ca. 100 km wide complex of multiple vertical shear zones and faults running NW-SE along the Savo belt and is generally considered the most important dividing factor between the NE Archean- and SW Paleoproterozoic domains of the Fennoscandian shield (Zaher et al. 2017). The Paleoproterozoic depositional formations in this region, namely Savo- and Pohjanmaa belt were defined by D_1 – D_4 deformation stages caused by early- and main phase Svecofennian orogeny (Laine et al. 2015). As previously mentioned, the Ylivieska group consists of various supracrustal rocks, of both sedimentary and volcanic origin (Geological survey of Finland 2026). Some of the volcanic rock formations in the wider Central Finland region are still undefined. In general, the Ylivieska group's volcanic rocks range from calc-alkaline basaltic- to potassium rich rhyolitic rocks (Kousa & Luukas 2004). Of the Ylivieska group's formations, closest to the RF are the Kuusaa formation (KF) and various undefined plagioclase porphyrite units deposited under the Rauhaperä formation's (RpF) turbiditic greywacke (Figure 1). The KF ca. 1.87 Ga is defined by plagioclase and uralite porphyritic felsic to mafic member volcanic rocks that, in some parts of the formation, has well preserved primary features (Figure 1). In mafic members, amygdaloidal- and flow-top breccias can be discerned, intermediate members have pyroclastic- and ash flow tuff features, and felsic members show signs of tuff and lapilli tuff features. The KF throughout calc-alkaline with a trend from basaltic andesites to high K rhyolites (Aho, 1979). The Pyhäsalmi group is defined by a clear bimodality between mafic and felsic members. The mafic member is defined by low – medium K tholeiitic basalts and basaltic andesites, which in some cases show well preserved shallow water deposition primary features eg. pillow lavas. The felsic member is defined by low – medium K rhyolites, represented by quartz porphyrites and volcanic breccias (Kousa 1994). The Vihanti group is defined by voluminous porphyric felsic to intermediate rocks that have been affected by strong deformation, so few primary features remain. The Vihanti intermediate volcanic rocks are interlaid by eg. calc-silicate rocks and graphite bearing schists (Huhma et al. 2021).

To the SW of the RF are various types of supracrustal rocks belonging to the Pohjanmaa Belt (Figure 1). Two most important lithological units are the Ylivieska group and Nivala group. The Ylivieska group, ca. 1.89 – 1.88 Ga, is a set of multiple volcanic formations overlain by redeposited volcano-sedimentary formations (Kousa 2008). Of the sedimentary formations, closest to the RF is the RpF which consists of turbiditic greywackes of volcanic sediment origin that most likely deposited on top of the volcanic formations of the Ylivieska group (Figure 1) (Kousa 2008). Meanwhile, the Nivala group (NG) ca. 1.96 – 1.91 Ga consists of mica paragneiss' that are defined as the lowermost strata in the area and thus overlain by the Ylivieska group sedimentary- and volcanic rocks. It is also to be mentioned that the granodiorites, granites and gneisses all intrude through both the Ylivieska group and Nivala group (Figure 1) (Kousa 2021).

The CFGC plutonic rocks in the region close to the RF can be divided into synkinematic Soutuperä granodiorite-tonalites and post kinematic bimodal Haapavesi granites (Figure 5). The Soutuperä granodiorite-tonalites locate on the SW side of the RF and belong to an undefined granodiorite unit of the CFGC that has not been researched further (Figure 1) (Luukas 2018b). These granodiorites have ages of ca. 1.91 – 1.88 Ga and most likely belong to the series of calc-alkaline intrusive rocks formed during the subduction under the Savo belt and are likely similar to more studied cases of similar rocks eg. the Pirkanmaa intrusive suite (Figure 2c) (Mikkola et al. 2018; Heilimo et al. 2018). The postkinematic ca. 1.88 – 1.87 Ga bimodal Haapavesi granites have been defined as belonging to the geochemically A-type Saarijärvi plutonic suite (Figure 2d) (Nironen 2018). Within and near the postkinematic Haapavesi granites exist large amounts of gabbro and some diabase dikes that are most likely the mafic phase of the bimodal Saarijärvi granites (Figure 1) (Luukas 2018a).

2.3.1 The Raahe-Ladoga Shear Complex

The deformation model, $D_1 – D_4$, in this study is after Laine et al. (2015) which is locally defined to the Vihanti-Pyhäslami region but is also applied to the Ylivieska group and the RF, due to spatial proximation and the scale of the deformation under consideration. Characteristic of the RLSC lithologies are strongly sheared rocks of different types, but also some well-preserved crustal components near the complex eg. the KF (Figure 1) (Zaher et al. 2017). The RLSC itself is made of various shear zones that all have their own characteristics, eg. Ruhaperä shear zone (RuSZ) by which the RF is located, yet the main shear sense of the RLSC is considered to be mainly dextral (Figure 1) (Roberts et al. 2003). The RLSC was formed by the complex evolution of the Svecofennian domain and has been active in multiple phases during its evolution (Zaher et al. 2017). The pre-Pohjanmaa belt and Ylivieska group D_1 and D_2 stages of the Svecofennian orogeny affected the older Savo belt and Pyhäsalmi group by NE directional thrusting- and flat laying folding F_1 and F_2. This thrusting of the Savo belt against the Archean Karelian province caused thrust fault zone with a NW – SE strike (Laine et al. 2015; Islam et al. 2025). This thrust fault zone is the RLSC. The Pohjanmaa belt supracrustal rocks deposited in between D_2 and D_3 and would be affected by the main phase of the Svecofennian orogeny and the subsequent D_3 and D_4 stages (Laine et al. 2015).

The D_3 stage was defined by SW – NE compression that refolded most of the D_1 and D_2 flat folds upright F_3 and created vertical shear zones and active shearing in the RLSC by the Archean border (Laine et al. 2015). The D_3 was the first stage of deformation that affected the Ylivieska group volcanic rocks. The cessation of the D_3 compression and following extension caused intrusion of voluminous porphyritic granites. The youngest deformation stage D_4 saw the direction of compression change from SW – NE to N – S. This was followed by extreme shearing in the RLSC and again, refolding of the F_3 into the F_4. This new direction of compression not only activated the RLSC again but also created new sinistral NE – SW trending shear zones in the region (Laine et al. 2015). After this, the RLSC mainly saw brittle faulting all around the complex (Laine et al. 2015).

As forementioned, the RLSC is also one of the most important economic ore potential regions on the Fennoscandian shield with many famous historical mining localities eg. Vihanti and Pyhäsalmi located on the RLSC. The deposits are usually hosted in either metasedimentary or metavolcanic rocks (Vaasjoki 1988). The RLSC's faults have acted as optimal pathways for ore bearing fluids that have in many cases been trapped in folds of the forementioned rock types.

3 Materials and methods

3.1 Fieldwork, bedrock observations and methods

Fieldwork in the Rytkynkylä locality of Haapavesi was started in May 2023 and lasted until the end of June 2023. Fieldwork was carried out by Hirsimäki, M. & Kirkonoja-Nummela, S. From 113 outcrops (Attachment A), recorded 41 samples were collected (Attachment B) and chosen for their representative features in the study area's geology. From the outcrops, observations on the coordinates; rock type; colour; grainsize; alterations; shearing; fractures; and other notable features were recorded on paper and later stored in Excel. The coordinate system used in this study is ETRS-TM35FIN. Of the samples, 27 thin sections were petrographically studied (Attachment C), and 27 samples geochemically analysed (Attachment D).

According to the fieldwork lithological observations, the outcrops recorded on the field were divided into three main groups, volcanic-; plutonic- and contact outcrops, of which based on field observations 73 volcanic-; 26 plutonic- and 14 contact outcrops. Nearly all the RF volcanic rocks were either altered or otherwise hard to distinguish from eachother on the field, thus most samples were described on the field as mafic volcanic rocks. Due to difficulty distinguishing the RF volcanic rocks on field, a more detailed categorization and naming was possible only after geochemical- and petrographic analyses. Most plutonic rocks were easily distinguishable from each other and further divided into two different groups, but some granites were given a field description of leucogranite when no dark minerals were present and thus have a very light colour.

U-Pb age determination on the RF volcanic rocks was attempted from a sample deemed best representing the unaltered RF during fieldwork. However, after the separation process, during the scanning electron microscopy (SEM), it was concluded that no zircon crystals were found from the volcanic sample rendering the age determination process unachievable.

3.2 Thin section materials, and petrographic naming

The thin sections on which petrographic was conducted, were first prepared in the University of Turku's Geohouse thin section laboratory and later analysed using a Meiji polarizing light microscope in the University of Turku's Geohouse microscope laboratory. These thin sections were used to determine modal compositions (vol %); textures; grain sizes; alterations; and other notable features, which were documented and listed (Attachment C). The samples were divided into three lithological units and further given the petrographic names based on thin sections' modal compositions. The RF samples were further divided into four groups, described and given petrographical names based on modal compositions. The thin sections were analysed and named after Le Maitre et al. (2004).

The RF volcanic rock thin sections were divided into four groups based on the modal compositions of quartz. Mafic amphibole porphyrites < 15 % quartz, intermediate amphibolite porphyrites 15 – 25 % quartz, quartz amphibole porphyrites > 25 % quartz, and metavolcanic rocks. The metavolcanic group only consists of a single sample that did not fit into the other groups due to extreme alteration. The thin sections within these groups were given specific names based on the studied modal compositions.

3.3 Data, and methods of whole-rock geochemistry

The geochemical dataset of 27 samples has 18 RF volcanic rock-, 4 Haapavesi granite-, 3 Soutuperä granodiorite-tonalite- and 2 Vattukylä gabbro samples (Attachment D). On the geochemical diagrams, the geochemical data is separated to RF volcanic rock- and plutonic rock datasets, including both Pyhäsalmi- and Ylivieska volcanic rock group's comparison datasets. Within the RF volcanic rock dataset, four different groups- and five subgroups have been established based on the petrographical descriptions.

The geochemical analysis was done using wavelength dispersive X-ray fluorescence spectrometry (WD-XRF) on a PANalytical Zetium in the University of Turku's and the Åbo Akademi's laboratory in Geohouse, Turku. The process began with the preparation of the samples for the analysis. The samples were first crushed using a Fritsch Pulverisette jaw crusher, and then further pulverized using a Fritsch Pulverisette 9 and a chromium-free steel 48.5510.00 pan to minimize contamination of the samples. The composition of the chromium-free pan is Fe 98.63 – 98.08 %, C 0.55 – 0.65 %, Si 0.15 – 0.4 %, Mn 0.6 – 0.8 %, P < 0.035 % and S < 0.035 %. Next, loss on ignition (LOI) was performed on the samples to ensure the erasure of crystalline water and any remaining possible organic matter. LOI was performed first at 105 °C overnight, then at 1000 °C for 1.5 hours. As the last preparation phase, the samples were divided in two, for the samples would be analysed as two different groups in the XRF, as pressed- and fused pellets. The pressed pellet samples were mixed with a CEREOX BM-0002-1 binding matter and pressed into pellets using a Paul Weber press under 20T of pressure. The fused pellets were similarly mixed with a Claisse lithium borate mixture, Li_2B_4O7 49.75 %, $LiBO_2$ 49.75 % and LiBr 0.5 %, and fused into glass pellets under 1000 °C using a Claisse Le Neo Fluxer. Major elements analysed as oxides in this study were Al_2O_3, CaO, Fe_2O_3, K_2O, MgO, MnO, Na_2O, P_2O_5, SiO_2 and TiO_2. Trace elements analysed were Ag, As, Ba, Cd, Ce, Cl, Co, Cr, Cs, Cu, Hf, La, Mo, Nb, Nd, Ni, Pb, Rb, S, Sc, Sm, Sn, Sr, Ta, Th, U, V, W, Y, Yb, Zn and Zr. The major elements were analysed using the pressed pellets, whilst the trace elements were analysed using the fused pellets. These results were achieved using the WD-XRF method. It is to be mentioned that the XRF measurements are very likely to be influenced by the matrix composition. Thus, variations in precision and accuracy might occur. Due to this, Fish Canyon Tuff, a dacitic standard by LGC183 standards, UK is used in the WD-XRF process to ensure the quality of the analysis.

For Quality Assurance and Quality Control (QA/QC), Ore Research and Exploration Assay Standards (OREAS) Certified Reference Materials (CRMs) CRM-85- and 185 OREAS were used. CRM-185 OREAS was used four times at 12 – 18 sample intervals. To ensure reproducibility of the XRF analysis, duplicate samples were used, one at the beginning and two at the end. In addition, two calcite standards from Pargas Quarry were used with a 24 sample difference to assess carryover effects from possibly ore potential samples. For more, see (Attachment B).

3.4 Comparison data, and data filtering

Comparison data for the whole-rock geochemical analysis in this study includes two papers by Nurmi et al. (1991), and Kousa et al. (1994). The paper by Nurmi et al. (1991) contains reference data of the Ylivieska group, whilst Kousa et al. (1994) provides reference data for the Pyhäsalmi group. The RF's volcanic rock data is compared to Ylivieska- and Pyhäsalmi volcanic group's datasets. The comparison datasets are presented as two different overlain fields which are drawn with 95 % accuracy. The data from these papers was compiled into their own tables using Excel (Attachment E).

The reference data, together with the 18 volcanic rock samples of the RF data, was filtered for alterations using the AI-CCPI diagram (Figure 3). The reference datapoints that fell outside the least altered box were singled out from the data pool, whilst the rest of the data was included in the geochemical analysis. With both RF- and reference data, values that would fall under the detection limits were replaced with values of 0.5 times the detection limit. The quite high limit values, AI 20 – 70 and CCPI 20 – 90, were chosen based on the commonly hydrothermally altered nature of the metavolcanic samples and reference data. The RF's and Ylivieska group's data all plot inside the least altered box, whilst the data from the Pyhäsalmi group fall outside on both hydrothermal and diagenetic sides of the diagram.

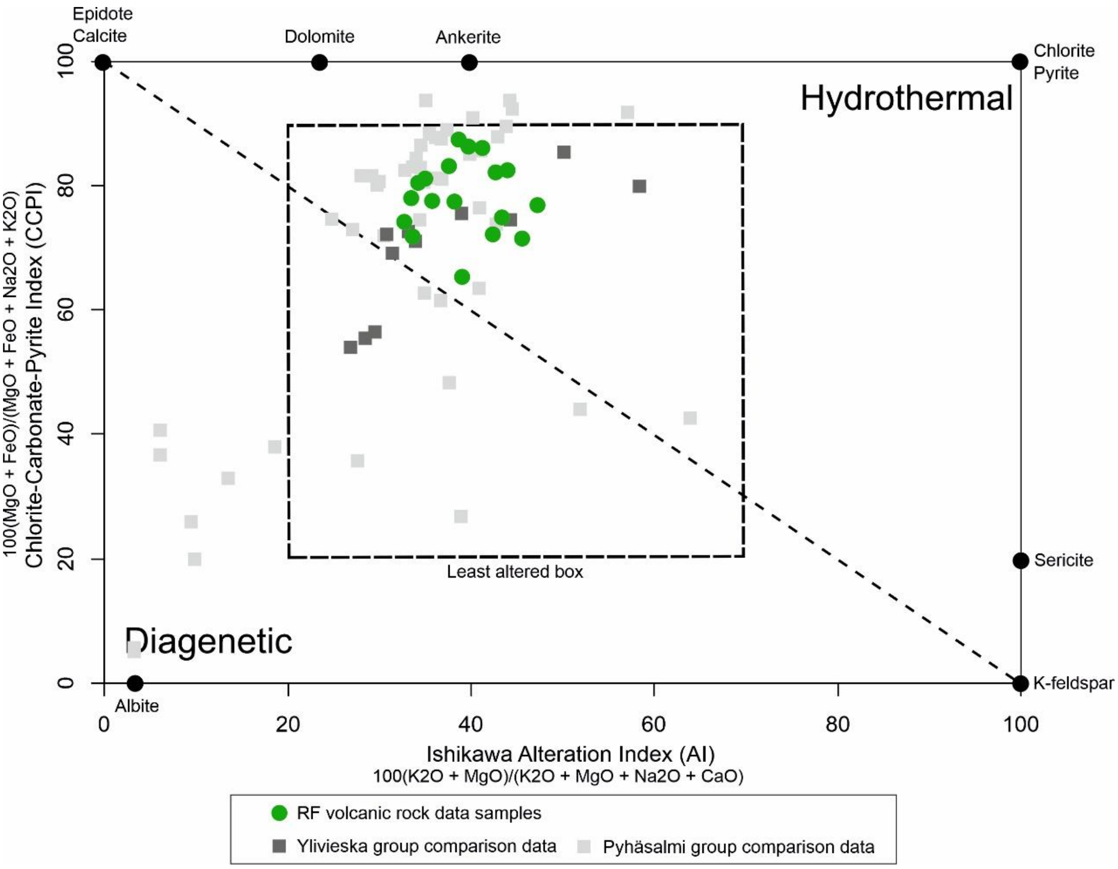

Figure 3. The AI-CCPI alteration index for Rytkynkylä formation-, Ylivieska group-, and Pyhäsalmi group samples. The least altered primary- and reference data samples are inside the least altered box. RF = Rytkynkylä formation. Modified after Large et al. (2001).

4 Results

4.1 Fieldwork, and mapping of the study area

A map of the study area was modified from the Geological Survey of Finland's Mineral Deposits and Exploration database, considering recorded field observations. The map shows an edited version of the RF with sample collection locations, and an edited interpretation of the dextral RuSZ's shearing in the area (Figure 4). The recorded contact outcrops played an integral role in editing of the map since they show boundaries between different lithological units, usually between the RF volcanic rock and either the Haapavesi granite or Soutuperä granodiorite-tonalite. The South side of the RF has a relatively simple and sharp boundary with the Soutuperä granodiorite-tonalite, but the Northern boundary of the RF, relative to the Haapavesi granite, is complicated with multiple heavily altered RF volcanic xenolithic inclusions inside of the Haapavesi granite, shown as flames on the map. The Soutuperä granodiorite-tonalite has also a few RF xenoliths. A small amount of the Vattukylä gabbro is visible on the map, and some of it was mistaken as RF volcanic rock on the field, resulting in three Vattukylä gabbro outcrops in the study area (Figure 4). These three small Vattukylä gabbro intrusions are marked as flames on the map. Some of the sedimentary supracrustal rocks of the Nivala group and Ylivieska group are visible on the map but aren't part of the study area either (Figure 4).

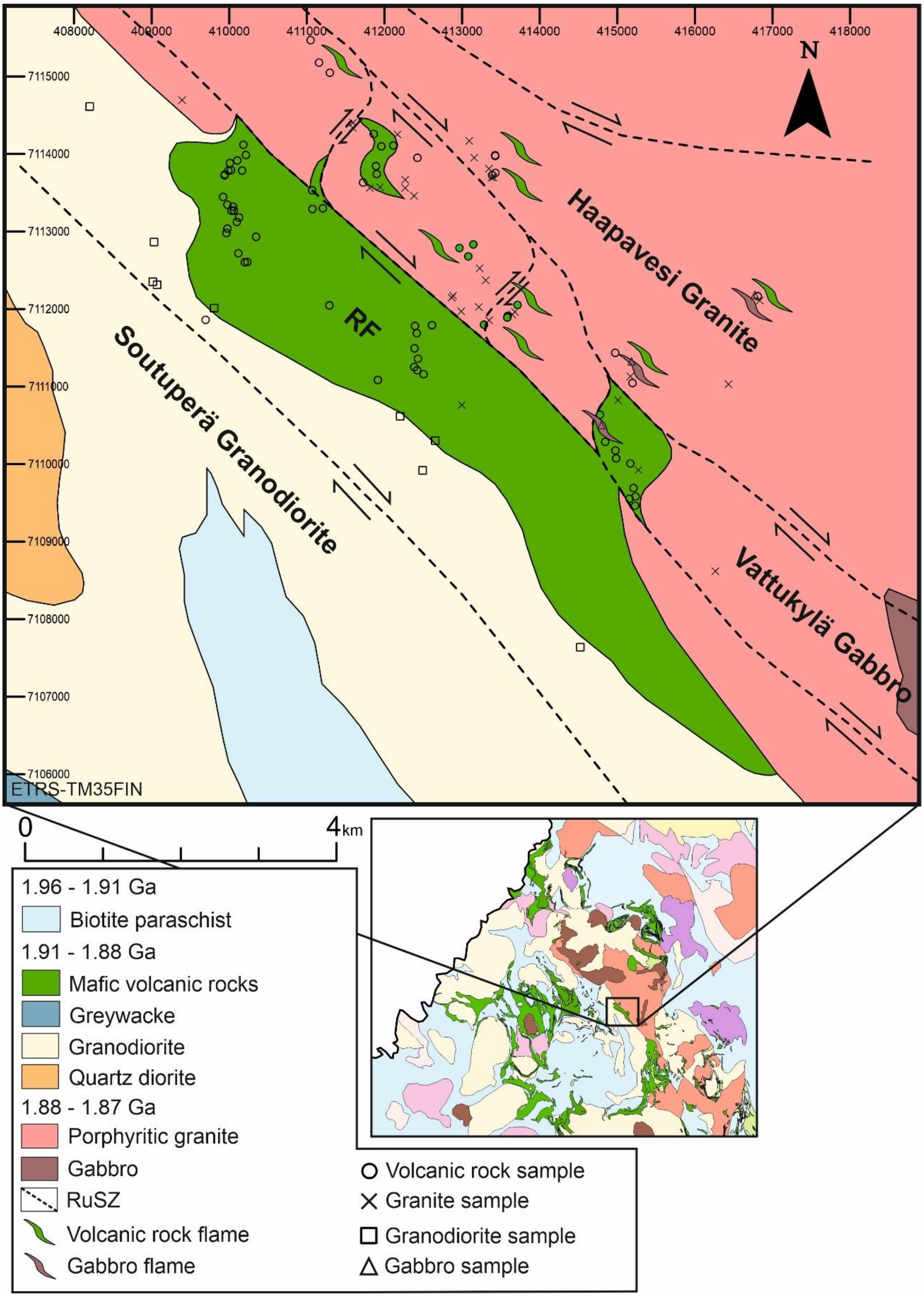

Figure 4. Geological map of the Rytkynkylä formation locality. RF = Rytkynkylä formation, RuSZ = Ruhaperä Shear Zone. Modified after Geological Survey of Finland (2026).

4.1.1 Rytkynkylä formation

Volcanic rocks belonging to the RF can be found as a ca. 7 km long NW – SE trending lithological unit in the middle of the study area ca. 9 km from the village of Haapavesi. The RF approximately follows the trend of both the RuSZ and the border of the Haapavesi granite and the Soutuperä granodiorite-tonalite. The entire study area is poorly exposed with some exceptions and has some small to medium sized moss-covered outcrops. The volcanic rocks collected from the study area were all categorized as basaltic due to them all retaining a similar messy dark appearance, grain size, texture and alterations without any significant differences. Only two cases of composition differences in the RF were found, and these primary features are most likely bedding of the original volcanic – sedimentary sequence (Figure 5e, f). Grainsizes recorded were medium ca. 1mm to fine < 1m with an aphanitic texture present in most outcrops (Figure 6b). Although the grainsizes were small, porphyritic texture was visible to eye in some samples (Figure 6a).

Epidote and quartz filled fractures were common in the volcanic rocks (Figure 5a, b), whilst granite dikes were more uncommon, but present especially in the NW parts of the RF (Figure 5d). Sinistral indicators are common in the brittle fractures filled with epidote and quartz. The dextral RuSZ's heavy shearing and the younger Haapavesi granite's intrusion has caused the RF to be heavily deformed and altered especially on the NE side of the formation. Contacts between the RF inclusions and Haapavesi granite are sharp and the volcanic rock is altered by contact metamorphism (Figure 5c). Inclusions of the RF inside the Haapavesi granite indicate clear age difference and relation. As for mineralisations, rusting was present in more mineralised outcrops, which were relatively common throughout the sequence. However, larger mineralisations were rare.

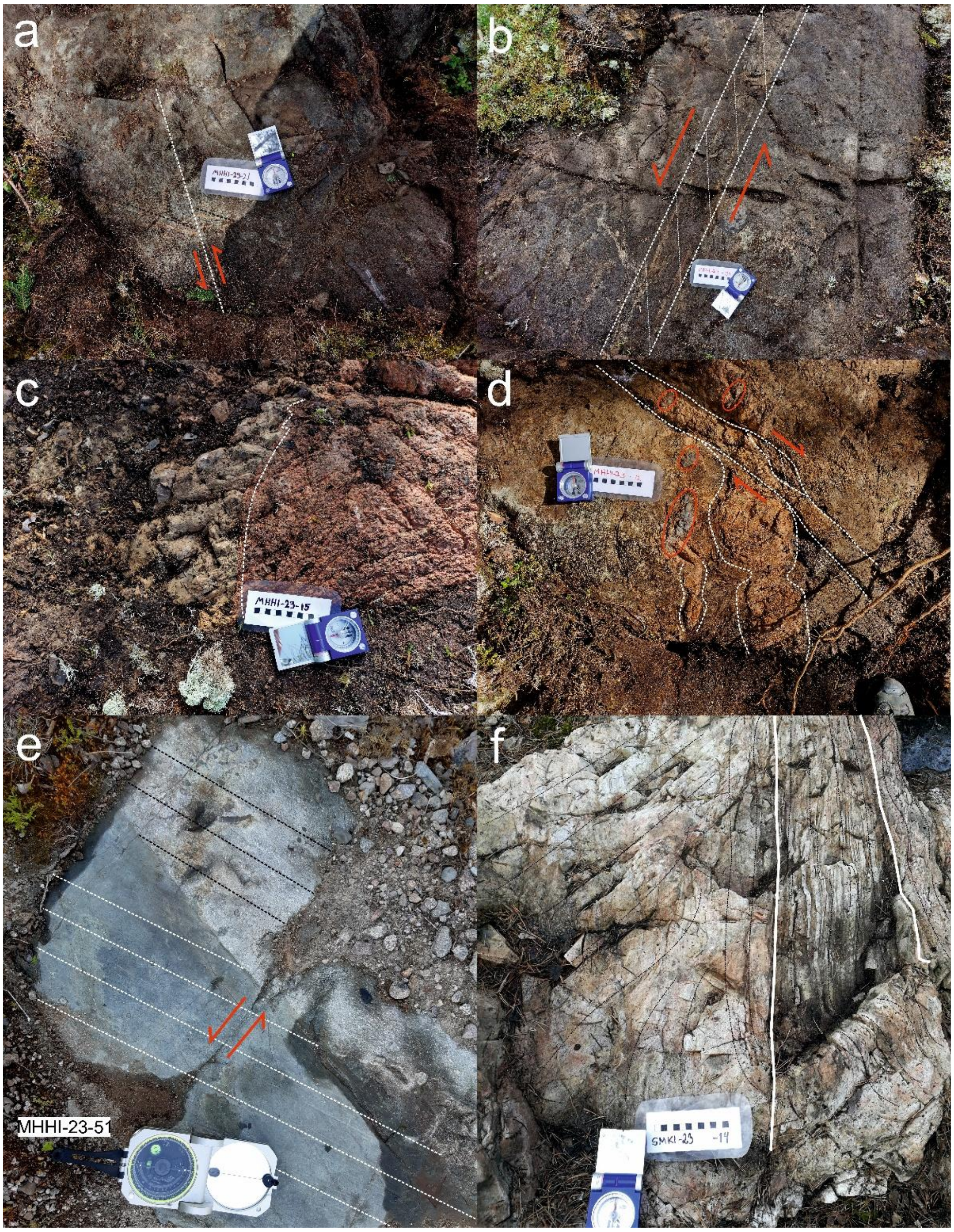

Figure 5. a) Altered presumably basaltic volcanic rock with an epidote filled fracture. The joint is cut by a sinistral fracture showing the sense of brittle deformation in the study area. MHHI-23-21.1. b) Another altered basaltic volcanic rock with epidote filled fractures. Between the two joints are en-echelon fractures that again show the sinistral sense of the brittle deformation. MHHI-23-13.2. c) A contact between the Rytkynkylä formation (RF) and the Haapavesi granite. The contact is extremely sharp, and the volcanic rock has been heavily altered. The volcanic rock is a part of one of the RF inclusions inside the Haapavesi granite. MHHI-23-15.1. d) Haapavesi granite dike, intruded inside the RF volcanic rock in the very NW part of the RF. The granite dike has round pinch and swell boudinage formed in ductile deformation. Some quartz has crystallized in the necks of the boudins that have later been displaced by sinistral brittle deformation. MHHI-23-12.1. e) An outcrop with primary bedding with a disconformity. The S layer is a basaltic ashflow with thin laminae. The N layer is more felsic, porphyroblastic, and with thin laminae, pointing at an andesitic ashflow. The bedding is cut by a sinistral fault. MHHI-23-51.1. f) The second outcrop with primary features. Folded bedding with two distinct unconformities. The center bed, where the thin layering is best seen, has parasitic S folds. The bed on the right has layers dipping perpendicularly to the center bed. SMKI-23-14.1.

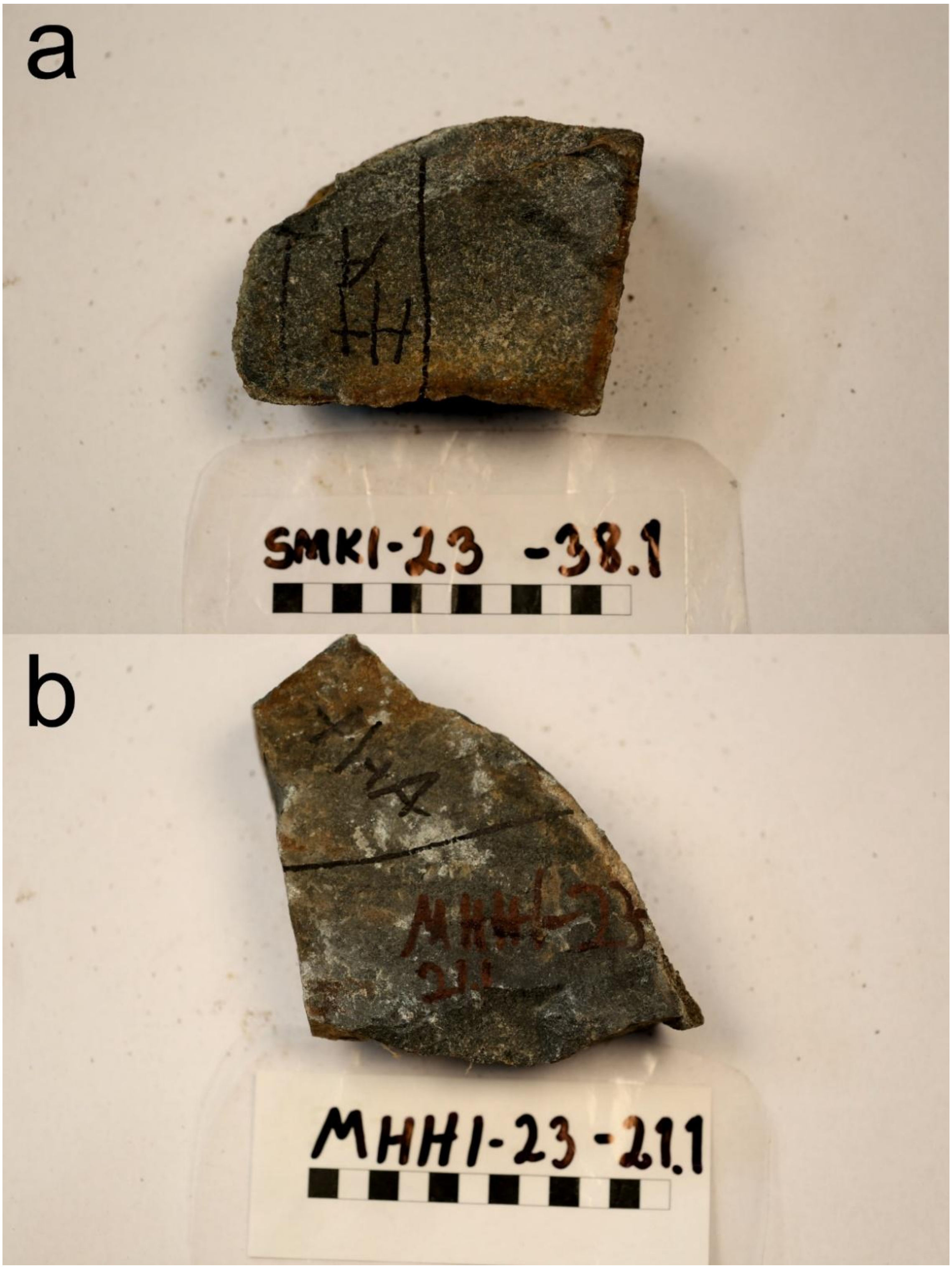

Figure 6. a) Rytkynkylä formation (RF) volcanic rock sample SMKI-23-38.1 with ca. 1mm medium grained porphyroblasts in a fine-grained matrix. b) A fine grained < 1mm RF volcanic rock sample MHHI-23-21.1 with aphanitic texture and silicification.

4.1.2 Haapavesi granite, Vattukylä gabbro

Haapavesi granite, a batholith of porphyritic granite is located to NE of the RF. The granite is bimodal with its mafic component, the Vattukylä gabbro located slightly further to the East of the RF (Figure 1). Aside from the gabbro intrusions, Haapavesi granite also has some leucogranite dikes located within. The leucogranite outcrops observed in the study area are all located by the RuSZ's main shears (Figure 7c). Observed along the RuSZ, on the contact between RF and Haapavesi granite, is a small quarry with an unakite outcrop. The unakite mineralisation follows the shear zone in a NW – SE trend (Figure 7d). Haapavesi granite's most common textures are porphyritic and phaneritic, which are seen in every outcrop (Figure 7a – c). The grainsizes of the porphyritic granites vary from large ca. 5mm to fine ca. 1mm. Some rare few granite outcrops show signs of ductile shearing induced foliation, indicated by deformed and elongated feldspar phenocrysts (Figure 7a). With these few exceptions, Haapavesi granite is mostly undeformed throughout the study area, except for the immediate area around the RuSZ. The gabbro and leucogranite grain sizes are small ca. 1mm to fine < 1mm, and the difference between the porphyritic- and leucogranite is clear (Figure 7c). The unakite is altered porphyritic granite, indicated by its large > 5mm phenocryst grainsizes and porphyritic texture (Figure 8a, b).

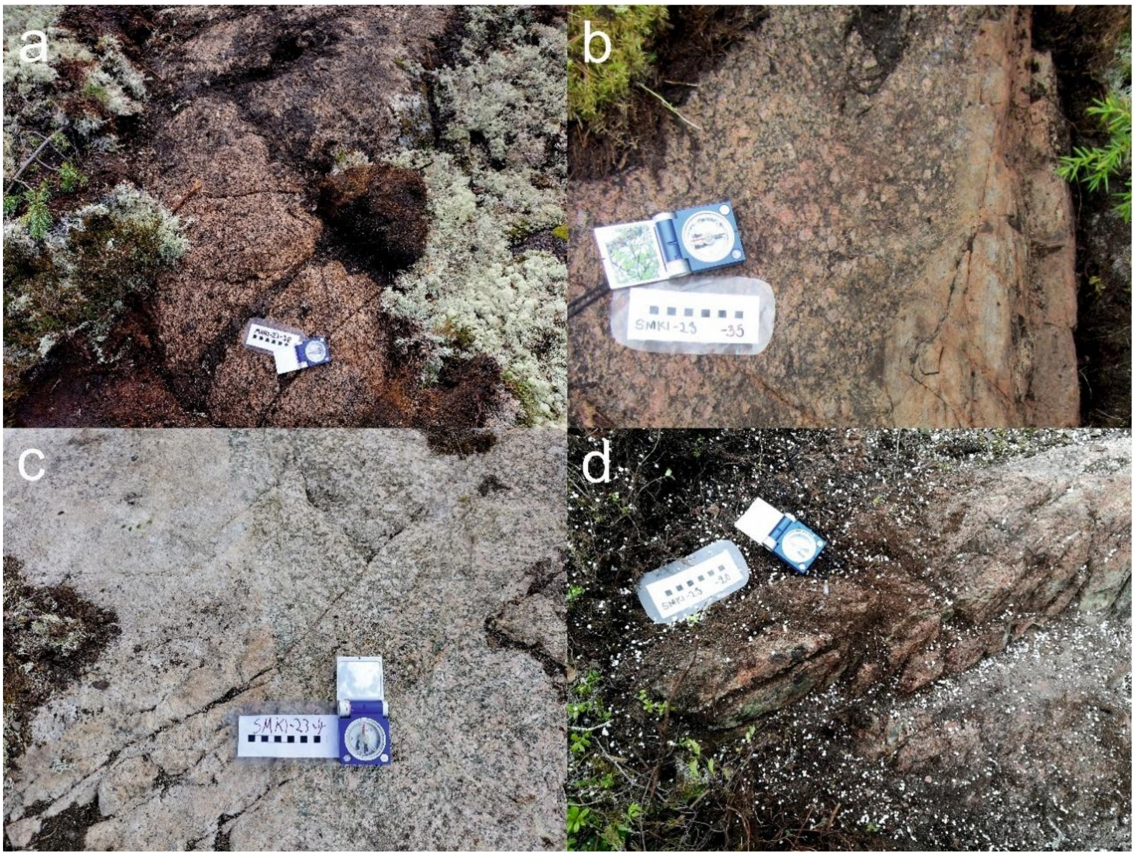

Figure 7. a) Porphyritic and slightly sheard Haapavesi granite from the NW border of the Rytkynkylä formation (RF). The shearing is indicated by elongated phenocrysts which show E – W trending shearing. MHHI-23-28.1. b) A contact outcrop between RF volcanic rock and Haapavesi porphyritic granite. Along the contact, the granite has a larger amount of mafic minerals in the matrix, and the phenocrysts are aligned following the contact. SMKI-23-35.1. c) Haapavesi granite’s leucogranite and porphyritic granite contact. The contact is sharp and difference in the two granites is clear. Some ductile shearing can be observed in the porphyritic granite. SMKI-23-4.1 d) An unakite outcrop within the Haapavesi granite, by one of the main Ruhaperä shear zone’s shears. All mafic minerals in the granite have altered to epidote, which is seen as the bright green mineral. SMKI-23-20.

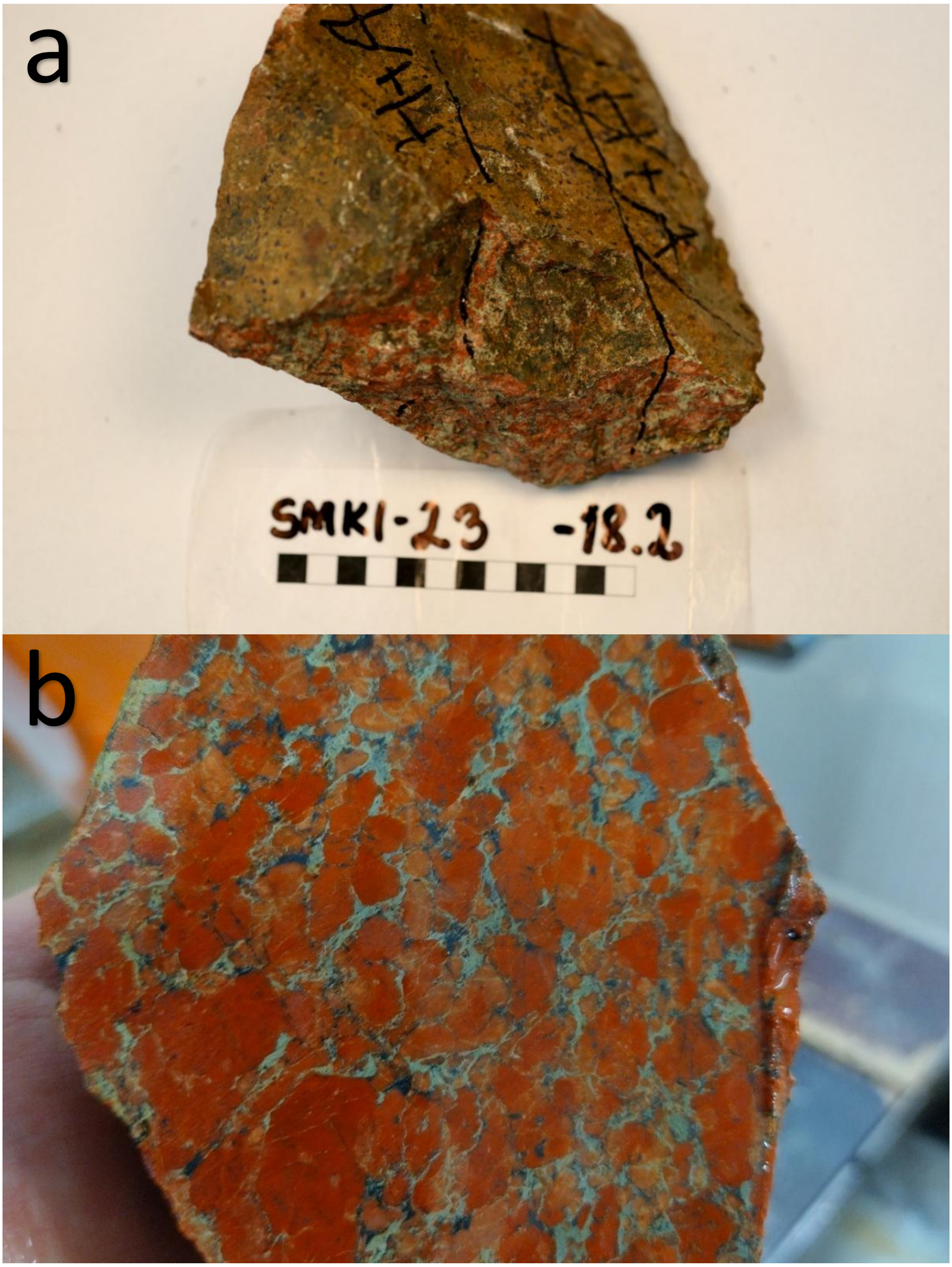

Figure 8. a) Haapavesi granite's unakite sample SMKI-23-18.2 which shows better the alteration the granite has gone through. b) A cut version of the same sample SMKI-23-18.2 where the alterations and texture can be seen on a fresh wet surface. The bright red feldspar and epidote indicate heavy metasomatic alteration. Some dark mafic minerals are still present between the feldspar phenocrysts, but most have metamorphosed to epidote.

4.1.3 Soutuperä granodiorite-tonalite

The SW side of the RF belongs largely to the Soutuperä granodiorite-tonalite. There is some quartz diorite, Ylivieska group greywacke, and Nivala group biotite paraschist in the same area to the West, but it lies outside the study area (Figure 4). The Soutuperä granodiorite-tonalite occurs on some outcrops more as a tonalite than granodiorite with a pale greyish and slightly darker appearance stemming from a very high plagioclase and content, whereas the granodiorite has a lighter pinkish appearance due to higher amounts of alkali feldspar (Figure 9a, b). Both granodiorites and tonalites have an even phaneritic texture, and their grainsizes vary from medium-, ca. 1mm – 5mm, to fine, < 1mm, grained (Figure 10a, b). One tonalite outcrop has dark patches of mafic enclaves as inclusions (Figure 9d). Quartz filled fractures are common in most Soutuperä granodiorite-tonalite outcrops, and ductile foliation is present in all granodiorite- and tonalite outcrops with varying directions, most likely caused by ductile shearing or conformity during intrusion to the RF (Figure 9c). Disseminated pyrite and chalcopyrite are observable in few outcrops.

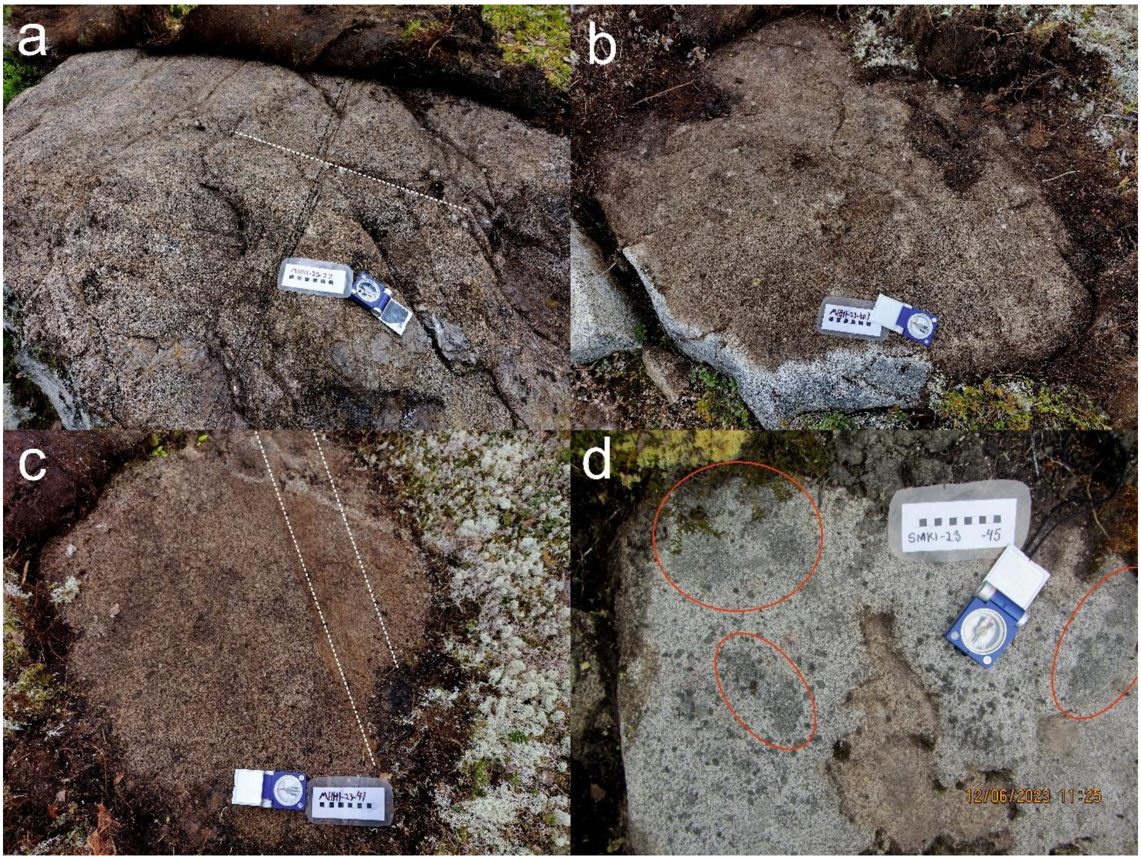

Figure 9. a) Soutuperä granodiorite-tonalite outcrop with multiple brittle deformation induced quartz joints and foliation. The granodiorite has a slightly pinkish color due to high alkali feldspar content. MHHI-23-22.1. b) Soutuperä tonalite outcrop with a slightly greyer color compared to the granodiorite and weak foliation. MHHI-23-40.1 c) Soutuperä granodiorite-tonalite with clear foliation, caused by either ductile shearing or conformity during intrusion to the Rytkynkylä formation. This outcrop has little stronger shearing compared to most other outcrops. MHHI-23-41.1 d) Soutuperä tonalite outcrop with multiple mafic enclaves. These mafic enclaves have a smaller grainsize, < 1mm, compared to the surrounding phaneritic tonalite. SMKI-23-45.1.

Figure 10. a) Soutuperä granodiorite-tonalite sample MHHI-23-22.1 with phaneritic texture and medium 1mm – 5mm grainsize. Weak foliation is visible in the sample. b) The Soutuperä tonalite sample MHHI-23-40.1 has more mafic minerals and a dark grey color compared to the granodiorite’s lighter pinkish color. The tonalite sample has same phaneritic texture and medium grainsize as the granodiorite.

4.2 Petrography

4.2.1 Thin section descriptions of the Rytkynkylä formation volcanic rocks

The mafic amphibole porphyrite group's major minerals are hornblende, plagioclase, epidote and in the case of the biotite plagioclase porphyrite, biotite. Trace minerals are quartz, chlorite, rutile, and some opaque minerals. The petrographical names given to the samples in the mafic amphibole porphyrite group are hornblende-plagioclase porphyrite, hornblende-plagioclase-epidote porphyrite, plagioclase-hornblende porphyrite, plagioclase-hornblende-epidote porphyrite and biotite-plagioclase porphyrite. The rough texture and mineral assemblage of hornblende-plagioclase porphyrites point to a crystallisation in either a magma chamber or a thick lava sill (Figure 11a, b), whereas hornblende-plagioclase-epidote porphyrites do not have as such clear texture but still could be an altered lava texture with larger phenocrysts from deeper in the magma chamber (Figure 11c, d). Plagioclase-hornblende porphyrite and plagioclase-hornblende-epidote porphyrite have ambiguous textures due to heavy alteration, but medium to large relict plagioclase and large uralite phenocrysts point to a lava origin (Figure 12). Compared to the other samples in this group, biotite-plagioclase porphyrite is clearly volcanic ash (Figure 13a, b).

Two hornblende-plagioclase porphyrite samples, MHHI-23-32.1 and SMKI-23-38.1, are medium grained, ca. 1 – 2 mm (Figure 11a, b). Major mineral modal compositions are hornblende 45 – 50 %, plagioclase 30 – 40 %. Accessory mineral modal compositions are chlorite 5 %, epidote < 1 – 10 %, quartz < 1 %, rutile < 1 %, and opaque minerals 5 – 10 %. Euhedral plagioclase crystals are enclosing anhedral hornblende crystals resulting in a subophitic texture. The hornblende crystals occupying the space between plagioclase have quartz inclusions which points to an alteration from clinopyroxene, thus hornblende being uralite. Some chlorite and epidote occur alongside opaque minerals. Many opaque mineral grains have a skeletal texture and always exist alongside chlorite.

The two hornblende-plagioclase-epidote porphyrite samples, MHHI-23-19.1 and MHHI-23-21.1, are fine grained, 0.2 – 1 mm (Figure 11c, d). Major mineral modal compositions are hornblende 45 – 55 %, plagioclase 25 – 30 % and epidote 10 – 15 %. Accessory mineral modal compositions are quartz 2 – 5 %, biotite 0 – 5 %, calcite 0 – 5 % and opaque minerals 2 – 3 %. Fine grained, ca. 0.1 – 0.2 mm, euhedral plagioclase phenocrysts and microcrystalline hornblende groundmass form an intergranular texture around fine grained, ca. 0.5 – 1 mm, hornblende phenocrysts. Zoning is present in some plagioclase phenocrysts. The hornblende phenocrysts retain a subhedral clinopyroxene structure, relict clinopyroxene twinning, and contain small quartz inclusions, thus remarking the hornblende phenocrysts as uralite. A lava flow direction can be observed due to the phenocrysts being aligned in the same general direction.

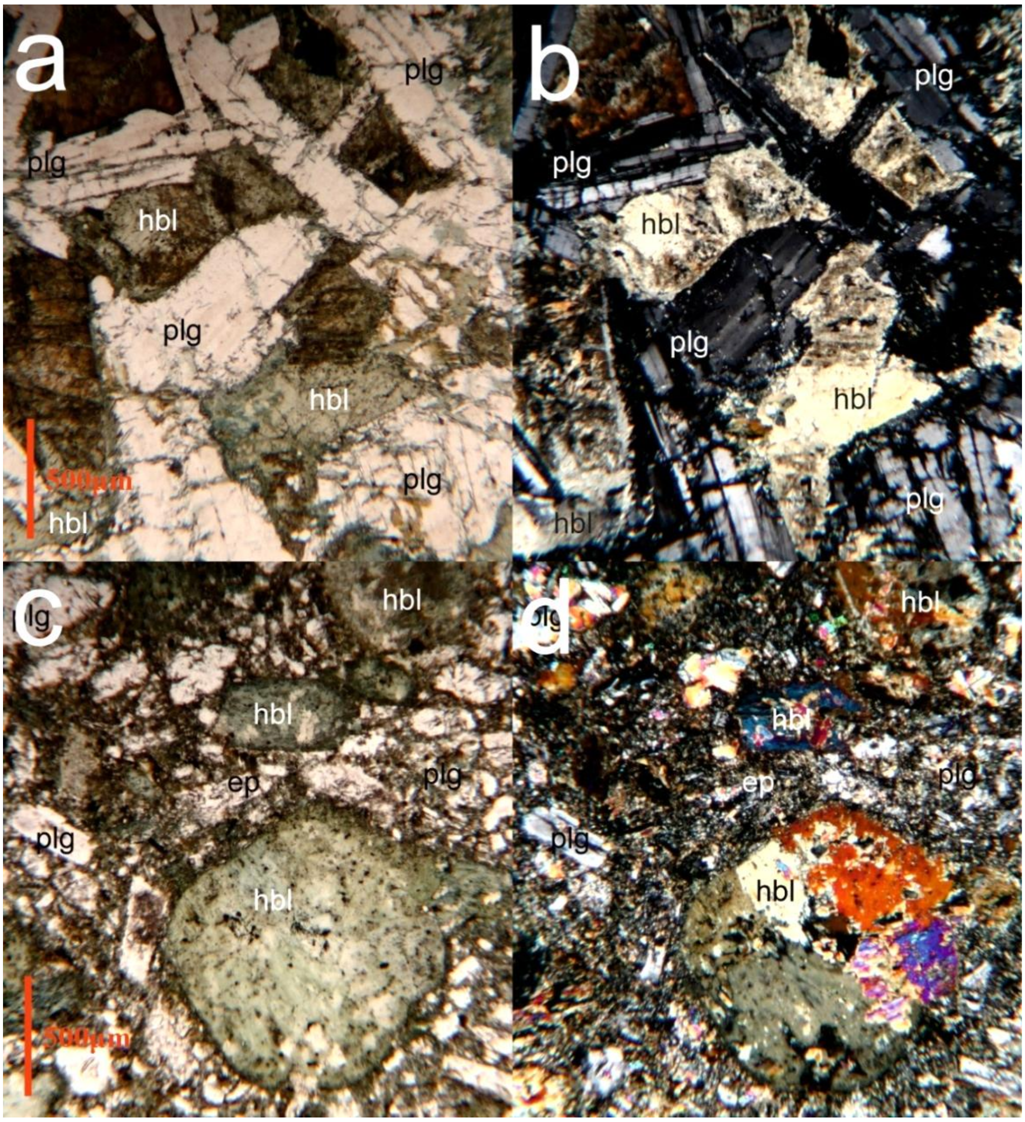

Figure 11. a) Sample SMKI-23-38.1, hornblende-plagioclase porphyrite. Medium grained, ca. 1mm, unaligned euhedral plagioclase grains with fine to medium grained hornblende in between. The plagioclase and hornblende form a subophitic texture. There is little alteration compared to all other RF volcanic rock samples. PPL. b) XPL version of the sample SMKI-23-38.1. c) Sample MHHI-23-21.1, hornblende-plagioclase-epidote porphyrite. Uralite phenocrysts with quartz inclusions, and smaller plagioclase phenocrysts in a hornblende groundmass. Most of the plagioclase has partly altered to epidote through saussuritization. PPL. d) XPL version of the sample MHHI-23-21.1.

The plagioclase-hornblende porphyrite sample, MHHI-23-7.1, is fine to medium grained, ca. 1 – 2 mm (Figure 12a, b). Major mineral modal compositions are plagioclase 40 % and hornblende 30 %. Accessory mineral modal compositions are quartz 5 %, biotite 5 %, opaque minerals 5 %, rutile 2 %, epidote 2 % and leucoxene 1 %. Subhedral hornblende phenocrysts form a glomeroporphyric texture within a fine grained, ca. 0.1 mm, plagioclase-hornblende-quartz groundmass. Quartz inclusions are observable in hornblende glomeroporphyres indicating alteration from clinopyroxene. Hornblende alters further into biotite. Likely ilmenite opaque minerals have leucoxene rims.

The plagioclase-hornblende-epidote porphyrite sample, MHHI-23-16.1, is medium grained, ca. 1 – 4 mm (Figure 12c, d). Major mineral modal compositions are plagioclase 40 %, hornblende 30 %, epidote 20 %. Accessory mineral modal compositions are chlorite 5 %, quartz 2 %, opaque minerals 2 % and rutile 1 %. Euhedral hornblende phenocrysts with quartz inclusions and twinning locate among fine grained, ca. 0.1 – 1 mm, euhedral altered plagioclase phenocrysts. All hornblende and chlorite are alteration products of clinopyroxene, whilst all plagioclase has partly altered to epidote. Quartz and epidote filled joints crosscut the sample throughout. The epidote filled joints show dextral semi brittle deformation cut quartz filled joints, thus are younger.

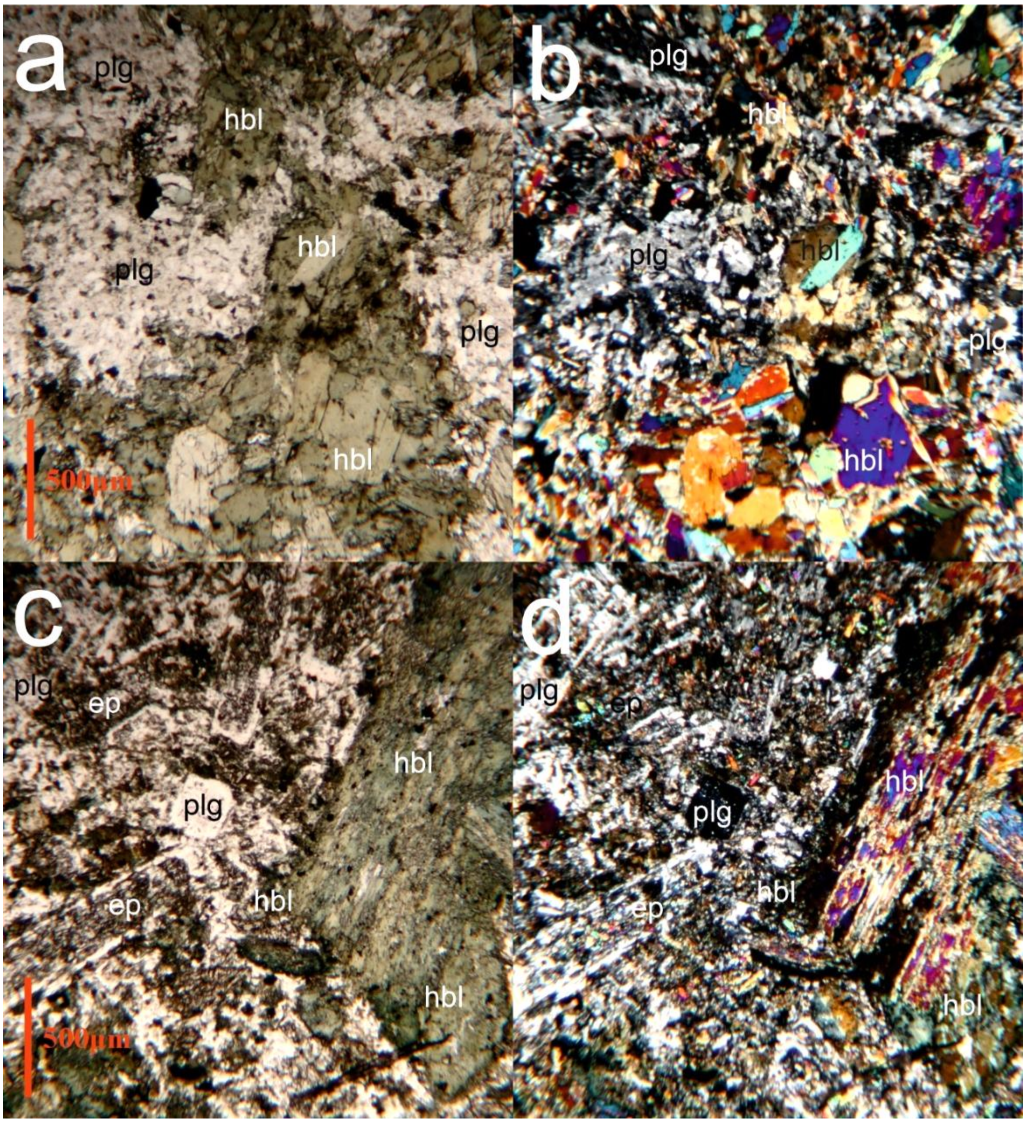

Figure 12. a) MHHI-23-7.1, plagioclase-hornblende porphyrite. Fine grained, 1 mm, hornblende glomeroporphyres among a plagioclase-quartz groundmass. PPL. b) XPL version of the sample MHHI-23-7.1. c) MHHI-23-16.1, plagioclase-hornblende-epidote porphyrite. Euhedral uralite phenocryst with relict clinopyroxene twinning and quartz inclusions among smaller, epidote altered, subhedral plagioclase phenocrysts. PPL. d) XPL version of the sample MHHI-23-16.1.

The biotite-plagioclase porphyrite sample, MHHI-23-36.1, has fine to medium grained, ca. 0.2 – 1 mm (Figure 13a, b). Major mineral modal compositions are biotite 50 % and plagioclase 30 %. Accessory mineral modal compositions are quartz 10 %, epidote 5 % and hornblende 5 %. Fine grained and microcrystalline, ca. < 0.1 mm, subhedral plagioclase grains are observable among a microcrystalline, < 0.1 mm, biotite groundmass. Some biotite form fine grained, ca. 0.3 mm, glomeroporphyres. A lava flow direction can be determined due to most of the plagioclase grains being aligned in the same direction.

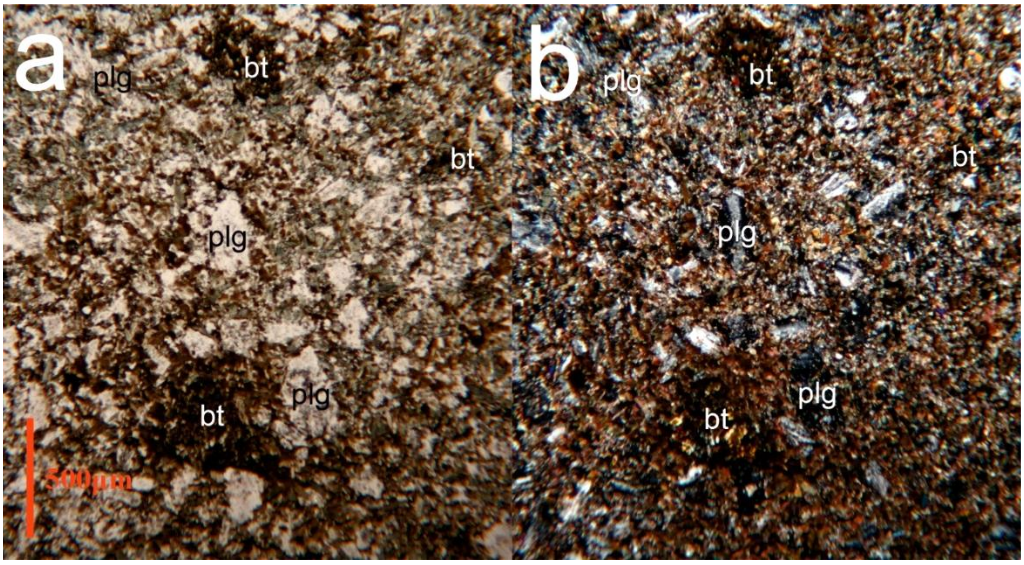

Figure 13. a) MHHI-23-36.1, biotite-plagioclase porphyrite. Subhedral plagioclase grains among a microcrystalline biotite groundmass. Most of the plagioclase crystals are aligned the same way, diagonally compared to the thin section pictures. Two biotite glomeroporphyres are observable due to their darker color on both PPL and XPL. PPL. b) XPL version of the sample MHHI-23-36.1.

The intermediate amphibole porphyrite group's major minerals are plagioclase, hornblende and quartz. Accessory minerals include biotite, epidote, rutile, chlorite, hematite, sericite, leucoxene and opaque minerals. All four of the intermediate amphibole porphyrite group's samples were given one petrographical name based on the modal compositions, plagioclase-hornblende-quartz porphyrite. The intermediate amphibole porphyrite group is by far the most ambiguous and varied as for the crystallisation environment and could be either or a mixture of lava and ash.

The four plagioclase-hornblende-quartz porphyrite samples, MHHI-23-13.1; MHHI-23-29.1; SMKI-23-47.2; SMKI-23-52.1, are fine grained, ca. 0.5 mm (Figure 14a, b). Major mineral modal composition is plagioclase 40 – 45 %, hornblende 20 – 35 % and quartz 15 – 20 %. Accessory mineral modal compositions are biotite 0 – 10 %, epidote < 1 – 5 %, leucoxene 0 – 5 %, opaque minerals < 1 – 5 %, rutile 0 – 5 %, chlorite < 1 % and hematite < 1 %. Hornblende- and plagioclase porphyrites occur among a fine grained, ca. 0.2 mm, quartz-hornblende-plagioclase groundmass. A clear sense of shearing is present throughout all the samples. Quartz inclusions in hornblende point to alteration from clinopyroxene, thus classifying the hornblende as uralite.

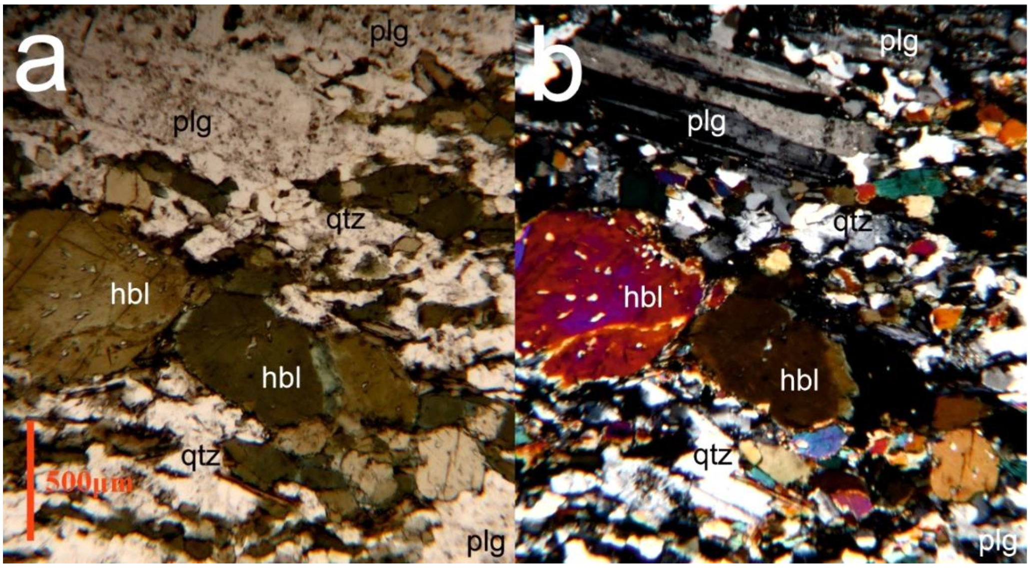

Figure 14. a) MHHI-23-29.1, plagioclase-hornblende-quartz porphyrite. A sheared sample with clearly visible quartz inclusions in the uralite phenocrysts. The quartz shows clear shearing induced recrystallization. PPL. b) XPL version of the sample MHHI-23-29.1.

The quartz amphibole porphyrite group's major minerals are quartz, hornblende, plagioclase, biotite and epidote. The formation environment is rather unclear from looking at the sample's textures but lean more in volcanic ash rather than a lava texture. Trace minerals include chlorite, calcite, rutile and opaque minerals. The petrographical names given to the samples in this group are hornblende-quartz-plagioclase porphyrite, hornblende-quartz-epidote porphyrite, quartz-hornblende-biotite porphyrite, quartz-plagioclase-biotite porphyrite and quartz-epidote-hornblende porphyrite. All of the samples in this group are volcanic ash or look that way by being extremely altered, like MHHI-23-2.1 with possible large relict plagioclase, aligned in a similar manner indicating a lava texture.

The hornblende-quartz-plagioclase porphyrite sample, SMKI-23-54.1, is fine grained, ca. 0.5 mm (Figure 15a, b). Major mineral modal compositions are hornblende 45 %, quartz 25 % and plagioclase 25 %. Accessory mineral modal compositions are biotite 5 % and epidote < 1 %. Fine grained, ca. 0.5mm, hornblende glomeroporphyres occur among a groundmass of fine and microcrystalline, < 0.1 mm, quartz and plagioclase.

The hornblende-quartz-epidote porphyrite sample, MHHI-23-38.1, has fine grained, ca. 0.5 mm phenocrysts, among a microcrystalline < 0.1 mm groundmass (Figure 15c, d). Major mineral modal compositions are hornblende 40 %, quartz 25 % and epidote 20 %.

Accessory mineral modal compositions are plagioclase 5 %, chlorite 5 %, calcite 5 % and biotite 5 %. The sample has sub ophitic texture with glomeroporphyres among the quartz dominated groundmass. Dextral joints cut hornblende porphyroblasts and are filled with epidote, quartz, chlorite, and calcite with typical calcite twinning.

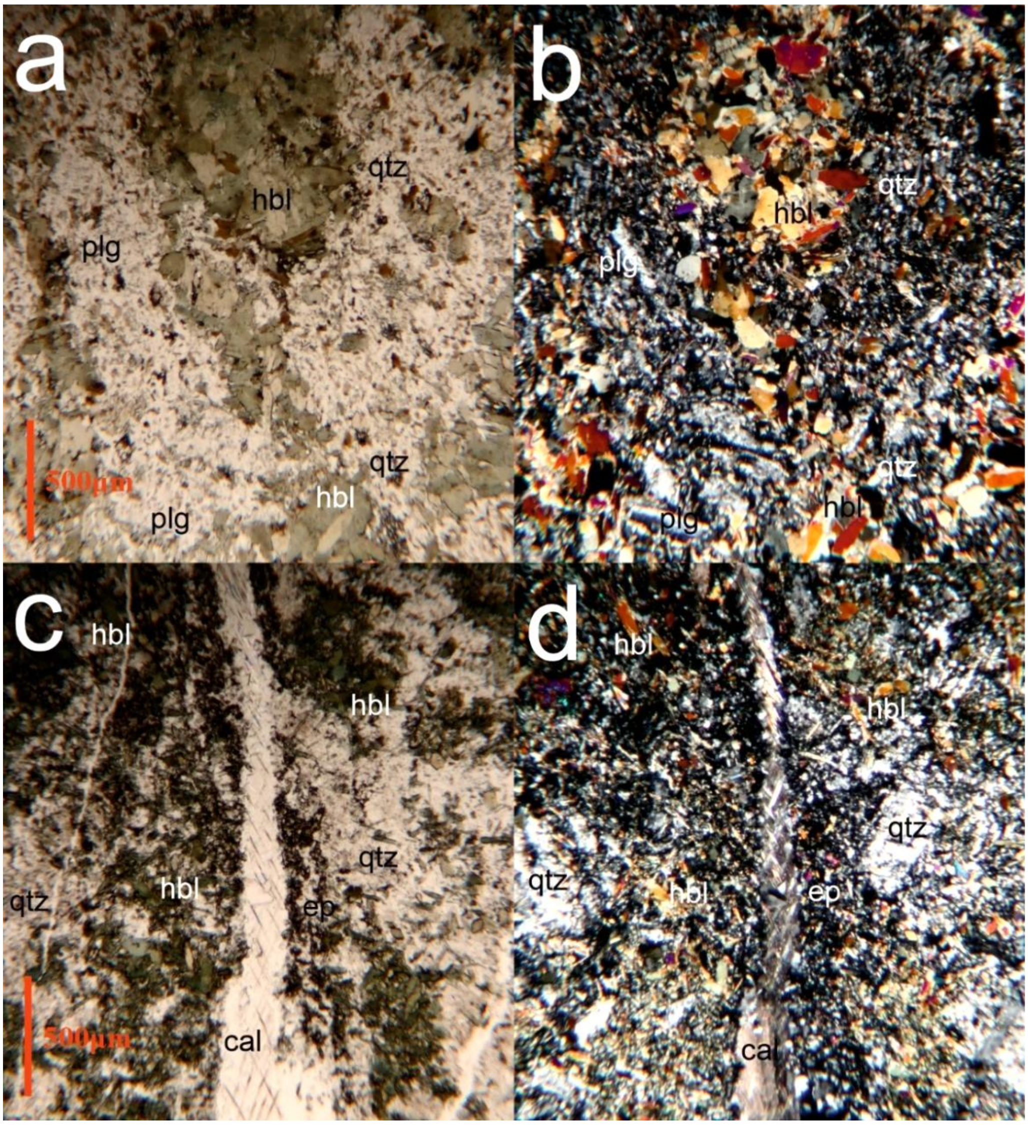

Figure 15. a) SMKI-23-54.1, hornblende-quartz-plagioclase porphyrite. Hornblende glomeroporphyres among a quartz and plagioclase groundmass. PPL. b) XPL version of the sample SMKI-23-54.1. c) MHHI-23-38.1, hornblende-quartz-epidote porphyrite. A calcite joint with typical calcite twinning cuts through groundmass of hornblende and quartz. PPL. d) XPL version of the sample MHHI-23-38.1.

The quartz-hornblende-biotite porphyrite sample, MHHI-37.2, is fine grained, ca. 0.3 mm (Figure 16a, b). Major mineral modal compositions are quartz 35 %, hornblende 25 % and biotite 25 %. Accessory mineral modal compositions are epidote 15 %, plagioclase 5 %, opaque minerals 5 % and chlorite < 1 %. Hornblende and biotite form glomeroporphyres among a microcrystalline quartz groundmass that contains only 5 % plagioclase. Quartz deformation is present and occurs throughout the sample as recrystallization.

The quartz-plagioclase-biotite porphyrite sample, MHHI-23-46.1, is microcrystalline to fine grained, ca. 0.5 – 1 mm (Figure 16c, d). Major mineral modal compositions are quartz 30 %, plagioclase 25 % and biotite 20 %. Accessory mineral modal compositions are epidote 15 %, hornblende 5 % and opaque minerals 5 %. The sample's biotite porphyrites have altered from hornblende, and further from clinopyroxene. The porphyrites formed of microcrystalline biotite grains retain euhedral shapes of the relict clinopyroxene. The opaque minerals in this sample are euhedral pyrite.

The two quartz-epidote-hornblende porphyrites, MHHI-23-2.1 and MHHI-23-43.1, are microcrystalline throughout the entire sample (Figure 16e, f). The main mineral modal compositions are quartz 30 – 40 %, epidote 25 – 30 % and hornblende 20 – 25 %. Accessory mineral compositions are plagioclase 5 – 15 %, chlorite 2 – 3 %, rutile 1 – 2 % and opaque minerals < 1 %. The samples groundmass has microcrystalline quartz, epidote and hornblende. Samples are classified as porphyrites due to relict plagioclase porphyrites being common throughout the samples and visible on PPL. Nearly all the plagioclase has altered to epidote.

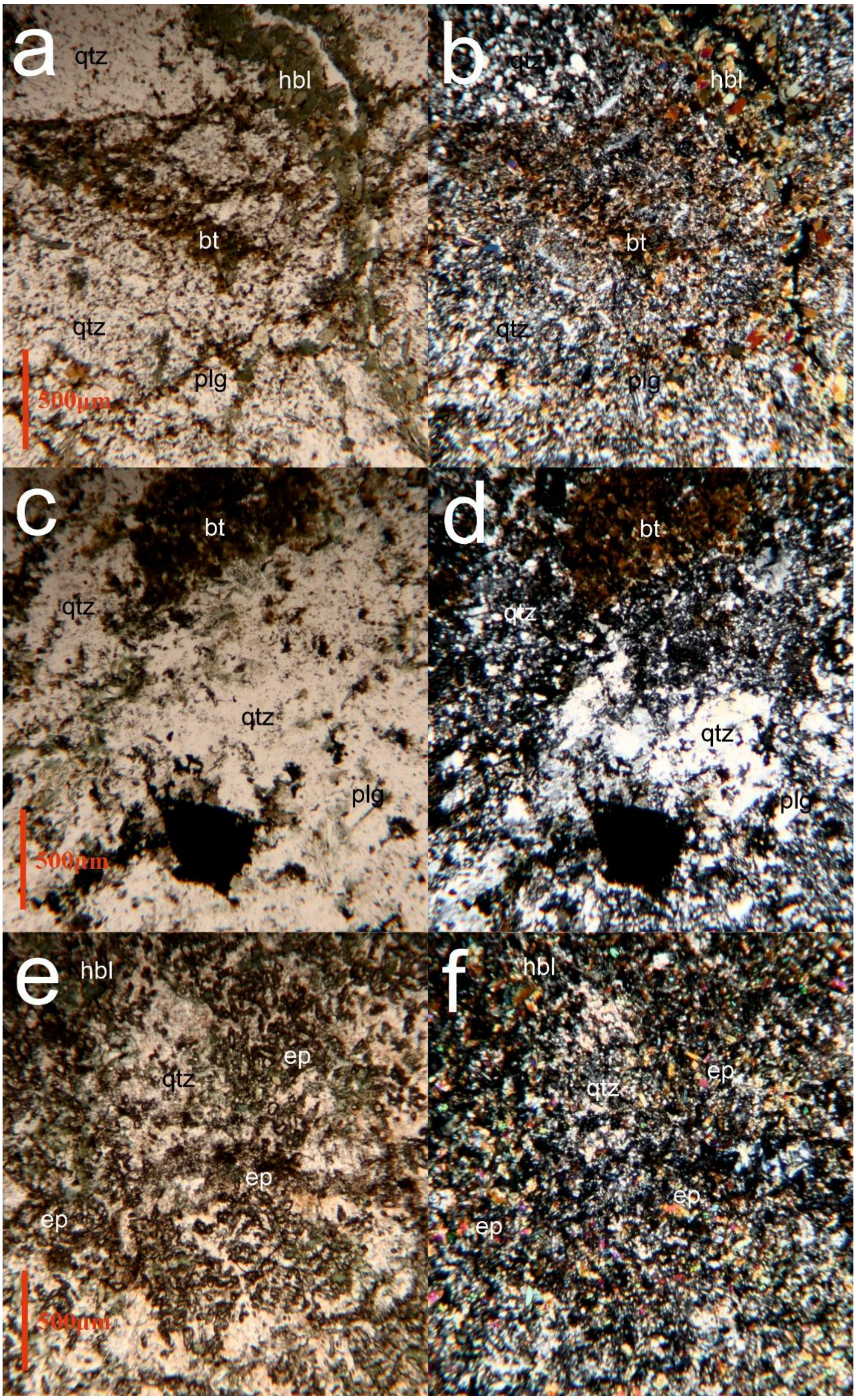

Figure 16. a) MHHI-23-37.2, quartz-hornblende-biotite porphyrite. Recrystallized quartz and biotite groundmass with hornblende bordering a quartz filled joint. PPL. b) XPL version of the sample MHHI-23-37.2. c) MHHI-23-46.1, quartz-plagioclase-biotite porphyrite. Biotite porphyrite with relict euhedral clinopyroxene porphyrite and a euhedral pyrite among a groundmass of quartz. PPL. d) XPL version of the sample MHHI-23-46.1. e) MHHI-23-2.1, quartz-epidote-hornblende porphyrite. Relict plagioclase porphyrites which have completely altered to epidote visible on PPL. PPL. f) XPL version of the sample MHHI-23-2.1.

The metavolcanic rock group contains only one sample that could not be placed in any other group due to its strong alteration. Major minerals are alkali feldspar and hornblende. Trace minerals are biotite, epidote, chlorite and opaque minerals. The alkali feldspar is an alteration product of plagioclase due to potassium metasomatism. Opaque minerals are common throughout the sample and constitute 10 % of the modal composition. The crystallisation environment of the alkali feldspar metavolcanic rock cannot be ascertained.

The alkali feldspar metavolcanic rock sample, SMKI-23-58.1, has fine grained, ca. 0.2 mm. (Figure 17a, b). Major mineral modal compositions are alkali feldspar 45 % and hornblende 20 %. Accessory mineral modal compositions are epidote 10 %, opaque minerals 10 %, biotite 5 % and chlorite 5 %. Some of the alkali feldspar occurs as microcline throughout the sample. The epidote occurs as joint filling. The chlorite only occurs by the epidote joints and has altered from hornblende due to hydrothermal alteration like the alkali feldspar.

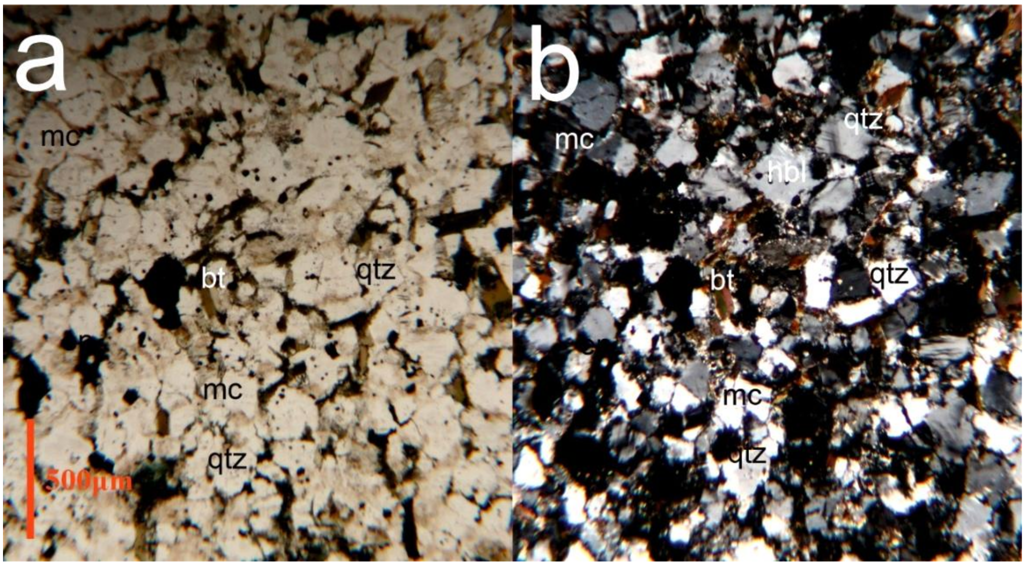

Figure 17. a) SMKI-23-58.1, alkali feldspar metavolcanic rock. Microcline visible on the top of the figure on XPL. Quartz occurs as roughly same size crystals among the microcline with biotite filling the gaps as smaller crystals. Opaque minerals occur disseminated all over the sample which is visible on PPL. PPL. b) XPL version of the sample SMKI-23-58.1.

4.2.2 Thin section descriptions of the Haapavesi granite, Vattukylä gabbro

The Haapavesi granite’s and Vattukylä gabbro’s main minerals present are quartz, alkali feldspar, plagioclase, biotite and sericite. Accessory minerals include epidote, titanite, chlorite, hornblende, calcite, ilmenite and opaque minerals. Grain sizes vary from fine to coarse, 0.2 mm-6 mm, with the two gabbro sample's groundmass being microcrystalline, < 0.2 mm, and phenocrysts varying from fine to medium, < 1 mm to 3 mm. All but one sample show deformation of quartz accompanied by indicators of shearing. Both gabbro samples have porphyritic textures. Myrmekite is present in one sample.

The three granite samples, SMKI-23-6.1; SMKI-23-30.1; SMKI-23-59.1, are fine- to coarse grained, ca. 0.1 – 5 mm (Figure 18a, b). Main mineral modal compositions are alkali feldspar 25 – 50 %, quartz 15 – 30 % and sericite 2 – 30 %. Accessory mineral modal compositions are plagioclase 4 – 15 %, biotite 0 – 10 %, hornblende 5 – 10 %, epidote 1 – 10 %, clinopyroxene 0 – 5 %, rutile 0 – 2 %, leucoxene 1 %, hematite 1 %, opaque minerals < 1 – 1 %, ilmenite < 1 %, zircon < 1 %, and apatite < 1 %. Plagioclase alters to epidote and sericite, whilst alkali feldspar alters to saussurite. Another alteration occurring is clinopyroxene to hornblende. Also, like in volcanic, ilmenite alters to leucoxene creating leucoxene rims. Majority of alkali feldspar is orthoclase with carlsbad twinning, but microcline is also abundant. Quartz deformation is present as recrystallization. Myrmekite is present along microcline.

A subtype of Haapavesi granites is leucogranite. The leucogranite sample's, SMKI-23-34.1, grain size is fine grained, ca. 0.1 – 1 mm (Figure 18c, d). Main mineral modal compositions are quartz 45 % and alkali feldspar 45 %. Accessory mineral modal compositions are biotite 5 %, epidote 2 %, plagioclase 1 %, sericite 1 % and opaque minerals 1 %. Due to quartz and alkali feldspar making up 90% of the modal composition with only 5 % biotite, the granite is considered a leucogranite. Quartz deformation is common as recrystallization and a sense of shearing is present.

The two Vattukylä gabbro samples classified as quartz gabbro, MHHI-23-34.1 and SMKI-23-25.1, are microcrystalline to medium grained, ca. < 1 – 3 mm (Figure 18e, f). Main mineral modal compositions are plagioclase 40 %, quartz 20 % and biotite 20 %. Accessory mineral modal compositions are sericite 10 – 15 %, epidote 2 – 5 %, opaque minerals 2 – 4 %, hornblende < 1 %, chlorite < 1 %, calcite < 1 % and leucoxene < 1 %. The complete lack of alkali feldspar points to a gabbroic origin. The sample also has an igneous texture ruling out volcanic origin. Quartz deformation and lineation due to shearing is observable. The quartz phenocrysts have biotite rims.

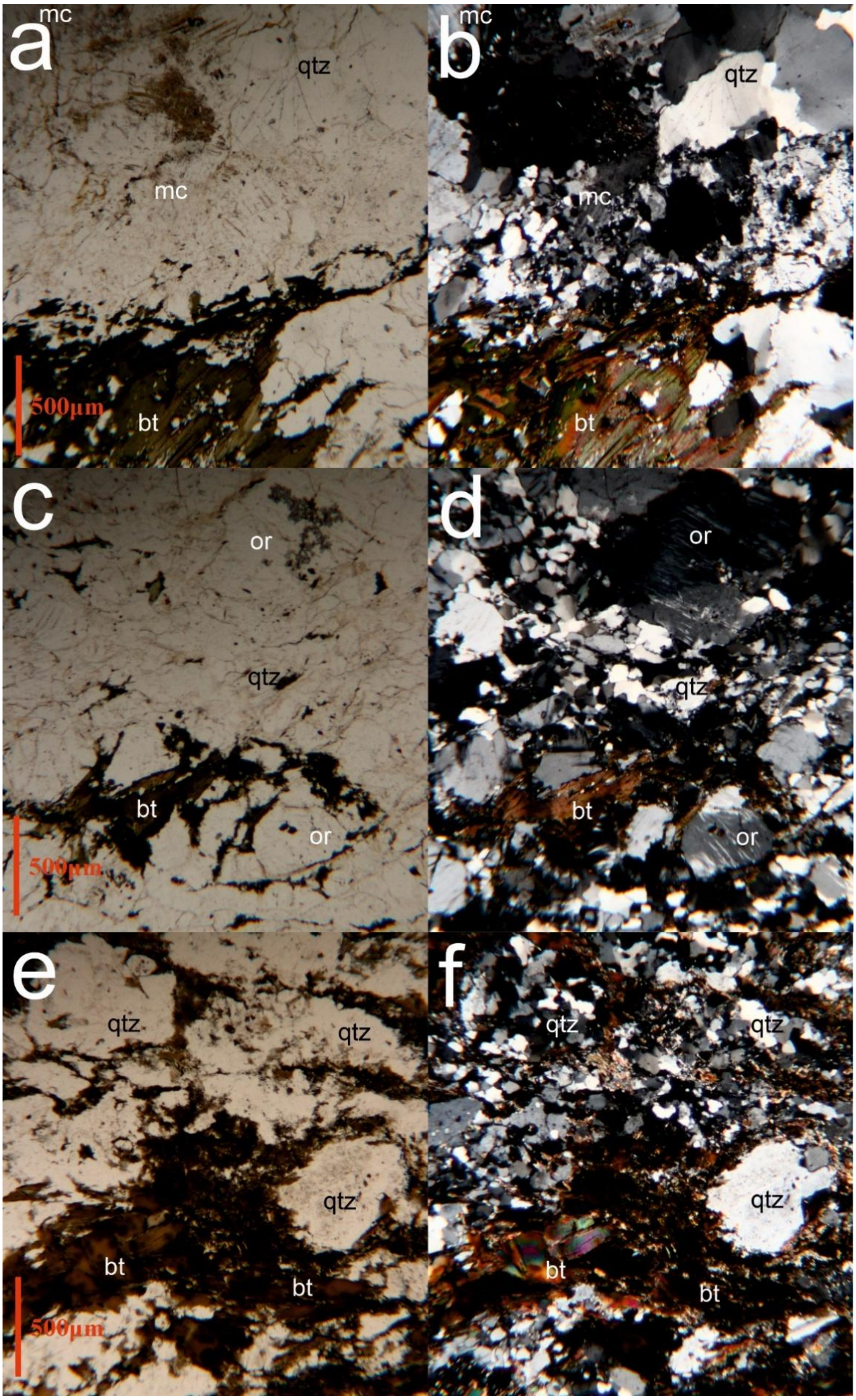

Figure 18. a) SMKI-23-59.1, granite. Microcline alkali feldspar with myrmekite is visible on XPL. Quartz deformation is also apparent. PPL. b) XPL version of the sample SMKI-23-59.1. c) SMKI-23-34.1, leucogranite. Alkali feldspar and quartz dominated leucogranite. Some accessory biotite is included. PPL. d) XPL version of the sample SMKI-23-34.1. e) SMKI-23-25.1, quartz gabbro. Recrystallized quartz biotite is pictured. PPL. f) XPL version of the sample SMKI-23-34.1.

4.2.3 Thin section descriptions of the Soutuperä granodiorite-tonalite

The Soutuperä granodiorite-tonalite's main minerals are plagioclase, quartz, alkali feldspar, biotite and hornblende. Accessory minerals are leucoxene, sericite, epidote, zircon and carbonate minerals. Alterations observed are plagioclase to sericite, ilmenite to leucoxene and hornblende to biotite. Two of the three samples are intergranular, and one is nesophitic. Other textures include quartz deformation, myrmekite in plagioclase and feldspar zoning. Grain sizes vary in from < 1 – 5 mm.

The two tonalite sample's, MHHI-23-40.1 and MHHI-23-50.1, have microcrystalline to coarse grain sizes, ca. < 1 – 5 mm (Figure 19a, b). Major mineral modal compositions are plagioclase 50 % and quartz 20 %. Accessory mineral modal compositions are biotite 10 – 15 %, hornblende 5 – 10 %, alkali feldspar 5 %, leucoxene < 1 – 2 %, sericite 1 %, zircon < 1 – 1 % and epidote < 1 %. Common alterations are plagioclase to epidote and sericite, hornblende to biotite, and ilmenite to leucoxene. The texture on both tonalites is intergranular with euhedral and subhedral plagioclase. The granodiorite sample, MHHI-23-22.1, has microcrystalline to medium gain size, ca. < 1 – 3 mm (Figure 19c, d). Major mineral modal compositions are plagioclase 40 %, quartz 20 %, hornblende 13 %, biotite 13 % and alkali feldspar 10 %. Accessory minerals modal compositions are sericite 1 %, leucoxene < 1 %, zircon < 1 %, calcite < 1 % and epidote < 1 %. The granodiorite differs from the tonalite with a larger amount of alkali feldspar, 10 % vs. 5 %. Hornblende alters to biotite, which have relict microstructures from hornblende. Quartz has some small fluid inclusions.

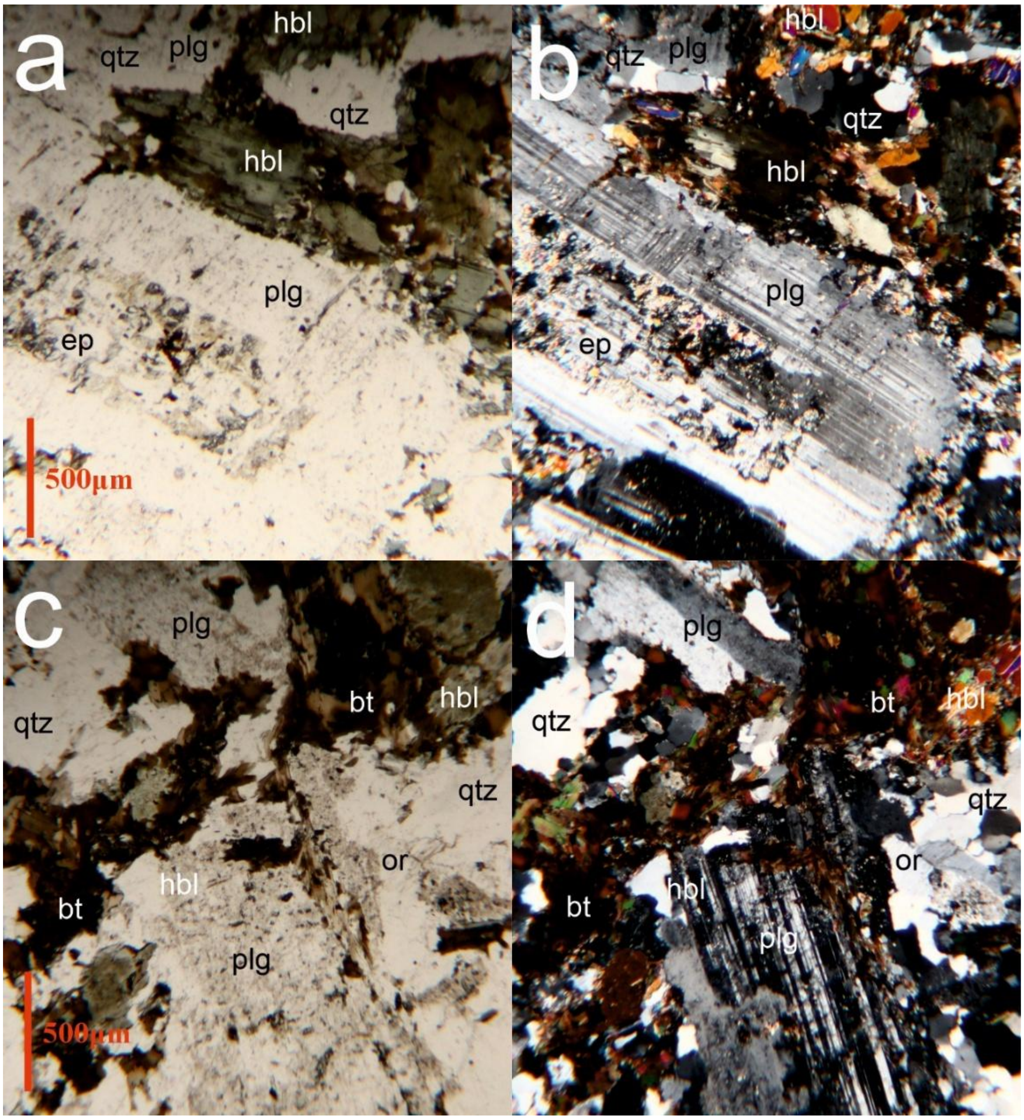

Figure 19. a) MHHI-23-40.1, tonalite. Zonal plagioclase alteration, where epidote alteration only affects the centre of the euhedral crystal. The hornblende show a glomeroporphyric texture. PPL. b) XPL version of the sample MHHI-23-40.1. c) MHHI-23-22.1, granodiorite. Euhedral to subhedral plagioclase crystals are surrounded mostly by biotite and quartz. Some orthoclase alkali feldspar is also present, which differs from the tonalite. PPL. d) XPL version of the sample MHHI-23-22.1.

4.3 Geochemistry

4.3.1 Geochemistry of the Rytkynkylä formation volcanic rocks

The RF volcanic rock data spreads to both tholeiite and calc-alkaline series on an AFM diagram, however the tholeiite series samples are consistent of only three subgroups of the mafic amphibole porphyrite group, hornblende plagioclase porphyrite; hornblende plagioclase epidote porphyrite; and plagioclase hornblende epidote porphyrite (Figure 20). The two remaining mafic amphibole porphyrite subgroups, plagioclase hornblende porphyrite and biotite plagioclase porphyrite fall into calc-alkaline series with all samples from the intermediate- and quartz porphyrite groups, and the metavolcanic group consisting of one sample. The intermediate amphibole porphyrite group plots closely together in the very centre of the calc-alkaline series, whilst the quartz amphibole porphyrite group has a wider spreading, with quartz plagioclase biotite porphyrite plotting in as most alkaline and hornblende quartz plagioclase porphyrite as most magnesian.

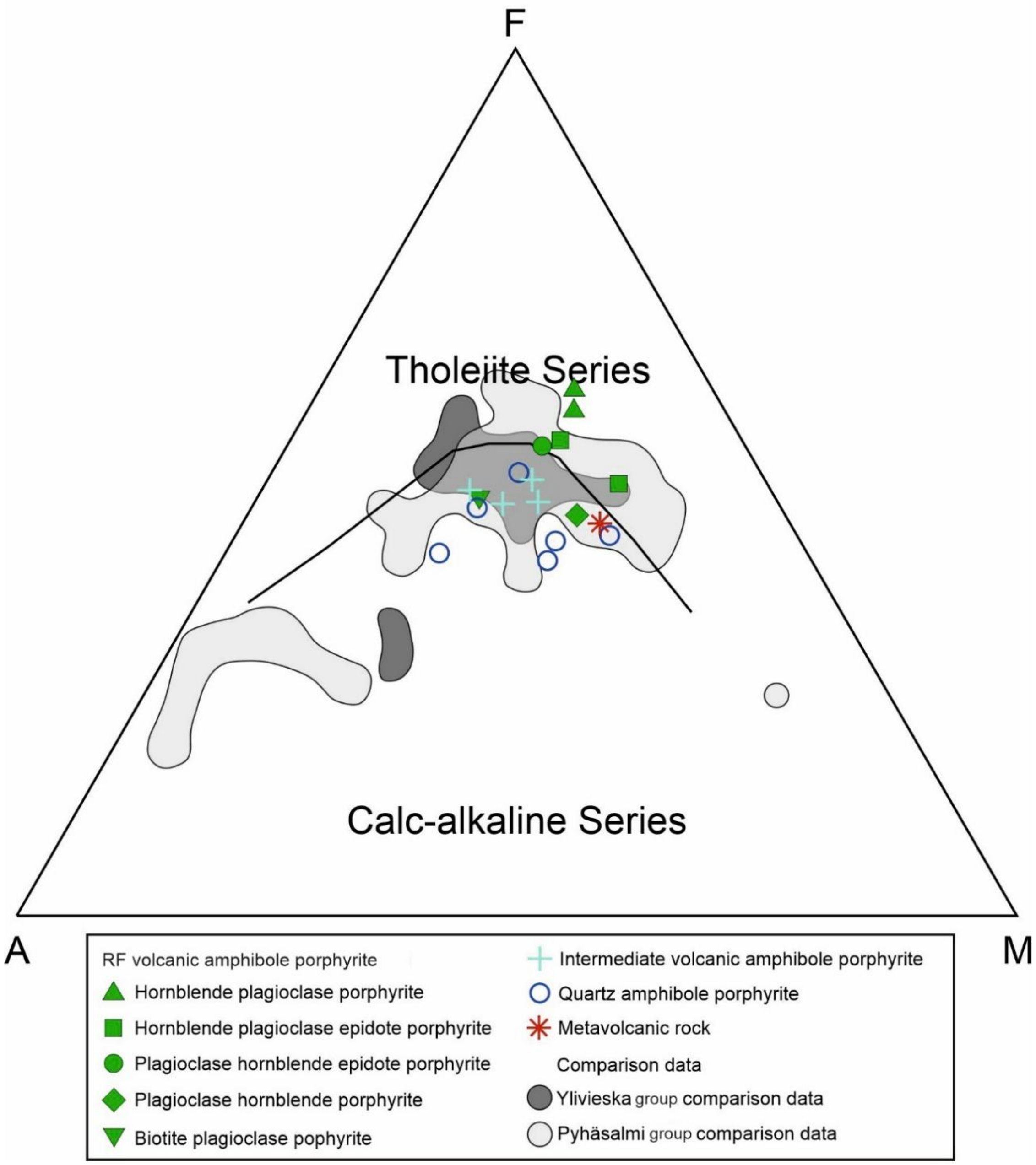

Figure 20. An Alkali-Iron-Magnesium (AFM) diagram (Irvine & Baragar 1971) to distinguish and classify the Rytkynkylä formation volcanic rock- and both comparison data (Nurmi et al. 1991; Kousa et al. 1994) samples into tholeiite- and calc-alkaline series. Ylivieska- and Pyhäsalmi group's comparison datasets are presented as grey fields. RF = Rytkynkylä formation.

On a total alkali versus silica (TAS) diagram, the RF's volcanic rock data forms a clear mafic to intermediate contingent (Figure 21). The RF mafic amphibole porphyrite group plots almost entirely on basalt and basaltic andesite, where hornblende plagioclase porphyrite subgroup plots distinctly in basalt. An exception is biotite plagioclase subgroup sample which plots in basaltic trachy-andesite. RF intermediate amphibole porphyrite plots in andesite, apart from one sample in basaltic andesite. RF quartz amphibole porphyrite group plot in both andesite and dacite fields, where the more SiO2 rich analyses plot in the dacite field. The RF metavolcanic rock group's one alkali metavolcanic rock plots in the andesite field.

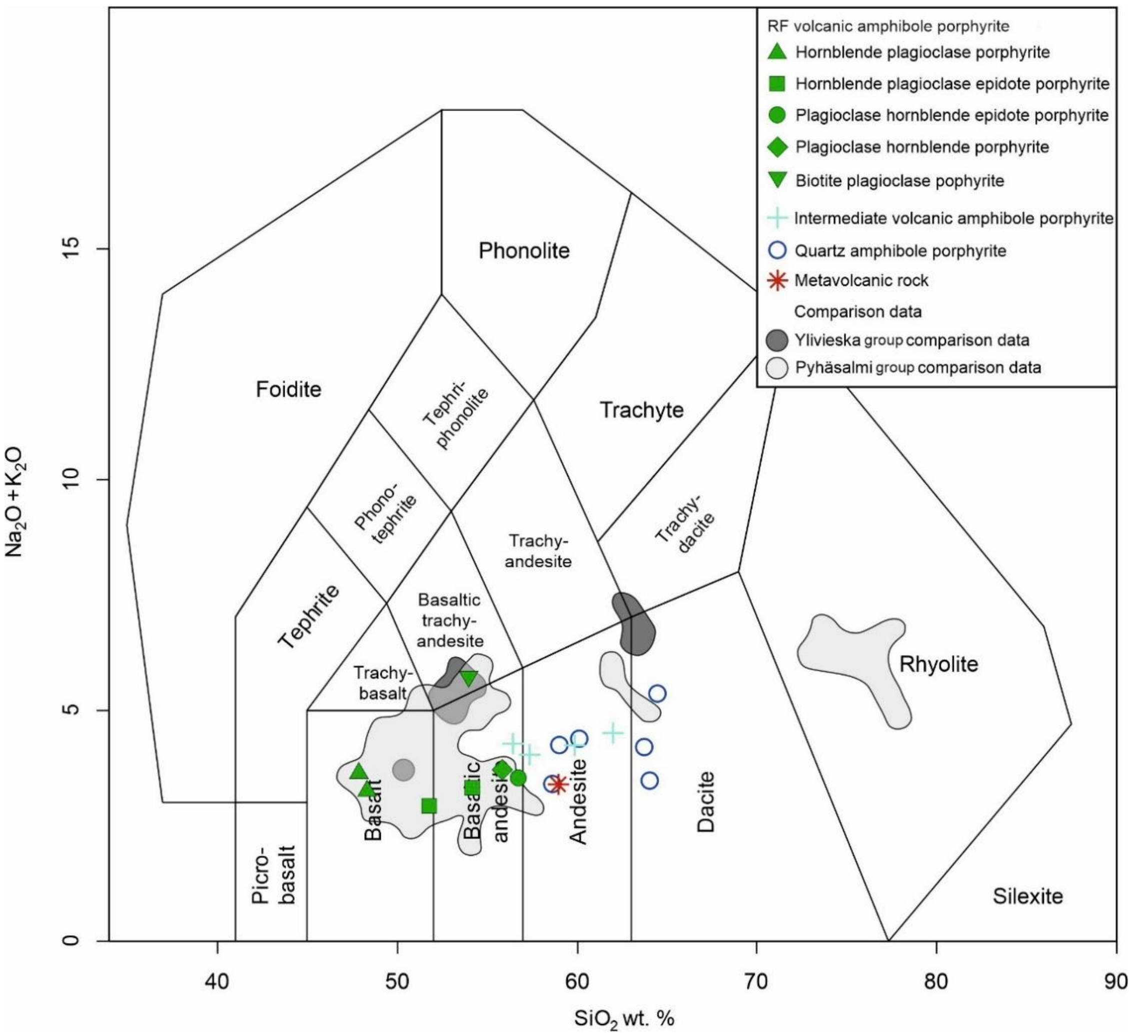

Figure 21. A total alkali versus silica (TAS) diagram (Middlemost, 1994) comparing the Rytkynkylä formation volcanic rock data to both Ylivieska- and Pyhäsalmi group's comparison datasets (Nurmi et al., 1991; Kousa et al., 1994). Ylivieska- and Pyhäsalmi group comparison datasets are presented as grey fields. RF = Rytkynkylä formation.

On major element binary plot diagrams (Figure 22), the silica (SiO_2) content of the RF volcanic rock data varies between 45 – 65 wt. %. The different groups and subgroups of the RF volcanic rocks form contingency based on the SiO_2 values. Al_2O_3-, Na_2O- and K_2O values vary respectively between 12 – 18 wt. %, 1 – 4 wt. %, and 0 – 3 wt. % (Figure 22a, d, g). All forementioned elements form a widespread plot with SiO2, where no clear contingency can be observed.

In turn, FeOt, MgO, and CaO all form negative correlations with SiO_2. FeOt (Figure 22d) varies between 6 – 14 wt. % and shows the clearest negative correlation out of all major elements. A clear distinction between the most mafic and intermediate samples can be observed. MgO (Figure 22e) and CaO (Figure 22h) vary respectively between 3 – 8 wt. % and 3 – 11 wt. %. MgO and CaO both form a negative correlation, but not to the same extent as FeOt with the biggest difference being the relatively lower concentration of both MgO and CaO in hornblende plagioclase porphyrite.

TiO_2 (Figure 22c) and P_2O_5 (Figure 22f) vary respectively between 0.5 – 2.5 wt. % and 0.1 – 0.6 wt. %. Both TiO_2 and P_2O_5 form a negative correlation with SiO_2 where all subgroups of the RF volcanic rocks form a low negative curve due to low concentrations. An exception with both TiO_2 and P_2O_5 is the hornblende plagioclase porphyrite subgroup, which shows extremely high concentrations of both elements compared to the rest of the subgroups, creating a steep curve in the negative correlation in the two diagrams.

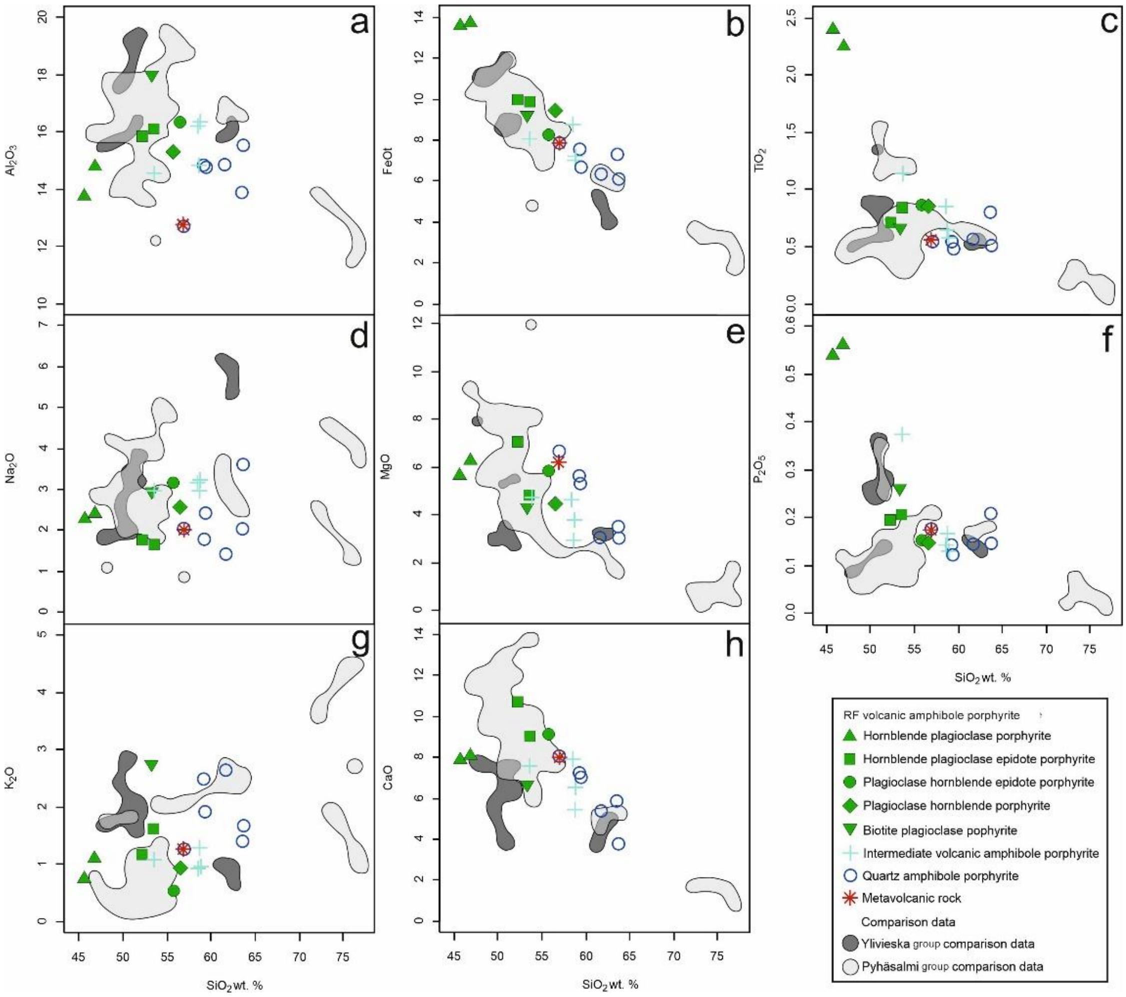

Figure 22. Major element binary plot diagrams presented as oxides. a) Al_2O_3 vs. SiO_2 wt. % b) FeOt vs. SiO_2 wt. % c) TiO_2 vs. SiO_2 wt. % d) Na_2O vs. SiO_2 wt. % e) MgO vs. SiO_2 wt. % f) P_2O_5 vs. SiO_2 wt. % g) K_2O vs. SiO_2 wt. % h) CaO vs. SiO_2 wt. %. Ylivieska- and Pyhäsalmi comparison datasets are presented as grey fields (Nurmi et al. 1991; Kousa et al. 1994). RF = Rytkynkylä formation.

On trace element binary plots, the SiO_2 content of the RF volcanic rock data is compared to trace elements Ce, La, Ba, Sr, Ni and Zr (Figure 23). The light rare earth elements (LREEs) Ce and La (Figure 24a, b) vary respectively between 7 – 53 ppm and 0 – 29 ppm and show a slight negative correlation with a widespread. To be noted is the relatively high values, 49 ppm and 28 ppm of both Ce and La in the alkali metavolcanic rock.

Large ion lithophile elements (LILEs) Ba and Sr (Figure 23c, d) do not show any correlation to SiO_2, only plotting as large shotgun spreads respectively between 215 – 1336 ppm and 125 – 651 ppm. However, like with Ce and La, the alkali metavolcanic rock sample has relatively high amounts, 1336 ppm and 536 ppm of both Ba and Sr.

Ni, both a mantle rock forming element (MRFE) and a siderophile element, forms a slight negative correlation with 1 – 61 ppm (Figure 23e). To be noted is the steep negative correlation of the Pyhäsalmi group's comparison data which reduces the visual effect of the RF volcanic rocks' negative correlation.

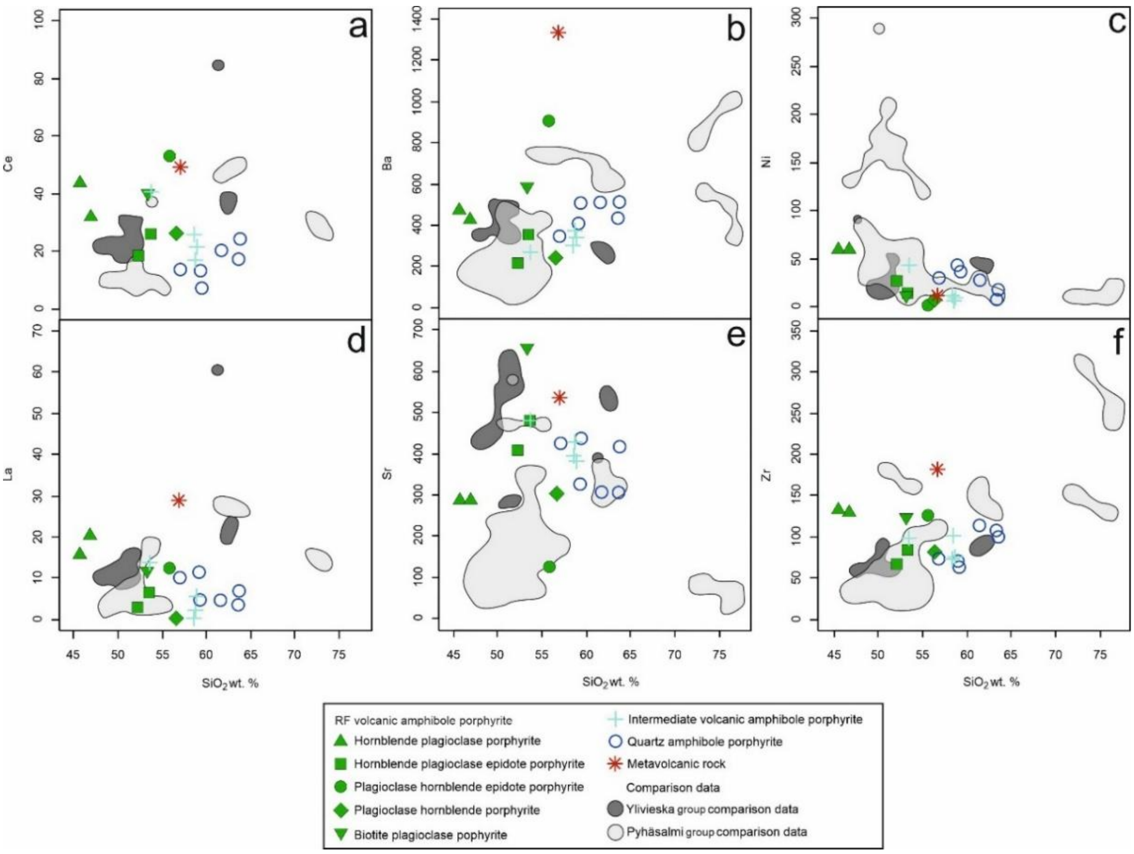

Figure 23. Trace element binary plot diagrams, a) Ce vs. SiO_2 wt. %. b) Ba vs. SiO_2 wt. %. c) Ni vs. SiO_2 wt. %. d) La vs. SiO_2 wt. %. e) Sr vs. SiO_2 wt. %. f) Zr vs. SiO_2 wt. %. Ylivieska- and Pyhäsalmi group's comparison datasets are presented as grey fields (Nurmi et al. 1991; Kousa et al. 1994). RF = Rytkynkylä formation.

On the primitive mantle spider diagram, the RF volcanic rock data follows generally the same wide pattern with some individual differences between different samples (Figure 24). All samples show clear enrichment of U and Pb, with primitive mantle normalized values 194 – 656 U_n and 91 – 254 Pb_n. La, Sm and Yb are somewhat depleted varying with different samples. La is depleted with two samples, the plagioclase hornblende porphyrite 0.35 La_n and the MHHI-23-29.1 of the plagioclase hornblende quartz porphyrite subgroup 0.59 La_n. Sm is depleted with hornblende quartz plagioclase porphyrite 0.76 Sm_n, MHHI-23-43.1 of the quartz epidote hornblende porphyrite subgroup 0.75 Sm_n and SMKI-23-52.1 of plagioclase hornblende quartz porphyrite subgroup 1.03 Sm_n. Yb is depleted in several different samples, most notably 0.1 Yb_n in

SMKI-23-52.1 of the plagioclase hornblende quartz porphyrite subgroup. The alkali metavolcanic rock subgroups' pattern differs somewhat from the rest, showing enrichment with LILEs and depletion with most ionically charged high field strength elements (HFSEs).

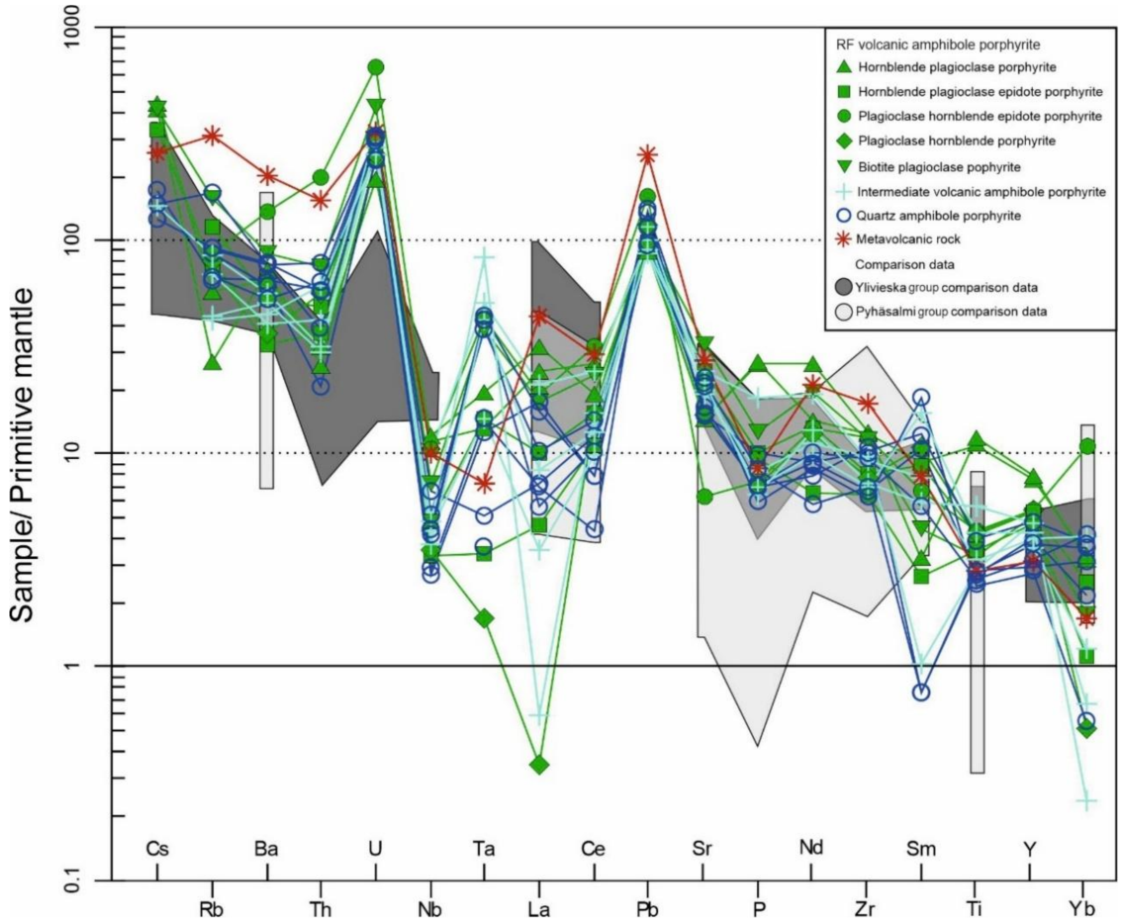

Figure 24. A Primitive mantle spider diagram with the Rytkynkylä formation volcanic rock primary data, and Ylivieska- and Pyhäsalmi group's comparison datasets (Nurmi et al. 1991; Kousa et al. 1994). The Ylivieska group's data lacks Th, U, Nb, Ta, Pb and Y values. The Pyhäsalmi group's data lacks Ta and Pb values. RF = Rytkynkylä formation.

4.3.2 Geochemistry of Haapavesi granite, Vattukylä gabbro, and Soutuperä granodiorite-tonalite

All analyses from Haapavesi granite, Vattukylä gabbro and Soutuperä granodiorite-tonalite plot clearly in the clac-alkaline field on an AFM diagram (Figure 25). Haapavesi granite and especially the leucogranite analyses plot strongly into the alkali corner, whilst both Vattukylä gabbro group's quartz gabbro-, and Soutuperä granodiorite-tonalite group's tonalite and granodiorite samples plot more into the centre of the calc-alkaline field.

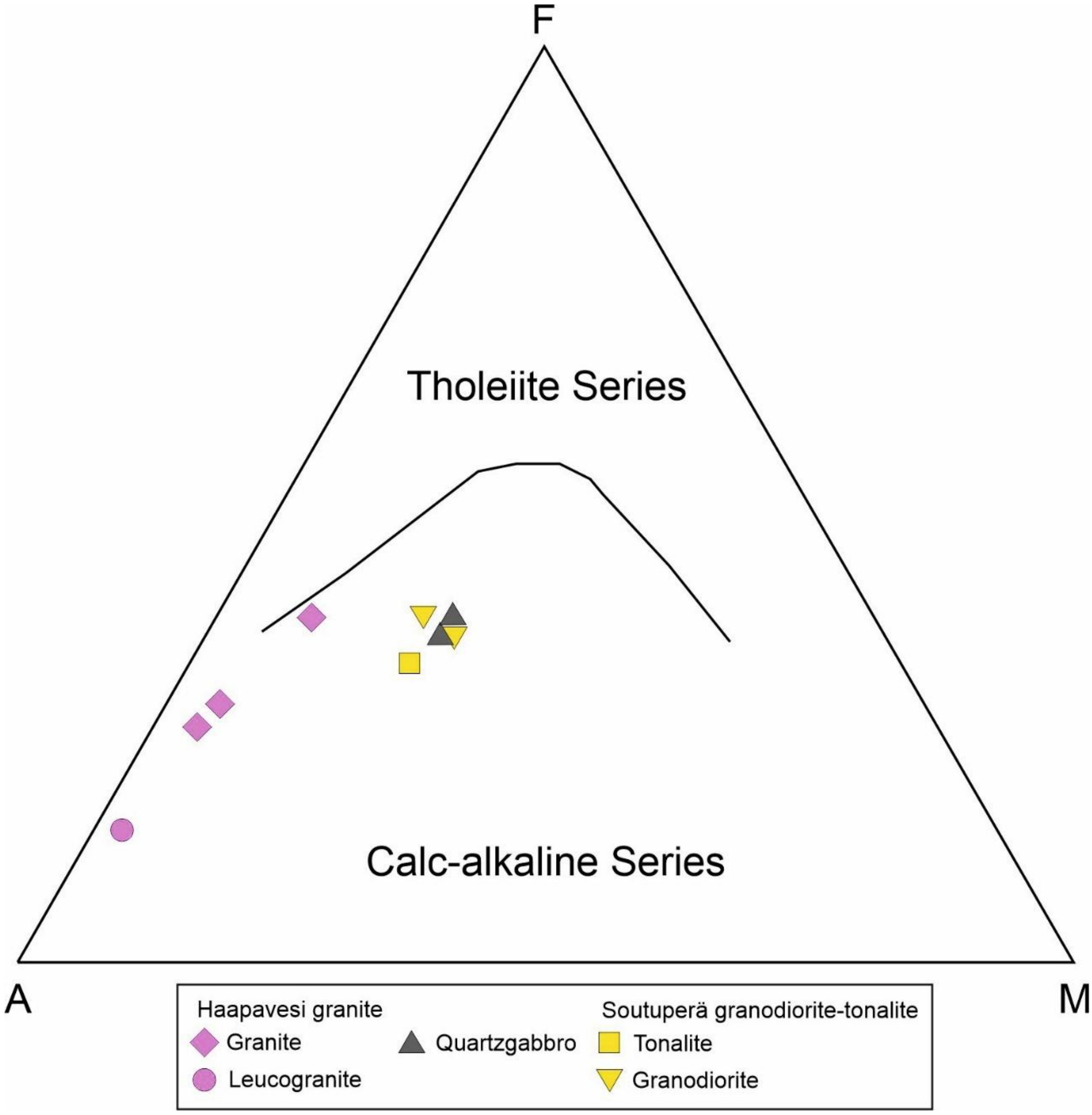

Figure 25. An AFM diagram (Irvine and Baragar 1971) with the Haapavesi granite-, Vattukylä gabbro- and Soutuperä granodiorite-tonalite group's samples.

On the TAS diagram, the Haapavesi granite group's analyses plot mostly in the granite field with one exception, a granite sample, in the quartz monzonite field. The leucogranite sample shows higher $Na_2O + K_2O$ values than the rest. The Vattukylä gabbro group's and Soutuperä granodiorite-tonalite group's samples all plot in the granodiorite field, with the quartz gabbro samples having lowest $Na_2O + K_2O$ values of all plutonic rock samples (Figure 26).

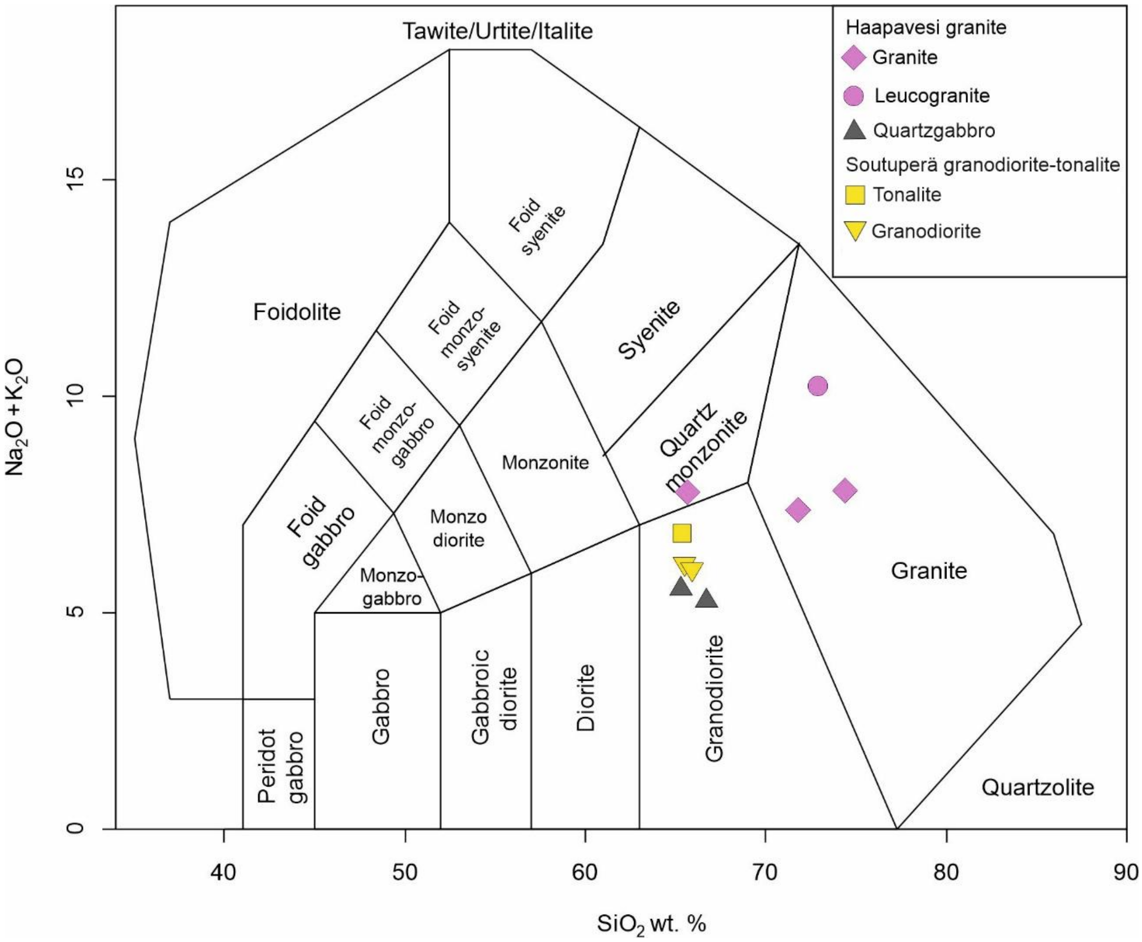

Figure 26. A TAS diagram (Middlemost 1994) with the Haapavesi granite-, Vattukylä gabbro- and Soutuperä granodiorite-tonalite group's samples.

5 Discussion

5.1 Field relationships and relative ages of the lithological units

The relative age differences in the RF study area are the following, 1. RF volcanic rocks; 2. Soutuperä granodiorite-tonalite; 3. Haapavesi granite, Vattukylä gabbro (Chapter 4.1). The relative ages have been derived from the lithological contacts and the cross-cutting relationships of the three forementioned lithological units. In addition, previous knowledge and studies observed from the region's plutonic rocks played an integral part in understanding the plutonic rock's age differences.

The RF can be considered as the oldest unit due to inclusions that can be observed in both Soutuperä granodiorite-tonalite and Haapavesi granite (Chapter 4.1). This gives a clear basis for the relative age relation between the RF and both intrusive plutonic rock units. The Soutuperä granodiorite-tonalite, as a part of the CFGC, can be considered a part of the calc-alkaline magmatism which reached its peak with the collision of the continental block from the South and the main phase of the Svecofennian orogeny in Finland, after the beginning of the Savo belt's volcanism (Figure 2d) (Mikkola et al. 2018). In addition to the known formation and its general age, the few RF inclusions and Soutuperä cross-cutting the RF volcanic rocks indicate the Soutuperä granodiorite-tonalite's relative younger age compared to the RF. Local ductile shearing induced foliation of the Soutuperä granodiorite-tonalite can be observed in all outcrops throughout the study area where the granodiorite-tonalite occurs (Chapter 4.1.3). This type of deformation is more uncommon in the Haapavesi granite, where foliation has been observed locally in fewer places. This indicates Soutuperä granodiorite-tonalite's older age compared to the Haapavesi granite, which remains mostly undeformed (Figure 7) (Chapter 4.1.2). The Haapavesi granite's contact with the RF is complex with a large scale volcanic breccia structure of the RF volcanic rocks inside the Haapavesi granite, further controlled by the RuSZ (Figure 4). This indicates a clear relative age difference where the RF is older compared to the Haapavesi granite. In some outcrops, alignment of alkali feldspar phenocrysts can be observed as following the contact with RF volcanic rock, which is yet further proof on the younger age and relative formation of Haapavesi granite to the RF (Figure 7b).

Unlike with the RF, the relative age differences of the two plutonic lithologies, Soutuperä granodiorite-tonalite and Haapavesi granite, is based just on comparing previous published data (Chapter 2.3) to the general field observations on the plutonic rocks. This is because outcrops with Soutuperä granodiorite-tonalite and Haapavesi granite were not found nor observed for data during fieldwork, and thus conclusions on the relative ages solely on field observations alone cannot be made. However, with previous knowledge that the calc-alkaline granodiorites and tonalites of CFGC are regarded as older than the geochemically A-type granites, a hypothesis on Soutuperä granodiorite-tonalite's and Haapavesi granite's relative age differences can be made (Nironen 2005). This concludes that Soutuperä granodiorite-tonalite is the second oldest unit and Haapavesi granite the youngest.

Due to lacking age determination data eg. U-Pb or other valid age determination data, this study bases the age relations of the RF, and Soutuperä granodiorite-tonalite and Haapavesi granite on field evidence of the contacts and cross-cutting relationships between the rocks, gathered during this study. Thus, this study can only procure relative ages of the lithologies, and no numerical ages. To confirm the relative age hypothesis made in this study and to gain accurate age data, an age determination study on the RF, and both Soutuperä granodiorite-tonalite and Haapavesi granite is required.

5.2 Correlation of deformation in the study area

The Vihanti-Pyhäsalmi regional deformation has been active in the RF study area in multiple phases (Chapter 2.3.1) (Laine et al. 2015; Zaher et al. 2017; Islam et al. 2025). From only a few field observations recorded around the RF study area (Figure 4), two different active deformation events can be observed and further correlated to the regional deformation stages D_3 and D_4 after Laine et al. (2015), with additional brittle deformation after D_4. D_1 and D_2 will not be discussed since they occurred prior to the formation of the Ylivieska group and the RF (Chapter 2.3.1). This is an extremely reserved interpretation and correlation of the study area's deformation due to a lack of observations. To create a solid understanding of the deformation history of the study area, a comprehensive structural study must be conducted.

The oldest regional deformation event affecting the RF, D_3, is related to the folding of RF volcanic rocks during the main phase of the Svecofennian Orogeny which can be correlated to the folding of the few primary features seen in some outcrops on the study area (Figure 6f). Only a small number of primary features were found, but the deformation seen on them may be correlated to the model after Laine et al. (2015). What changed with D_3 compared to the earlier regional deformation D_1 and D_2, is that the thrust zone which formed during D_1 and D_2 reactivated multiple times during D_3 and D_4 (Chapter 2.3.1). With regional D_3, the deformation style was not only compressional but included shearing along the reactivated RLSC. D_3 shearing of the RuSZ on the RF study area created large scale dextral en echelon structures that dominate the NE side of the RF (Figure 4). D_3 shearing likely occurred before the intrusion of the Haapavesi granite, since RF volcanic rocks and Soutuperä granodiorite-tonalite show more prominent signs of ductile deformation as foliation. (Figure 9). According to Laine et al. (2015), the cessation of the D_3 compression and following extension allowed porphyritic granites to intrude, which would correlate to the formation of the Haapavesi granite around this time. Thus in the RF study area, D_3 can be mainly presumed as dextral shearing, seen as shearing induced foliation in the RF and Soutuperä granodiorite-tonalite which had intruded by this point in time (Mikkola et al. 2018).

Regionally the D_4 was characterized by another compressional stage with a change in the direction of the stress from SW – NE to N – S that refolded D_3 folds (Laine et al. 2015). The D_4 also caused reactivation of dextral shearing along the RLSC, which would have also reactivated the RuSZ and the large en echelon structures now by both the RF and Haapavesi granite (Kärki et al. 1993). Signs of ductile or semi-ductile deformation related to D_4 are present in the Haapavesi granite as foliation near the shear zone. The ductile or semi-ductile deformation of the Haapavesi granite is also apparent due to the rounded boudinage of the granite dikes inside the RF volcanic rocks (Figure 5d). The rounding of the boudinage acting as an indicator for ductility. With this evidence in mind, it is somewhat misleading generalizing the geochemically A-type Haapavesi granite as "postkinematic" when they were affected by D_4 in at least some degree (Mikkola et al. 2018). In addition, D_4 also created a SW – NE Oulujärvi shear zone, which differs from other RLSC zones like the RuSZ by being sinistral rather than dextral (Kärki et al. 1993). Sinistral sense of deformation is also seen commonly in the RF, but with more brittle features.

Regarding the study area's younger brittle deformation, the sense of deformation changes in observed outcrops from dextral to sinistral, and most brittle faults are ca. N-S oriented rather than E-W or SE-NW, coinciding more with the direction of eg. Oulujärvi shear zone (Figure 5a) (Kärki et al. 1993). Multiple different generations of brittle sinistral deformation can be observed on most outcrops where joints filled with different minerals crosscut each other with clear age differences (Figures 5a, 9a). The sinistral sense is best seen in en echelon microstructures by brittle fractures (Figure 5b). The brittle deformation seen on the study area can be correlated with the regional brittle faulting that superseded D_4 (Laine et al. 2015).

As for hydrothermal activity, it is evident to have taken place during the D_3 and D_4 events as the unakite by the main shearing of the RuSZ points to large scale fluid activity during shearing, and all the brittle joints filled with epidote and quartz to fluid activity long afterwards (Figures 5a, 7d, 8). The unakite formed most likely after D_3 and perhaps during D_4 as Haapavesi granite which intruded along the RuSZ was exposed to voluminous amounts of fluids causing alteration to unakite. The unakite and another mineralisation along the shearing speaks for hydrothermal activity throughout the RF and explains the degree of alteration seen locally in the study area.

5.3 Geochemical comparison of Rytkynkylä formation vs. Ylivieska- and Pyhäsalmi groups

The whole-rock geochemical analysis shows that the RF volcanic rocks belong to the Ylivieska group rather than the Pyhäsalmi group, due to a clear distinction from the Pyhäsalmi group rocks' data (Figures 20 – 24). The geochemical data also gives indication that the RF formed possibly in subduction related process' during the main phase of the Svecofennian orogeny along with the rest of the Ylivieska group.

Via a detailed analysis of geochemical data, it can be concluded that the RF's and Ylivieska group's similarities on most diagrams are pronounced as they overlap and form similar positive- and negative correlations on eg. Fe-, MgO-, Ni- and Zr vs SiO_2 wt. % diagrams. On the TAS diagram (Figure 21) both RF and Ylivieska group form a very similar basalt-dacite continuation, reminiscent of a typical island arc field. The Ylivieska group is slightly more enriched with Na_2O+K_2O compared to the RF, but this can simply be regarded as a result of higher degree of alteration.

Compared to the similarities between RF and Ylivieska group, the differences between RF and Pyhäsalmi group are more pronounced and provide good evidence to the conclusion that the RF belongs to the Ylivieska group. The most evident dissimilarity to the Pyhäsalmi group is its bimodality seen on most geochemical plot diagrams (Figures 20 – 23). Based on the data RF, Ylivieska- and Pyhäsalmi group all have both tholeiitic and calc-alkaline affinities, but only the Pyhäsalmi group has a distinct evolved alkaline group (Figure 20). Seen on all plot diagrams as SiO_2 rich, the Pyhäsalmi group's felsic member is composed of evolved calc-alkaline rhyolites that stand out from the rest of the samples of all three datasets, even from the rest of the Pyhäsalmi group data (Figures 20, 21). These SiO_2 -rich samples are also enriched with Zr, indicating possible high degree differentiation or crustal melting and contamination of the melt (Watson & Harrison 1983).

What further supports the bimodality of Pyhäsalmi group is the Mg-rich end member of the tholeiitic series shown on the AFM diagram (Figure 20), and the high negative correlation of Ni vs. SiO_2 wt. %. Both Mg and Ni are indicators of mantle derived primitive mafic magmas, where Mg forms olivine and pyroxenes early in the fractionation process (Schmidt & Jagoutz 2017). Ni as a mantle rock forming element (MRFE) is highly compatible and fractionates early along the Mg-rich olivine and pyroxenes (Sato 1977). The tholeiitic data of neither RF or Ylivieska group do not show Mg enrichment of this degree, rather they show Fe enrichment which is typical for more evolved tholeiitic magma after the fractionation of Mg-rich minerals and overall depletion of Mg from the melt, typical for volcanic back arc basin related magmatism (Figure 21) (Chen et al. 2023). The Pyhäsalmi group instead has two distinct types of melts, that would erupt simultaneously as bimodal volcanism (Kousa et al. 1994).

Another noteworthy similarity between the RF and Ylivieska group is the similar enrichment of LILEs Cs, Rb, Ba, Sr and Pb (Figure 24). LILEs are fluid mobile and thus indicators of possible subduction related magmatism, which would fit well into the framework of both RF's and Ylivieska group's compositions (Figure 2c) (Zheng 2019). Taking this into consideration, it is to be noted that LILEs remain mobile post magmatism and are susceptible to hydrothermal alteration or mineralisation, even though mineralised samples were avoided in this study (Karakaya et al. 2012). This has most likely affected the metavolcanic rock sample, which shows higher LILE concentrations than all other samples (Figure 24). However, a subduction related magmatic origin should not be disregarded. More evidence to a subduction relation in RF and Ylivieska groups is the similar depletion in HFSEs Nb and Ta, common with subduction related magma (Figure 24) (Zheng 2019; Kalimenze et al. Submitted).

5.4 Assessment of Rytkynkylä formation's geotectonic formation environment

Based on all the geochemical data presented, the RF represents an intermediate calc-alkaline island arc type volcanic setting by most of the RF's volcanic rocks, accompanied by a back arc spreading environment represented by a few tholeiitic samples (Kalimenze et al. Submitted). The study area's plutonic rocks, Soutuperä granodiorite-tonalite and Haapavesi granite each intruded during mid to late phases of the Svecofennian orogeny (Lahtinen 2015; Mikkola et al. 2018).

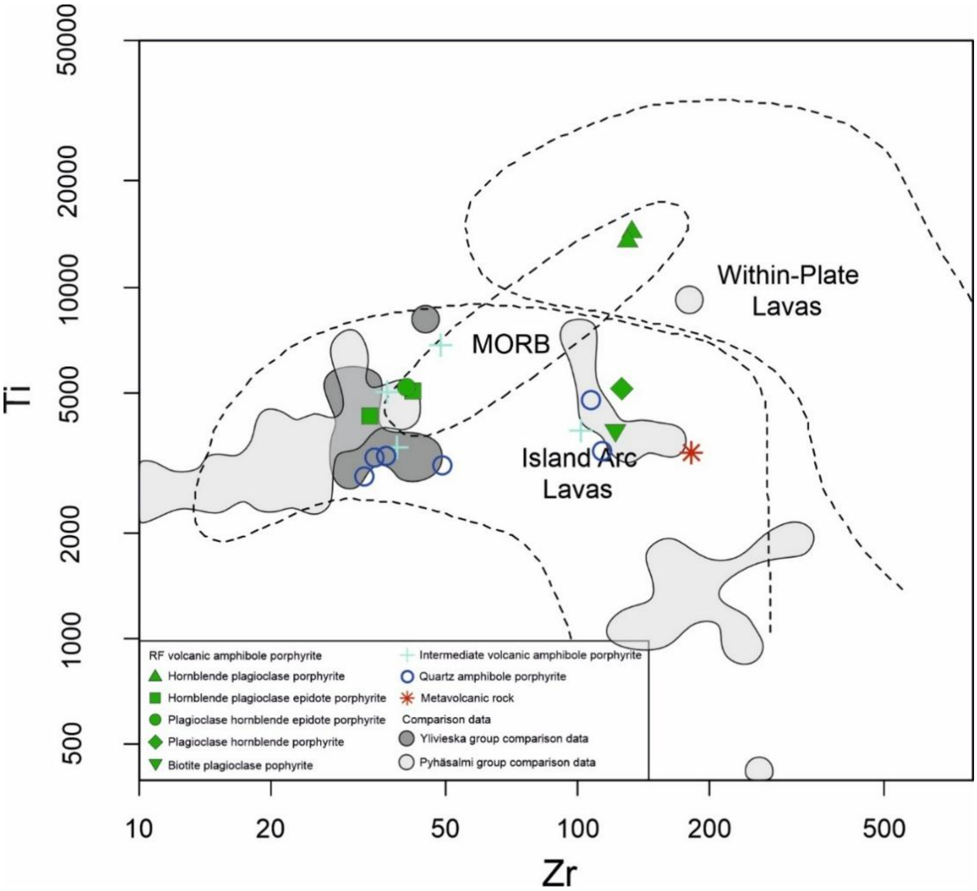

Figure 27. Zr vs. Ti geotectonic diagram (Pearce 1982) comparing the Rytkynkylä formation volcanic rock data to both Ylivieska- and Pyhäsalmi groups' data (Nurmi et al. 1991; Kousa et al. 1994). The Ylivieska- and Pyhäsalmi group comparison datasets are presented as grey fields. RF = Rytkynkylä formation.

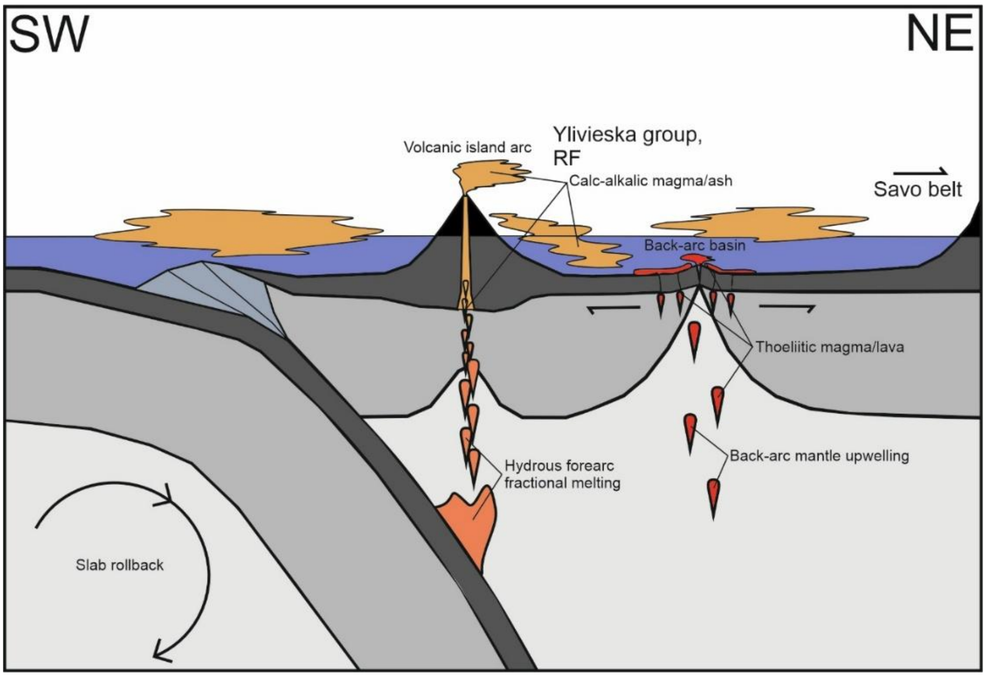

Figure 28. A figure of the formation environment of the Rytkynkylä formation, and the Ylivieska group. The proposed island arc and back-arc basin environment does not consider the formation nor the subduction model of the Savo belt and only proposes a contextual formation model for the RF's rocks. RF = Rytkynkylä formation.

The original geotectonic formation environment of the RF rocks can be assessed by using geochemical Zr vs. Ti diagram (Figure 27). Most of the samples fall onto the island arc lavas -field, except for two tholeiitic end members of the RF (Figure 20) that plot in the MORB -field and within-plate lavas -field. With the context of the RF, the samples plotting in MORB -field can be regarded rather as volcanic island back-arc spreading related lavas, than MORBs (Figure 27).

Knowing this, the RF volcanic rocks represent island arc magmatism and shallow water back-arc basin volcanism induced by intra-oceanic subduction (Figure 28). The tholeiitic rocks formed in the subduction related extensional back arc basin environment and hydrothermal volcanism (Figure 28). Evidence for this, that also supports geochemical data is the petrographical descriptions (Chapter 4.2.1). The two tholeiitic samples in mafic amphibole porphyrite group show a clear lava texture which stand out from the rest of the RF volcanic rock samples with fine grained volcanic ash textures (Figure 11). These tholeiitic samples with lava textures most likely represent either thick sills that intruded the ocean floor strata or magma chambers close to the oceanic crust, both related to extension in the back-arc basin (Figure 28). The rest of the samples with varying kinds of volcanic ash textures formed in eruptions and settled around the island arc (Figure 28). As the RF is considered a part of the Ylivieska group, the RF was most likely closely associated with the KF (Figure 1). However, through extensive dextral shearing, the RF has most likely moved at least some distance NW along the Western side of the RuSZ it's the current locale.

The Soutuperä granodiorite-tonalite most likely represents the plutonic counterpart of the calc-alkaline Ylivieska group volcanic rocks (Figure 25) (Wyllie 1984). These plutonic calc-alkaline magmas like the Soutuperä granodiorite-tonalite started magmatic intrusion during the onset of the main phase of the Svecofennian orogeny, forming most of the CFGC (Figure 2c, d) (Mikkola et al. 2018).

The felsic, geochemically A-type member Haapavesi granite most likely formed from crustal melts in the Svecofennian orogeny, heated by mantle upwelling (Figures 25, 26) (Virtanen & Heilimo 2018). Haapavesi granite is bimodal with the local mafic member being the Vattukylä gabbro (Figures 25, 26), accompanied by voluminous other gabbro intrusions thought the Haapavesi batholith (Figure 1) (Virtanen & Heilimo 2018). Both felsic and mafic members started intruding during synorogenic transtensional faulting, and further during post orogenic relaxation of the crust and subsequent extension seen regionally around the RF (Laine et al. 2015). In addition, leucogranitic portions can be observed inside the Haapavesi granite.

6 Conclusions

1. Based on the available whole-rock geochemical data, the RF volcanic rocks are a part of the Ylivieska group, rather than the Pyhäsalmi group. The similarities between the RF and the Ylivieska group, and the Pyhäsalmi group's distinctive yet differing bimodality is not present in either RF or Ylivieska group, drawing a clear conclusion on the parental group of the RF.

2. The RF formed in an island-arc volcanic environment with active subduction and back arc basin extensional spreading related volcanism. This is indicated by the rocks found in the study area being both calc-alkaline- and tholeiitic. Petrographical descriptions of the calc-alkaline- and tholeiitic sample thin sections show lava and volcanic ash textures, where the geochemically tholeiitic correspond with lava- and geochemically calc-alkaline with ash textures.

3. The relative ages of the study area's lithologies, based on lithological contacts and crosscutting observations, are as follows: 1. RF, due to being present as inclusions is both Soutuperä granodiorite-tonalite and Haapavesi granite, indicating older relative age to both plutonic rocks; 2. Soutuperä granodiorite-tonalite, based on literary sources and published data indicating calc-alkaline granodiorites and tonalites of the CFGC as older than geochemically A-type granites like Haapavesi granite (Nironen 2005; Mikkola et al. 2018); 3. Haapavesi granite, Vattukylä gabbro; for the same reason as Soutuperä granodiorite-tonalite. Vattukylä gabbro is a mafic counterpart of the bimodal Haapavesi granite and is regarded as one.

4. According to Laine et al. (2015), the region surrounding the RF has witnessed four deformation events D_1, D_2, D_3, D_4 and further brittle deformation. RF can be correlated with two of these deformation events D_3 and D_4, and the following brittle deformation. D_3 is seen on the RF as large dextral en echelon structures by the RuSZ and foliation of the RF volcanic rocks and Soutuperä granodiorite-tonalite. D_4 is reactivation of the RuSZ after the intrusion of the Haapavesi granite, seen as foliation in all three lithologies of the study area. This would somewhat misplace calling the geochemically A-type Haapavesi granite "postkinematic". Brittle deformation is seen on RF commonly as sinistral fractures of many generations.

Acknowledgements

First and foremost, I would like to express my deepest gratitude to my master's thesis supervisor Esa Heilimo from University of Turku for brilliant and persevering guidance throughout the long making of this study. Most importantly, I would like to thank the K.H. Renlund's foundation for funding. Further, I am grateful to Susanna Kirkonoja-Nummela for partnership and company during fieldwork, preparation and laboratory analysis of the study's rock samples. I also offer my thanks to laboratory technicians Sören Fröjdö from Åbo Akademi, and Arto Peltola from University of Turku for their invaluable technical assistance in whole-rock geochemistry (WD-XRF) and thin section creation respectively. Finally, I would like to thank Tuukka Mäkiranta, Ville Paalumäki, Perttu Heiskanen, Camilla Westerlund, and all other dear friends who've been supporting me during the writing process of this thesis.

References

Aho, L. 1979. Petrogenetic and geochronological studies of metavolcanic rocks and associated granitoids in the Pihtipudas area, Central Finland. *Geological Survey of Finland Bulletin* 300, 22 p.

Ahtonen, N., Hölttä, P. & Huhma, H. 2007. Intracratonic Palaeoproterozoic granitoids in northern Finland: prolonged and episodic crustal melting events revealed by Nd isotopes and U – Pb ages on zircon. *Geological Society of Finland Bulletin* 79, 143–174. https://doi.org/10.17741/bgsf/79.2.002

Bogdanova, S., Gorbatschev, R., Skridlaite, G., Soesoo, A., Taran, L. & Kurlovich, D. 2015. Trans–Baltic Palaeoproterozoic correlations towards the reconstruction of supercontinent Columbia/Nuna. *Precambrian Research* 259, 5–33. https://doi.org/10.1016/j.precamres.2014.11.023

Chen, K., Tang, M., Hu, Z. & Liu, Y. 2023. Generation of tholeiitic and calc- alkaline arc magmas and its implications for continental growth. *Geochimica et Cosmochimica Acta* 355, 173–183. https://doi.org/10.1016/j.gca.2023.07.002

Daly, J.S., Balagansky, V.V., Timmermann, M.J. & Whitehouse, M.J. 2006. The Lapland – Kola orogen: Palaeoproterozoic collision and accretion of the northern Fennoscandian lithosphere. *In:* Gee, D.G. & Stephenson, R.A. (eds.) *European Lithosphere Dynamics. Geological Society London Memoirs* 32, 579–598. https://doi.org/10.1144/GSL.MEM.2006.032.01.35

Geological survey of Finland (2026) Mineral deposits and exploration. Accessed: 29.5.2026. https://gtkdata.gtk.fi/mdae/index.html

Gorbatschev, R. & Bogdanova, S. 1993. Frontiers in the Baltic Shield. *Precambrian Research* 64, 3–21. https://doi.org/10.1016/0301-9268(93)90066-B

Hanski, E. & Huhma, H. 2005. Central Lapland greenstone belt. *In:* Lehtinen, M., Nurmi, P.A. & Rämö, O.T. (eds.) *Precambrian Geology of Finland – Key to the Evolution of the Fennoscandian Shield*, 139–194. https://doi.org/10.1016/S0166-2635(05)80005-2

Heilimo, E., Ahven, M. & Mikkola, P. 2018. Geochemical characteristics of the plutonic rock units present at the southeastern boundary of the Central Finland Granitoid Complex. *Geological Survey of Finland Bulletin* 407, 106–129. https://doi.org/10.30440/bt407.6

Huhma, H., Kousa, J. & Luukas, J. 2021. Geochronology of the Paleoproterozoic Pyhäsalmi – Vihanti district, Central Finland. *Geological Survey of Finland Open File Research Report 8/2021*, 31 p.

Hermansson, T., Stephens, M.B., Corfu, F., Page, I.M. & Andersson, J. 2008. Migratory tectonic switching, western Svecofennian orogen, central Sweden: Constraints from U/Pb zircon and titanite geochronology. *Precambrian Research* 161, 250–278. https://doi.org/10.1016/j.precamres.2007.08.008

Hölttä, P., Heilimo, E., Huhma, H., Kontinen, A., Mertanen, S., Mikkola, P., Paavola, J., Peltonen, P., Semprich, J., Slabunov, A. & Sorjonen-Ward, P. 2012. The Archaean of the Karelia Province in Finland. *Geological Survey of Finland Special Paper* 54, 21–73.

Islam, S.R., Heilimo, E. & Kuva, J. 2025. Decoding multiple ore mineral remobilization processes during polyphase deformational phases from the Precambrian Pyhäsalmi VMS deposit halo, Central Finland: new insights from mineralogy, mineral chemistry and micro-CT. *International Journal of Earth Science* 114, 727–747. https://doi.org/10.1007/s00531-025-02511-4

Kalimenze, J.D., Hirsimäki, M., Kirkonoja-Nummela, S., Ranta, E., Jansson, N.F. & Heilimo, E. Submitted. Geochemical Signature of Rytkynkylä Volcanic Sequences in Central Finland: Implications for Ore Formation and Exploration. *Ore Geology Reviews*, 54 p.

Kousa, J., Marttila, E. & Vaasjoki, M. 1994. Petrology, geochemistry and dating of Paleoproterozoic metavolcanic rocks in the Pyhäjärvi area, Central Finland. *In:* Nironen, M. & Kähkönen, Y. (eds.) *Geological Survey of Finland Special Paper 19*, 7–27.

Kousa, J. & Luukas, J. 2004. Vihannin ympäristön kallioperä- ja malmitutkimukset vuosina 1992 – 2003. *Geological Survey of Finland archive report M10.4/2004/2*, 143 p. https://tupa.gtk.fi/raportti/arkisto/m10_4_2004_2.pdf

Kousa, J. 2008. Geological Unit Report 210502. *Geological Survey of Finland*.

Kousa, J. 2021. Geological Unit Report 211106. *Geological Survey of Finland*.

Kähkönen, Y. 2005. Chapter 8 Svecofennian supracrustal rocks. *Developments in Precambrian Geology* 14, 343–405. https://doi.org/10.1016/S0166-2635(05)80009-X

Kärki, A., Laajoki, K. & Luukas, J. 1993. Major Palaeoproterozoic shear zones of the central Fennoscandian Shield. *Precambrian Research* 64, 207–223. https://doi.org/10.1016/0301-9268(93)90077-F

Lahtinen, R., Korja, A. & Nironen, M. 2005. Paleoproterozoic tectonic evolution. *In:* Lehtinen, M., Nurmi, P.A. & Rämö, O.T. (eds.) *Precambrian Geology of Finland – Key to the Evolution of the Fennoscandian Shield*, 481–532.

Lahtinen, R. 2012. Main geological features of Fennoscandia. *Geological Survey of Finland Special Paper* 53, 13–18.

Lahtinen, R., Huhma, H., Lahaye, Y., Kousa, J. & Luukas, J. 2015. Archean – Proterozoic collision boundary in central Fennoscandia: Revisited. *Precambrian Research* 261, 127–165. https://doi.org/10.1016/j.precamres.2015.02.012

Large, R., Gemmell, B., Paulick, H. & Huston, D. 2001. The Alteration Box Plot: A Simple Approach to Understanding the Relationship between Alteration Mineralogy and Lithogeochemistry Associated with Volcanic-Hosted Massive Sulfide Deposits. *Economic Geology* 96, 957–971. https://doi.org/10.2113/gsecongeo.96.5.957

Le Maitre, R.W., Streckeisen, A., Zanettin, B., Le Bas, M.J., Bonin, B. & Bateman, P. 2004. Igneous Rocks: A Classification and Glossary of Terms. *In:* Le Maitre, R.W., Streckeisen, A., Zanettin B., Le Bas, M.J., Bonin, P. & Bateman, P. (eds.) *Igneous Rocks: A Classification and Glossary of Terms*, 252 p.

Luukas, J. 2018. Geological Unit Report 2104. *Geological Survey of Finland*.

Mikkola, P., Heilimo, E., Luukas, J., Kousa, J., Aatos, S., Makkonen, H., Niemi, S., Nousiainen, M., Ahven, M., Romu, I. & Hokka, J. 2018. Geological evolution and structure along the southeastern border of the Central Finland Granitoid Complex. *Geological Survey of Finland Bulletin* 407, 5–27. https://doi.org/10.30440/bt407.1

Karakaya, M.C., Karakaya, N., Küpeli, Ş. & Yavuz, F. 2012. Mineralogy and geochemical behavior of trace elements of hydrothermal alteration types in the volcanogenic massive sulfide deposits, NE Turkey. *Ore Geology Reviews* 48, 197–224. https://doi.org/10.1016/j.oregeorev.2012.03.007

Nironen, M. 1997. The Svecofennian orogen: a tectonic model. *Precambrian Research* 86, 21–44. https://doi.org/10.1016/S0301-9268(97)00039-9

Nironen, M., Elliott, B.A. & Rämö, O.T. 2000. 1.88 – 1.87 Ga post-kinematic intrusions of the Central Finland Granitoid Complex: a shift from C-type to A-type magmatism during lithospheric convergence. *Lithos* 53, 37–58. https://doi.org/10.1016/S0024-4937(00)00007-4

Nironen, M. 2005. Chapter 10 Proterozoic orogenic granitoid rocks. *In:* M. Lehtinen, P.A. Nurmi, O.T. Rämö (eds.) *Developments in Precambrian Geology* 14, 443–479. https://doi.org/10.1016/S0166-2635(05)80011-8

Nironen, M. 2017. Bedrock of Finland at the scale 1:1 000 000 – Major stratigraphic units, metamorphism and tectonic evolution. *Geological Survey of Finland Special Paper* 60, 41–76. https://minsysfin.gtk.fi/wp-content/uploads/sp_060.pdf

Nurmi, P., Lestinen, P. & Niskavaara, H. 1991. Geochemical characteristics of mesothermal gold deposits in the Fennoscandian shield, and a comparison with selected Canadian and Australian deposits. *Geological Survey of Finland Bulletin* 351, 104 p.

Roberts M.D., Oliver N.H.S., Fairclough M.C., Hölttä P.S. & Lahtinen R. 2003. Geochemical and oxygen isotope signature of sea-floor alteration associated with a polydeformed and highly metamorphosed massive sulfide deposit, Ruostesuo, Central Finland. *Economic Geology* 98, 535–556. https://doi.org/10.2113/gsecongeo.98.3.535

Saalmann, K., Mänttäri, I., Ruffet, G. & Whitehouse, M.J. 2009. Age and tectonic framework of structurally controlled Palaeoproterozoic gold mineralization in the Häme belt of southern Finland. *Precambrian Research* 174, 53–77. https://doi.org/10.1016/j.precamres.2009.06.005

Sato, H. 1977. Nickel content of basaltic magmas: identification of primary magmas and a measure of the degree of olivine fractionation. *Lithos* 10, 113–120. https://doi.org/10.1016/0024-4937(77)90037-8

Schmidt, M.W. & Jagoutz, O. 2017. The global systematics of primitive arc melts. *Geochemistry, Geophysics, Geosystems* 18, 2817–2854. https://doi.org/10.1002/2016GC006699

Vaasjoki, M. & Sakko, M. 1988. The Evolution of the Raahe-Ladoga zone in Finland: isotopic constraints. *Geological Survey of Finland Bulletin* 343, 7–32.

Virtanen, V. & Heilimo, E. 2018. Petrology of the geochemically A-type Saarijärvi suite: evidence for bimodal magmatism. *Geological Survey of Finland Bulletin* 407, 130–150. https://doi.org/10.30440/bt407.7

Vuollo, J. & Huhma, H. 2005. Chapter 5 Paleoproterozoic mafic dikes in NE Finland. *In:* Lehtinen, M., Nurmi, P.A. & Rämö, O.T. (eds.) *Precambrian Geology of Finland – Key to the Evolution of the Fennoscandian Shield*, 195–236. https://doi.org/10.1016/S0166-2635(05)80006-4

Watson, E.B. & Harrison, T.M. 1983. Zircon saturation revisited: temperature and composition effects in a variety of crustal magma types. *Earth and Planetary Science Letters* 64, 295–304. https://doi.org/10.1016/0012-821X(83)90211-X

Wyllie, P.J. 1984. Sources of granitoid magmas at convergent plate boundaries. *Physics of the Earth and Planetary Interiors* 35, 12–18. https://doi.org/10.1016/0031-9201(84)90030-X

Zheng, Y.F. 2019. Subduction zone geochemistry. *Geoscience Frontiers* 10, 1223–1254. https://doi.org/10.1016/j.gsf.2019.02.003

Zaher, M.A., Pirttijärvi, M. & Korja, T. 2017. Geophysical Studies of the Raahe-Ladoga Shear Complex in the Iisalmi Area of Finland. *Geophysica* 52, 43–67. https://www.geophysica.fi/pdf/geophysica_2017_52_2_031_abdelzaher.pdf

Attachments

Attachment A. The total list of recorded outcrops in the study area with coordinates (ETRS-TM35FIN), sample names and initially used field naming.

no.	x	y	Sample	Field naming
1	412381	7113457	SMKI-23-1	Granite
2	412267	7113558	SMKI-23-2	Granite
3	412267	7113665	SMKI-23-3	Granite
4	413398	7113695	SMKI-23-4	Granite/Leucogranite
5	413346	7113807	SMKI-23-5	Granite
6	411549	7114654	SMKI-23-6	Granite/Leucogranite
7	411594	7114399	SMKI-23-7	Granite/Mafic Volcanic rock
8	411591	7114335	SMKI-23-8	Granite
9	413430	7113753	SMKI-23-9	Mafic Volcanic rock
10	413092	7114166	SMKI-23-10	Granite
11	413156	7113948	SMKI-23-11	Mafic Volcanic rock/Granite
12	412866	7112145	SMKI-23-12	Mafic Volcanic rock/Granite
13	412883	7112170	SMKI-23-13	Granite/Mafic Volcanic rock
14	413215	7112025	SMKI-23-14	Mafic Volcanic rock/Granite
15	413305	7112369	SMKI-23-15	Granite
16	413714	7112051	SMKI-23-16	Mafic Volcanic rock
17	413680	7111961	SMKI-23-17	Granite
18	413282	7111797	SMKI-23-18	Mafic Volcanic rock
19	413347	7111853	SMKI-23-19	Mafic Volcanic rock/Granite
20	413647	7111928	SMKI-23-20	Granite
21	413587	7111908	SMKI-23-21	Mafic Volcanic rock
22	413582	7111889	SMKI-23-22	Mafic Volcanic rock
23	415196	7111045	SMKI-23-23	Mafic Volcanic rock
24	415169	7111131	SMKI-23-24	Granite
25	415184	7111323	SMKI-23-25	Mafic Volcanic rock
26	414973	7111434	SMKI-23-26	Mafic Volcanic rock
27	411862	7114254	SMKI-23-27	Mafic Volcanic rock
28	411960	7114095	SMKI-23-28	Mafic Volcanic rock/Unakite
29	412114	7114107	SMKI-23-29	Mafic Volcanic rock
30	412169	7114249	SMKI-23-30	Granite
31	412966	7112785	SMKI-23-31	Mafic Volcanic rock
32	413080	7112677	SMKI-23-32	Mafic Volcanic rock
33	413226	7112523	SMKI-23-33	Mafic Volcanic rock/Granite
34	413145	7112831	SMKI-23-34	Mafic Volcanic rock

35	411942	7113568	SMKI-23-35	Granite/Mafic Volcanic rock
36	411811	7113559	SMKI-23-36	Mafic Volcanic rock/Granite
37	411724	7113629	SMKI-23-37	Mafic Volcanic rock
38	411891	7113841	SMKI-23-38	Mafic Volcanic rock
39	411900	7113738	SMKI-23-39	Mafic Volcanic rock
40	411296	7115044	SMKI-23-40	Mafic Volcanic rock
41	411157	7115175	SMKI-23-41	Mafic Volcanic rock
42	411048	7115464	SMKI-23-42	Mafic Volcanic rock
43	407898	7118299	SMKI-23-43	Mafic Volcanic rock
44	409696	7111859	SMKI-23-44	Mafic Volcanic rock
45	409016	7112350	SMKI-23-45	Granodiorite
46	416432	7111029	SMKI-23-46	Granite
47	409940	7113723	SMKI-23-47	Mafic Volcanic rock
48	410023	7113788	SMKI-23-48	Mafic Volcanic rock
49	410166	7113783	SMKI-23-49	Mafic Volcanic rock
50	411206	7113296	SMKI-23-50	Mafic Volcanic rock
51	415155	7109554	SMKI-23-51	Mafic Volcanic rock
52	411072	7113288	SMKI-23-52	Mafic Volcanic rock
53	411068	7113529	SMKI-23_53	Mafic Volcanic rock
54	409976	7113344	SMKI-23-54	Mafic Volcanic rock
55	410030	7113266	SMKI-23_55	Mafic Volcanic rock
56	413427	7113972	SMKI-23_56	Mafic Volcanic rock
57	412425	7113948	SMKI-23_57	Mafic Volcanic rock
58	413426	7113981	SMKI-23_58	Mafic Volcanic rock
59	416834	7112108	SMKI-23-59	Granite
60	416810	7112164	SMKI-23-60	Mafic Volcanic rock
61	416772	7112183	SMKI-23-61	Gabbro
62	410346	7112929	MHHI-2023-1	Mafic Volcanic rock
63	409964	7112979	MHHI-2023-2	Mafic Volcanic rock
64	409977	7113036	MHHI-2023-3	Mafic Volcanic rock
65	410098	7113121	MHHI-2023-4	Mafic Volcanic rock
66	410126	7113179	MHHI-2023-5	Mafic Volcanic rock
67	410061	7113268	MHHI-2023-6	Mafic Volcanic rock
68	410050	7113317	MHHI-2023-7	Mafic Volcanic rock
69	409921	7113444	MHHI-2023-8	Mafic Volcanic rock
70	413388	7113724	MHHI-2023-9	Mafic Volcanic rock
71	409943	7113732	MHHI-2023-10	Mafic Volcanic rock
72	409989	7113783	MHHI-2023-11	Mafic Volcanic rock
73	410008	7113880	MHHI-2023-12	Mafic Volcanic rock
74	410104	7113914	MHHI-2023-13	Mafic Volcanic rock

75	410215	7113984	MHHI-2023-14	Mafic Volcanic rock
76	412989	7111969	MHHI-2023-15	Mafic Volcanic rock/Granite
77	412612	7111791	MHHI-2023-16	Mafic Volcanic rock
78	412393	7111780	MHHI-2023-17	Mafic Volcanic rock
79	412416	7111686	MHHI-2023-18	Mafic Volcanic rock
80	412387	7111492	MHHI-2023-19	Mafic Volcanic rock
81	412431	7111358	MHHI-2023-20	Mafic Volcanic rock
82	412384	7111251	MHHI-2023-21	Mafic Volcanic rock
83	412492	7109919	MHHI-2023-22	Granodiorite
84	412655	7110302	MHHI-2023-23	Granodiorite
85	412202	7110616	MHHI-2023-24	Mafic Volcanic rock/Granodiorite
86	412504	7111158	MHHI-2023-25	Mafic Volcanic rock
87	412421	7111210	MHHI-2023-26	Mafic Volcanic rock
88	411914	7111084	MHHI-2023-27	Mafic Volcanic rock
89	409393	7114691	MHHI-2023-28	Granite
90	410182	7114116	MHHI-2023-29	Mafic Volcanic rock
91	409031	7112862	MHHI-2023-30	Granodiorite
92	409805	7112011	MHHI-2023-31	Granodiorite
93	414776	7110637	MHHI-2023-32	Mafic Volcanic rock
94	415010	7110825	MHHI-2023-33	Granite/Mafic Volcanic rock
95	414795	7110501	MHHI-2023-34	Mafic Volcanic rock
96	414844	7110287	MHHI-2023-35	Mafic Volcanic rock
97	411291	7112046	MHHI-2023-36	Mafic Volcanic rock
98	410199	7112602	MHHI-2023-37	Mafic Volcanic rock
99	410118	7112717	MHHI-2023-38	Mafic Volcanic rock
100	410233	7112606	MHHI-2023-39	Mafic Volcanic rock
101	409070	7112311	MHHI-2023-40	Granodiorite
102	408202	7114609	MHHI-2023-41	Granodiorite
103	416263	7108619	MHHI-2023-42	Granite
104	415229	7109463	MHHI-2023-43	Mafic Volcanic rock
105	415235	7109582	MHHI-2023-44	Mafic Volcanic rock
106	415209	7109692	MHHI-2023-45	Mafic Volcanic rock
107	415272	7109924	MHHI-2023-46	Mafic Volcanic rock
108	415168	7110008	MHHI-2023-47	Mafic Volcanic rock
109	414985	7110074	MHHI-2023-48	Mafic Volcanic rock
110	414976	7110175	MHHI-2023-49	Mafic Volcanic rock
111	414523	7107640	MHHI-2023-50	Granodiorite
112	415272	7109924	MHHI-2023-51	Volcanic rock contact
113	413404	7113695	MHHI-2023-52	Granite/Mafic Volcanic rock

Attachment B. The total list of recorded samples gathered during field work in the QA/QC order for geochemical analysis.

no.	Sample	Rock type	QA/QC
1	Stand-1	Standard	CRM-185 OREAS
2	MHHI-23-2.1	Volcanic rock	
3	Dupl-1	Volcanic rock	MHHI-23-46.1
4	MHHI-23-6.1A	Volcanic rock	
5	MHHI-23-6.1B	Volcanic rock	
6	MHHI-23-6.1C	Volcanic rock	
7	MHHI-23-6.1D	Volcanic rock	
8	MHHI-23-6.1E	Volcanic rock	
9	MHHI-23-6.1F	Volcanic rock	
10	MHHI-23-7.1	Volcanic rock	
11	MHHI-23-11.1	Volcanic rock	
12	Blank-1	Blank	Calcite
13	MHHI-23-13.1	Volcanic rock	
14	MHHI-23-16.1	Volcanic rock	
15	MHHI-23-19.1	Volcanic rock	
16	MHHI-23-21.1	Volcanic rock	
17	MHHI-23-22.1	Granodiorite	
18	MHHI-23-29.1	Volcanic rock	
19	MHHI-23-32.1	Volcanic rock	
20	Stand-2	Standard	CRM-185 OREAS
21	MHHI-23-34.1	Volcanic rock	
22	MHHI-23-36.1	Volcanic rock	
23	MHHI-23-37.2	Volcanic rock	
24	MHHI-23-38.1	Volcanic rock	
25	MHHI-23-40.1	Granodiorite	
26	MHHI-23-43.1	Volcanic rock	
27	MHHI-23-46.1	Volcanic rock	
28	Blank-2	Blank	Calcite
29	MHHI-23-50.1	Granodiorite	
30	SMKI-23-6.1	Granite	
31	SMKI-23-7.1	Granite/Volcanic rock	
32	SMKI-23-13.1	Volcanic rock	
33	Stand-3	Standard	CRM-185 OREAS
34	SMKI-23-16.1	Volcanic rock	

35	SMKI-23-18.1	Volcanic rock/Granite	
36	SMKI-23-18.2	Granite	
37	SMKI-23-18.3	Granite/Volcanic rock	
38	SMKI-23-25.1	Volcanic rock	
39	SMKI-23-27.1	Granite/Volcanic rock	
40	SMKI-23-30.1	Granite	
41	SMKI-23-34.1	Granite	
42	SMKI-23-38.1	Volcanic rock	
43	SMKI-23-47.2	Volcanic rock	
44	SMKI-23-52.1	Volcanic rock	
45	SMKI-23-54.1	Volcanic rock	
46	SMKI-23-58.1	Volcanic rock	
47	SMKI-23-59.1	Granite	
48	Dupl-2	Volcanic rock	SMKI-23.54.1
49	Stand-4	Standard	CRM-185 OREAS
50	OLK MM30A		Related to other study
51	OLK MM30C		Related to other study
52	Dupl-3	Granodiorite	MHHI-23-50.1

Attachment C. Petrographical descriptions of the studied Rytkynkylä formation's samples with coordinated (ETRS-TM35FIN).

Sample	**MHHI-23-19.1**	**MHHI-23-21.1**	**MHHI-23-32.1**
x	412387	412384	414776
y	7111492	7111251	7110637
Field naming	Mafic Volcanic rock	Mafic Volcanic rock	Mafic Volcanic rock
Lithological names	Central Volcanic rock	Central Volcanic rock	Central Volcanic rock
Grouping names	Amphibole porphyrites	Amphibole porphyrites	Amphibole porphyrites
Petrographical names	Hornblende plagioclase epidote porphyrite	Hornblende plagioclase epidote porphyrite	Hornblende plagioclase porphyrite
Mineral percentages	Hornblende 45 %, plagioclase 25 %, epidote 15 %, quartz 5 %, biotite 5 %, chlorite 3 %, opaques 2 %	Hornblende 55 %, plagioclase 30 %, epidote 10 %, quartz 2 %, opaques 3 %	Hornblende 50 %, plagioclase 30 %, chlorite 5 %, epidote 10 %, quartz 1 %, rutile 1 %, opaques 5 %
Alterations	Plag > epidote, clinopyroxene > hornblende/chlorite	Plag > epidote, clinopyroxene > hornblende	Plag > sericite/epidote, clinopyroxene > hornblende
Textures	Porphyritic, Intergranular, Zoned plagioclase, Glomeroporphyric	Porphyritic, Intergranular, Trachytic, Glomeroporphyric, zoned plagioclase	Ophitic, glomeroporphyric, porphyritic, altered, zoned plagioclase
Grain size (diameter)	Groundmass: < 0.1 mm Phenocrysts: ca. < 1 – 1 mm	Groundmass: < 0.1mm Phenocrysts: ca. < 1 – 3 mm	Groundmass: < 0.1 mm Phenocrysts: < 1 – 3 mm

Sample	**SMKI-23-38.1**	**MHHI-23-36.1**	**MHHI-23-16.1**
x	411891	411291	412612
y	7113841	7112046	7111791
Field naming	Mafic Volcanic rock	Mafic Volcanic rock	Mafic Volcanic rock
Lithological names	Central Volcanic rock	Central Volcanic rock	Central Volcanic rock
Grouping names	Amphibole porphyrites	Amphibole porphyrites	Amphibole porphyrites
Petrographical names	Hornblende plagioclase porphyrite	Biotite plagioclase pophyrite	Plagioclase hornblende epidote porphyrite
Mineral percentages	Hornblende 45 %, plagioclase 40 %, chlorite 5 %, epidote < 1 %, opaque 10 %	Biotite 50 %, plagioclase 30 %, epidote 5 %, hornblende 5 %, quartz 10 %	Plagioclase 40 %, hornblende 30 %, epidote 20 %, chlorite 5 %, rutile 1 %, quartz 2 %, opaques 2 %
Alterations	Plag > sericite/epidote, clinopyroxene > hornblende/uralite	Plag > sericite/epidote, clinopyroxene > hornblende > biotite	Plag > epidote, clinopyroxene > hornblende/chlorite

Textures	Ophitic, glomeroporphyric, porphyritic, altered, sheared	Porphyritic, Intergranular, trachytic, geroplomorphyric	Porphyritic, Intergranular, semi trachytic, Glomeroporphyric
Grain size (diameter)	ca. 2 mm	Groundmass: < 0.1 mm Phenocrysts: < 1 – 1 mm	Groundmass: < 0.1 mm Phenocrysts: ca. < 1 – 2 mm
Sample	**MHHI-23-7.1**	**SMKI-23-52.1**	**MHHI-23-29.1**
x	410050	411072	410182
y	7113317	7113288	7114116
Field naming	Mafic Volcanic rock	Mafic Volcanic rock	Mafic Volcanic rock
Lithological names	Central Volcanic rock	Central Volcanic rock	Central Volcanic rock
Grouping names	Amphibole porphyrites	Sheared amphibole porphyrites	Sheared amphibole porphyrites
Petrographical names	Plagioclase hornblende porphyrite	Plagioclase hornblende quartz porphyrite	Plagioclase hornblende quartz porphyrite
Mineral percentages	Plagioclase 40 %, hornblende 40 %, opaque 5 % quartz 5 %, leucoxene 2 %, epidote 2 %, biotite 5 %, leucoxene 1 %	Plagioclase 40 %, hornblende 25 %, quartz 15 %, biotite 10 %, rutile 3 %, chlorite 1 %, hematite 1 %, epidote 5 %, opaque < 1 %	Plagioclase 45 %, hornblende 35 %, quartz 20 %, epidote < 1 %, opaques 1 %
Alterations	Clinopyroxene > Hornblende/quartz > biotite, plag > epidote, opaque > titanite	Plag >sericite/epidote, clinopyroxene > uralite/hornblende > biotite	Plag > epidote, clinopyroxene > hornblende/uralite
Textures	Quartz deformation, uralite with Q inclusions, shearing with en echelon filled w opaques	Porphyritic, Intergranular, glomeroporphyric, zoned plagioclase	Porphyritic, Intergranular, Glomeroporphyric
Grain size (diameter)	> 1 mm – 2 mm	Groundmass: 0.1 mm Phenocrysts: < 1 – 2 mm	Groundmass: > 0.1 mm Phenocrysts: 1 – 4 mm
Sample	**MHHI-23-13.1**	**SMKI-23-47.2**	**MHHI-23-38.1**
x	410104	409940	410118
y	7113914	7113723	7112717
Field naming	Mafic Volcanic rock	Mafic Volcanic rock	Mafic Volcanic rock
Lithological names	Central Volcanic rock	Central Volcanic rock	Central Volcanic rock
Grouping names	Sheared amphibole porphyrites	Sheared amphibole porphyrites	Quartz amphibole porphyrites
Petrographical names	Plagioclase hornblende quartz porphyrite	Plagioclase hornblende quartz porphyrite	Hornblende quartz epidote porphyrite

Mineral percentages	Plagioclase 45 %, hornblende 30 %, quartz 20 %, epidote 2 %, sericite 2 %, opaque 2 %, rutile 2 %	Plagioclase 40 %, hornblende 20 %, quartz 20 %, epidote 5 %, biotite 1 %, rutile 5 %, leucoxene 5 %, hematite 1 %, opaque 5 %	Hornblende 40 %, quartz 25 %, epidote 20 %, plagioclase 5 % chlorite 5 %, calcite 5 %, biotite 5 %
Alterations	Plag > sericite/epidote, clinopyroxene > uralite/hornblende	Plag > sericite/epidote, clinopyroxene > hornblende > biotite	Plag > epidote, clinopyroxene > hornblende/chlorite
Textures	Porphyritic, Intergranular, glomeroporphyric	Porphyritic, trachytic, geroplomorphyric	Porphyritic, Subophitic, Zoned plagioclase, Glomeroporphyric
Grain size (diameter)	Groundmass: > 0.1 mm Phenocrysts: 1 – 3 mm	Groundmass: < 0.1 mm Phenocrysts: < 1 mm – 1 mm	Groundmass: < 0.1 mm Phenocrysts: ca. < 1 – 1 mm

Sample	**SMKI-23-54.1**	**MHHI-23-37.2**	**MHHI-23-46.1**
x	409976	410199	415272
y	7113344	7112602	7109924
Field naming	Mafic Volcanic rock	Mafic Volcanic rock	Mafic Volcanic rock
Lithological names	Central Volcanic rock	Central Volcanic rock	Central Volcanic rock
Grouping names	Quartz amphibole porphyrites	Quartz amphibole porphyrites	Quartz amphibole porphyrites
Petrographical names	Hornblende quartz plagioclase porphyrite	Quartz hornblende biotite porphyrite	Quartz plagioclase biotite porphyrite
Mineral percentages	Hornblende 45 %, quartz 25 %, plagioclase 25 %, biotite 5 %, epidote < 1 %	Quartz 35 %, hornblende 25 %, biotite 25 %, epidote 15 %, plagioclase 5 %, opaque 5 %, chlorite < 1 %	Quartz 30 %, plagioclase 25 %, biotite 20 %, epidote 15 %, hornblende 5 %, opaques 5 %
Alterations	Plag > sericite/epidote, clinopyroxene > uralite/hornblende > biotite		Plag > epidote, hornblende > biotite
Textures	Porphyritic, Intergranular, glomeroporphyric	Quartz deformation	Quartz deformation,
Grain size (diameter)	Groundmass: < 0.1 mm Phenocrysts: 1 – 3 mm	> 1 mm – 1 mm	Groundmass: < 0.1 mm Porphyrite: 1 – 3 mm

Sample	**MHHI-23-2.1**	**MHHI-23-43.1**	**SMKI-23-58.1**
x	409964	415229	413426
y	7112979	7109463	7113981
Field naming	Mafic Volcanic rock	Mafic Volcanic rock	Mafic Volcanic rock
Lithological names	Central Volcanic rock	Central Volcanic rock	Central Volcanic rock

Grouping names	Quartz amphibole porphyrites	Quartz amphibole porphyrites	Meta Volcanic rock
Petrographical names	Quartz epidote hornblende meta volcanic rock	Quartz epidote hornblende meta volcanic rock	Alkalifeldspar meta volcanic rock
Mineral percentages	Quartz 30 %, epidote 25 %, hornblende 25 %, plagioclase 15 %, chlorite 2 %, rutile 2 %, opaques 1 %	Quartz 40 %, epidote 30 %, hornblende 20 %, plagioclase 5 % chlorite 3 %, rutile 1 %, opaque 1 %	Alkali feldspar 45 %, hornblende 20 %, biotite 5 %, epidote 10 %, chlorite 5 %, opaques 10 %
Alterations	Plag > epidote, clinopyroxene > hornblende	Plag > sericite/epidote	Feldspar > sericite, biotite > chlorite
Textures	Intergranular, Zoned plagioclase, geroplomorphyric	Porphyritic, Intergranular, trachytic, geroplomorphyric	Epidote joints,
Grain size (diameter)	< 0.1 mm	Groundmass: < 0.1 mm Phenocrysts: 1 – 4 mm	> 1 mm

Sample	**MHHI-23.40.1**	**MHHI-23-50.1**	**MHHI-23-22.1**
x	409070	414523	412492
y	7112311	7107640	7109919
Field naming	Granodiorite	Granodiorite	Granodiorite
Lithological names	Southern plutonic	Southern plutonic	Southern plutonic
Grouping names			
Petrographical names	Tonalite	Tonalite	Granodiorite
Mineral percentages	Plagioclase 50 %, quartz 20 %, alkali feldspar 5 %, biotite 10 %, hornblende 10 %, zircon < 1 %, leucoxene < 1 %, sericite 1 %, epidote < 1 %	Plagioclase 50 %, quartz 20 %, alkali feldspar 5 %, hornblende 5 %, biotite 15 %, leucoxene 2 %, sericite 1 %, zircon 1 %, carbonates 2 %	Plagioclase 40 %, quartz 20 %, alkali feldspar 10 %, hornblende 13 %, biotite 13 %, leucoxene < 1 %, sericite 1 %, zircon < 1 %, carbonate < 1 %, epidote < 1 %
Alterations	Plag > sericite, ilmenite > titanite, hornblende > biotite	Plag > sericite, ilmenite > titanite, hornblende > biotite	Plag > sericite, ilmenite > titanite, hornblende > biotite
Textures	Intergranular, myrmekite, zoned feldspars, quartz deformation	Intergranular, quartz deformation	Nesophitic, quartz deformation
Grain size (diameter)	< 1 mm – 5 mm	< 1 mm – 3 mm	< 1 mm – 3 mm

Sample	**MHHI-23-34.1**	**SMKI-23-25.1**	**SMKI-23-6.1**
x	414795	415184	411549
y	7110501	7111323	7114654
Field naming	Mafic Volcanic rock	Mafic Volcanic rock	Granite/Leucogranite

Lithological names	Northern plutonic	Northern plutonic	Northern plutonic
Grouping names			
Petrographical names	Quartz gabbroid	Quartz gabbroid	Granite
Mineral percentages	Plagioclase 40 %, biotite 20 %, quartz 20 %, sericite 10 %, chlorite 1 %, leucoxene < 1 %, epidote 5 %, calcite < 1 %, opaques 4 %	Plagioclase 40 %, biotite 20 %, quartz 20 %, sericite 15 %, hornblende 1 %, epidote 2 %, opaques 2 %	Quartz 30 %, sericite 30 %, epidote 10 %, alkali feldspar 25 % plagioclase 4 %, opaques 1 %
Alterations	Plag > sericite/epidote, hornblende > biotite	Plag > sericite/epidote, hornblende > biotite	Plag > epidote/sericite
Textures	Porphyritic, Intergranular, trachytic	Sheared, porphyritic, quartz deformation	Quartz deformation
Grain size (diameter)	Groundmass: < 0.1 mm Phenocrysts: ca. 2 – 3 mm	Groundmass: < 0.1 mm Phenocrysts: ca. < 1 – 2 mm	< 1 mm – 3 mm

Sample	**SMKI-23.59.1**	**SMKI-23-30.1**	**SMKI-23-34.1**
x	416834	409031	413145
y	7112108	7112862	7112831
Field naming	Granite	Granite	Mafic Volcanic rock
Lithological names	Northern plutonic	Northern plutonic	Northern plutonic
Grouping names			
Petrographical names	Granite	Granite	Leucogranite
Mineral percentages	Alkali feldspar 40 %, quartz 30 %, plagioclase 5 % biotite 10 %, hornblende 5 %, leucoxene 1 %, ilmenite < 1 %, epidote 2 %, sericite 2 %, zircon < 1 %, opaques < 1 %	Alkali feldspar 50 %, quartz 15 %, plagioclase 15 %, hornblende 10 %, clinopyroxene 5 %, rutile 2 %, epidote 1 %, apatite < 1 %, zircon < 1 %, hematite 1 %, opaques 1 %	Quartz 45 %, alkali feldspar 45 %, plagioclase 1 %, biotite 5 %, epidote 2 %, sericite 1 % opaques 1 %
Alterations	Sericite, saussurite, ilmenite > titanite,	Clinopyroxene > hornblende, plagioclase > sericite,	Plagioclase > epidote/sericite
Textures	Myrmekite, quartz deformation	Quartz deformation and strain, microcline, myrmekite	Quartz deformation, shearing
Grain size (diameter)	< 1 mm – > 5 mm	< 1 mm – 10 mm	< 1 mm – 1 mm

Attachment D. Geochemical data of the Rytkynkylä formation used in this study. Oxides are given as weight percentages (wt. %) and trace element data as parts per million (ppm). Values below detection limit are marked (b.d.l.).

Sample	**SMKI-23-59.1**	**SMKI-23-58.1**	**SMKI-23-54.1**	**SMKI-23-52.1**	**SMKI-23-47.2**
Petrographical name	Granite	Alkalifeldspar meta volcanic rock	Hornblende quartz plagioclase porphyrite	Plagioclase hornblende quartz porphyrite	Plagioclase hornblende quartz porphyrite
AI	57.11	42.67	43.92	33.60	35.73
CCPI	31.78	81.93	82.27	71.52	77.26
Al_2O_3	12.40	12.78	12.72	14.82	14.54
CaO	1.22	8.04	8.10	5.43	7.59
Fe_2O_3	3.15	8.73	8.73	7.77	8.94
K_2O	4.93	1.27	1.27	1.29	1.07
MgO	0.47	6.22	6.68	2.96	4.79
MnO	0.04	0.16	0.16	0.12	0.13
Na_2O	2.83	2.03	2.05	2.98	2.97
P_2O_5	0.07	0.18	0.17	0.17	0.37
SiO_2	73.90	56.97	57.07	58.75	53.66
TiO_2	0.38	0.56	0.55	0.65	1.14
Ag	3.36	2.12	b.d.l.	0.97	b.d.l.
As	10.35	12.57	10.35	24.02	48.83
Ba	506.83	1336.07	349.49	375.77	268.93
Cd	11.82	11.24	6.88	9.24	10.58
Ce	174.58	49.33	13.32	16.65	40.54
Cl	22.48	b.d.l.	305.67	497.59	178.37
Co	3.92	13.88	25.24	13.96	18.05
Cr	9.51	34.83	431.86	47.00	208.99
Cs	2.22	5.48	3.62	3.03	b.d.l.
Cu	5.85	9.75	20.93	53.95	70.75
Hf	10.56	5.71	4.71	4.44	2.61
La	86.48	28.90	10.22	2.31	13.79
Mo	3.06	0.01	b.d.l.	b.d.l.	1.08
Nb	15.54	6.58	2.93	2.85	6.62
Nd	84.66	26.39	7.29	13.83	23.63
Ni	3.52	11.20	30.31	5.57	42.84
Pb	30.66	38.11	14.09	17.29	15.13
Rb	130.53	187.45	40.80	50.79	41.94
S	17.59	9.81	26.39	21.50	1329.96

Sc	6.28	16.46	40.61	24.65	30.17
Sm	19.07	b.d.l.	b.d.l.	0.42	3.12
Sn	15.27	12.25	12.31	13.46	18.07
Sr	91.73	536.25	424.69	428.67	480.57
Ta	1.85	b.d.l.	1.63	0.54	1.89
Th	12.61	12.33	5.17	2.54	3.41
U	6.55	6.49	6.28	5.73	6.44
V	16.61	160.35	169.32	146.91	201.60
W	2.32	1.97	1.45	2.87	4.17
Y	48.52	13.41	16.07	20.15	18.24
Yb	6.61	0.75	1.58	0.10	b.d.l.
Zn	85.67	73.45	113.88	103.33	89.54
Zr	346.07	182.40	73.19	101.69	98.31

Sample	**SMKI-23-38.1**	**SMKI-23-34.1**	**SMKI-23-30.1**	**SMKI-23-25.1**	**SMKI-23-6.1**
Petrographical name	Hornblende quartz epidote porphyrite	Leucogranite	Granite	Quartz gabbroid	Granite
AI	38.68	76.86	52.45	39.79	39.54
CCPI	87.15	18.64	48.96	59.54	35.40
Al_2O_3	13.78	13.54	15.95	16.20	13.67
CaO	7.95	0.36	1.90	3.47	2.30
Fe_2O_3	15.18	1.94	6.04	5.11	3.36
K_2O	0.77	7.85	4.39	1.83	3.40
MgO	5.70	0.34	1.32	2.83	0.56
MnO	0.20	0.02	0.06	0.06	0.04
Na_2O	2.31	2.10	3.28	3.57	3.75
P_2O_5	0.54	0.03	0.21	0.13	0.09
SiO_2	45.72	70.98	64.63	63.35	69.71
TiO_2	2.39	0.21	0.76	0.53	0.31
Ag	1.70	5.11	10.96	0.29	1.45
As	19.84	8.72	13.35	12.26	14.14
Ba	473.95	919.40	1564.41	862.01	967.17
Cd	4.72	12.05	14.43	8.07	8.08
Ce	44.00	49.02	41.13	80.45	42.78
Cl	b.d.l.	b.d.l.	b.d.l.	b.d.l.	b.d.l.
Co	39.36	1.85	5.54	10.44	4.25
Cr	102.02	5.94	12.99	236.71	11.94
Cs	b.d.l.	1.49	b.d.l.	7.78	b.d.l.

Cu	43.42	0.09	15.66	7.41	8.25
Hf	3.43	7.75	11.67	5.89	7.48
La	15.80	17.27	22.98	42.05	15.94
Mo	0.49	0.32	1.18	b.d.l.	b.d.l.
Nb	7.50	7.44	16.85	7.91	4.16
Nd	33.07	26.24	29.15	35.41	16.03
Ni	60.86	1.85	4.20	6.28	3.12
Pb	13.43	32.09	20.32	25.02	18.46
Rb	16.29	152.25	84.08	79.94	81.42
S	350.24	8.20	6.51	211.14	6.49
Sc	40.35	5.21	22.46	16.19	7.16
Sm	b.d.l.	b.d.l.	1.62	6.88	5.03
Sn	8.50	14.68	15.39	12.57	12.60
Sr	289.86	113.07	226.81	550.80	292.20
Ta	0.48	2.76	1.64	1.24	b.d.l.
Th	2.09	14.52	3.87	17.27	5.78
U	4.88	4.61	4.58	7.22	5.60
V	217.21	6.28	37.41	80.39	30.58
W	3.98	0.64	1.72	1.27	b.d.l.
Y	33.89	10.63	27.56	19.92	11.85
Yb	b.d.l.	3.26	2.13	1.56	3.72
Zn	154.59	25.99	110.73	68.84	39.84
Zr	133.32	286.62	516.00	217.43	227.83

Sample	**MHHI-23-50.1**	**MHHI-23-46.1**	**MHHI-23-43.1**	**MHHI-23-40.1**	**MHHI-23-38.1**
Petrographical name	Tonalite	Quartz plagioclase biotite porphyrite	Quartz epidote hornblende meta volcanic rock	Tonalite	Hornblende quartz epidote porphyrite
AI	50.25	39.02	45.55	44.99	43.41
CCPI	60.56	65.03	71.21	59.04	74.77
Al_2O_3	13.80	15.51	14.85	14.49	14.76
CaO	3.93	3.80	5.36	4.35	7.00
Fe_2O_3	5.67	6.78	7.02	5.78	7.45
K_2O	3.25	1.67	2.64	3.11	1.89
MgO	3.41	3.09	3.04	2.74	5.34
MnO	0.08	0.12	0.14	0.09	0.15
Na_2O	2.66	3.63	1.43	2.80	2.42
P_2O_5	0.14	0.15	0.14	0.12	0.12

SiO_2	63.95	63.75	61.70	65.30	59.43
TiO_2	0.65	0.52	0.57	0.59	0.48
Ag	4.01	2.47	0.86	0.59	b.d.l.
As	21.93	12.24	9.12	9.64	5.89
Ba	564.44	515.29	510.52	594.57	508.36
Cd	8.53	9.96	7.34	11.66	3.33
Ce	41.11	23.89	20.18	58.77	7.34
Cl	149.14	b.d.l.	b.d.l.	419.59	41.31
Co	16.09	17.10	19.39	14.69	24.56
Cr	164.83	104.49	145.35	64.97	229.26
Cs	2.10	2.65	3.12	5.66	b.d.l.
Cu	24.77	15.27	19.68	25.93	b.d.l.
Hf	7.83	6.48	5.16	6.65	4.40
La	18.14	6.68	4.68	25.86	4.56
Mo	1.50	b.d.l.	b.d.l.	1.95	b.d.l.
Nb	7.42	3.40	4.43	6.31	1.88
Nd	21.09	12.56	9.95	27.15	10.61
Ni	33.49	17.67	26.69	12.55	36.50
Pb	27.32	17.21	17.50	31.92	20.50
Rb	130.22	55.22	100.69	120.67	54.57
S	37.17	562.53	9.27	135.28	28.30
Sc	22.26	24.88	22.27	23.89	35.38
Sm	7.34	2.31	0.31	b.d.l.	7.44
Sn	15.08	11.73	11.95	13.00	10.73
Sr	275.06	415.78	306.57	259.22	436.74
Ta	0.68	1.41	b.d.l.	1.05	0.53
Th	10.93	4.74	6.31	11.92	3.06
U	7.38	6.03	6.06	7.16	5.98
V	114.72	113.42	147.15	112.32	136.86
W	1.02	1.37	2.34	2.90	1.68
Y	20.08	13.58	17.33	22.03	11.78
Yb	2.75	1.85	0.95	2.10	b.d.l.
Zn	88.14	105.52	96.89	93.31	74.03
Zr	168.35	98.53	113.73	234.34	65.23

Sample	MHHI-23-37.2	MHHI-23-36.1	MHHI-23-34.1	MHHI-23-32.1	MHHI-23-29.1
Petrographical name	Quartz hornblende biotite porphyrite	Biotite plagioclase porphyrite	Quartz gabbroid	Hornblende plagioclase porphyrite	Plagioclase hornblende quartz porphyrite
AI	38.13	42.37	44.28	41.24	33.44
CCPI	77.18	71.92	61.92	85.88	77.70
Al_2O_3	13.89	17.93	14.64	14.83	16.19
CaO	5.93	6.60	3.79	8.12	7.91
Fe_2O_3	8.08	10.17	5.50	15.31	9.73
K_2O	1.40	2.72	2.34	1.11	0.95
MgO	3.51	4.27	2.93	6.30	4.62
MnO	0.15	0.11	0.06	0.20	0.17
Na_2O	2.03	2.92	2.84	2.44	3.17
P_2O_5	0.21	0.26	0.10	0.56	0.14
SiO_2	63.63	53.35	65.65	46.93	58.58
TiO_2	0.80	0.65	0.51	2.26	0.85
Ag	b.d.l.	b.d.l.	1.56	b.d.l.	4.68
As	9.31	9.88	30.62	33.10	9.20
Ba	431.85	578.21	382.11	430.99	300.14
Cd	4.04	7.34	10.15	8.64	15.25
Ce	17.45	39.32	25.03	32.01	25.90
Cl	477.31	1066.58	b.d.l.	b.d.l.	709.99
Co	12.46	13.34	15.10	37.92	20.47
Cr	53.86	86.16	91.06	84.66	70.49
Cs	b.d.l.	8.77	1.82	b.d.l.	b.d.l.
Cu	35.39	1.96	115.51	44.19	28.32
Hf	4.17	6.79	4.59	4.95	3.23
La	3.70	11.44	8.62	20.53	b.d.l.
Mo	1.04	0.37	0.55	0.89	0.33
Nb	2.82	4.79	5.47	7.98	3.14
Nd	11.26	24.34	15.25	17.91	12.23
Ni	6.95	10.19	24.26	60.30	11.36
Pb	20.34	15.57	23.04	13.90	12.98
Rb	40.15	95.48	120.00	35.03	25.37
S	1554.85	40.58	70.27	551.31	153.44
Sc	28.18	30.05	18.06	38.84	38.88
Sm	5.04	b.d.l.	10.44	3.66	6.25
Sn	11.46	12.51	11.59	10.54	15.39
Sr	305.35	651.48	267.16	288.42	394.37

Ta	1.60	1.43	1.79	b.d.l.	3.11
Th	4.68	6.01	11.19	2.56	4.94
U	4.99	8.52	7.77	3.87	5.10
V	153.26	127.50	95.33	199.12	240.02
W	2.25	0.06	1.54	2.64	1.85
Y	20.71	22.09	17.54	32.66	17.14
Yb	1.69	0.77	1.97	b.d.l.	1.79
Zn	157.00	65.51	65.56	152.16	89.63
Zr	107.02	121.99	134.81	130.21	73.15

Sample	**MHHI-23-22.1**	**MHHI-23-21.1**	**MHHI-23-19.1**	**MHHI-23-16.1**	**MHHI-23-13.1**
Petrographical name	Granodiorite	Hornblende plagioclase epidote porphyrite	Hornblende plagioclase epidote porphyrite	Plagioclase hornblende epidote porphyrite	Plagioclase hornblende quartz porphyrite
AI	51.36	39.74	37.61	34.98	32.73
CCPI	55.15	86.03	82.89	80.93	73.90
Al_2O_3	15.31	15.84	16.11	16.33	16.33
CaO	3.67	10.70	9.04	7.40	6.53
Fe_2O_3	5.37	11.06	10.98	10.51	8.01
K_2O	3.91	1.17	1.62	0.94	0.95
MgO	3.08	7.05	4.83	4.44	3.79
MnO	0.09	0.19	0.18	0.17	0.13
Na_2O	2.96	1.77	1.65	2.59	3.22
P_2O_5	0.11	0.20	0.21	0.15	0.13
SiO_2	65.70	52.27	53.60	56.61	58.90
TiO_2	0.54	0.71	0.84	0.86	0.58
Ag	2.77	b.d.l.	5.11	b.d.l.	0.60
As	16.51	9.89	9.61	8.05	9.61
Ba	555.29	214.79	351.44	244.98	338.31
Cd	9.60	8.72	13.25	6.59	7.04
Ce	52.69	18.47	25.95	26.14	21.34
Cl	199.72	152.67	199.67	113.36	470.19
Co	15.14	31.25	22.85	20.94	17.93
Cr	102.59	231.71	119.31	77.12	50.87
Cs	4.48	b.d.l.	b.d.l.	b.d.l.	b.d.l.
Cu	19.35	5.34	54.90	13.56	19.61
Hf	8.81	4.41	7.93	4.76	4.30
La	26.06	2.98	6.60	0.23	5.43
Mo	1.76	0.07	1.03	0.23	b.d.l.

Nb	7.04	2.20	3.19	2.30	2.45
Nd	26.85	8.23	16.96	15.58	16.04
Ni	31.49	27.47	14.58	6.66	9.53
Pb	27.31	14.68	17.88	17.67	13.61
Rb	157.84	45.46	70.15	48.10	26.43
S	63.41	18.32	82.00	20.90	28.39
Sc	16.76	52.34	47.77	42.71	32.59
Sm	6.31	1.08	3.54	4.40	2.41
Sn	15.63	10.90	10.88	8.93	10.92
Sr	270.51	407.65	480.57	302.03	381.02
Ta	1.22	b.d.l.	0.54	0.06	1.58
Th	13.54	2.94	3.92	4.52	2.41
U	9.64	5.43	6.01	5.11	5.56
V	93.93	252.55	240.55	241.71	209.90
W	0.94	1.18	2.11	2.34	2.99
Y	19.93	20.42	22.78	23.37	15.42
Yb	2.79	0.49	b.d.l.	0.23	0.54
Zn	75.37	117.78	122.41	95.80	105.21
Zr	152.43	67.11	84.04	81.75	75.53

Sample	**MHHI-23-7.1**	**MHHI-23-2.1**
Petrographical name	Plagioclase hornblende porphyrite	Quartz epidote hornblende meta volcanic rock
AI	34.20	47.25
CCPI	80.19	76.65
Al_2O_3	15.29	14.83
CaO	9.14	7.25
Fe_2O_3	9.16	8.37
K_2O	0.54	2.47
MgO	5.85	5.62
MnO	0.17	0.17
Na_2O	3.16	1.79
P_2O_5	0.15	0.14
SiO_2	55.82	59.26
TiO_2	0.87	0.55
Ag	1.88	1.32
As	1203.88	16.70
Ba	905.80	404.01

Cd	9.13	7.34
Ce	52.90	13.18
Cl	b.d.l.	63.49
Co	2.95	25.02
Cr	8.73	412.99
Cs	b.d.l.	b.d.l.
Cu	26.37	0.19
Hf	6.50	2.77
La	12.35	11.34
Mo	1.56	b.d.l.
Nb	6.95	1.78
Nd	16.57	11.27
Ni	1.46	43.00
Pb	23.97	14.73
Rb	52.15	52.79
S	666.86	16.02
Sc	6.53	33.79
Sm	2.70	4.31
Sn	12.97	14.02
Sr	125.03	326.17
Ta	1.59	0.47
Th	15.70	1.65
U	13.13	4.86
V	5.12	132.35
W	0.59	2.69
Y	23.30	12.60
Yb	4.78	b.d.l.
Zn	12.85	117.38
Zr	125.89	69.50

Attachment E. Geochemical comparison data of Ylivieska- and Pyhäsalmi groups (Nurmi et al. 1991; Kousa et al. 1994). Oxides are given as weight percentages (wt. %) and trace element data as parts per million (ppm). Unavailable data are marked as not analyzed (n.a.).

Group	**Ylivieska**	**Ylivieska**	**Ylivieska**	**Ylivieska**
Sample	**Antinoja1**	**Antinoja2**	**Antinoja3**	**Vesiperä1**
Lithology	**Intermediate plag-horn porphyrite**	**Intermediate plag-horn porphyrite**	**Intermediate plag-horn porphyrite**	**Intermediate plag porphyrite**
AI	26.82	29.55	28.41	33.12
CCPI	53.64	56.16	55.13	72.38
Al_2O_3	16.00	15.80	16.40	19.20
CaO	4.83	3.75	4.95	7.44
Fe_2O_3	4.42	5.91	4.63	9.44
K_2O	0.70	0.95	0.97	1.77
MgO	3.24	3.21	3.11	3.48
MnO	0.07	0.06	0.07	0.15
Na_2O	5.92	6.17	5.33	3.16
P_2O_5	0.13	0.15	0.14	0.25
SiO_2	62.60	61.30	62.40	50.80
TiO_2	0.53	0.51	0.56	0.86
Ag	0.08	0.21	0.03	0.20
As	7.90	80.00	99.00	390.00
Ba	249.00	291.00	263.00	347.00
Cd	0.20	0.20	0.20	0.20
Ce	37.50	84.50	35.70	19.90
Cl	143.00	132.00	87.00	149.00
Co	10.00	8.00	7.00	13.00
Cr	110.00	64.00	87.00	36.00
Cs	1.00	3.00	3.00	3.00
Cu	286.00	819.00	101.00	152.00
Hf	2.10	2.50	2.60	1.50
La	22.50	60.40	20.30	9.60
Mo	1.00	38.00	1.00	1.00
Nb	12.00	13.00	12.00	12.00
Nd	13.90	22.10	15.60	12.40
Ni	44.00	46.00	40.00	21.00
Pb	2.00	2.00	2.00	2.00
Rb	26.00	41.00	56.00	48.00
S	270.00	1420.00	130.00	1400.00
Sc	12.90	11.50	13.00	18.50

Sm	2.30	3.10	2.90	2.80
Sn	2.00	7.00	2.00	7.00
Sr	528.00	388.00	543.00	614.00
Ta	1.00	1.00	1.00	1.00
Th	1.30	1.00	2.10	0.60
U	0.90	1.50	1.00	0.80
V	110.00	120.00	100.00	200.00
W	0.50	0.50	0.50	6.00
Y	9.00	9.00	11.00	16.00
Yb	0.90	1.00	1.40	1.90
Zn	30.20	57.00	29.30	137.00
Zr	92.00	84.00	88.00	62.00

Group	**Ylivieska**	**Ylivieska**	**Ylivieska**	**Ylivieska**
Sample	Vesiperä2	Vesiperä3	Ängesneva1	Ängesneva2
Lithology	Intermediate plag porphyrite	Intermediate plag porphyrite	Intermediate plag-horn porphyrite	Intermediate plag porphyrite
AI	33.96	30.79	58.35	38.93
CCPI	70.79	71.92	79.60	75.19
Al_2O_3	18.00	18.90	15.90	17.60
CaO	6.74	7.59	3.87	5.80
Fe_2O_3	9.76	9.58	13.30	12.50
K_2O	1.95	1.63	2.83	2.45
MgO	3.28	3.25	5.31	2.93
MnO	0.13	0.16	0.12	0.10
Na_2O	3.43	3.38	1.94	2.64
P_2O_5	0.24	0.25	0.36	0.26
SiO_2	50.60	51.40	50.80	49.70
TiO_2	0.81	0.87	1.35	0.88
Ag	1.80	0.32	0.49	4.20
As	13000.00	1300.00	1100.00	12000.00
Ba	373.00	369.00	481.00	500.00
Cd	0.20	0.20	0.20	0.20
Ce	18.10	19.90	29.80	22.10
Cl	123.00	174.00	376.00	314.00
Co	17.00	20.00	12.00	23.00
Cr	35.00	36.00	29.00	38.00
Cs	2.00	2.00	7.00	5.00
Cu	279.00	180.00	550.00	1490.00
Hf	1.40	1.70	2.20	1.30

La	8.50	9.10	13.80	10.80
Mo	1.00	2.00	1.00	1.00
Nb	12.00	11.00	15.00	12.00
Nd	11.10	12.10	18.40	13.60
Ni	18.00	21.00	14.00	20.00
Pb	2.00	2.00	2.00	2.00
Rb	54.00	42.00	75.00	72.00
S	12000.00	3110.00	10100.00	30800.00
Sc	17.20	18.10	27.40	19.00
Sm	2.70	2.80	4.40	3.00
Sn	8.00	2.00	5.00	12.00
Sr	551.00	631.00	278.00	456.00
Ta	1.00	1.00	1.00	1.00
Th	0.70	0.90	1.30	0.90
U	0.60	0.70	2.10	0.50
V	200.00	200.00	320.00	220.00
W	92.00	13.00	4.00	6.00
Y	14.00	15.00	22.00	16.00
Yb	1.60	2.10	2.60	1.90
Zn	95.20	112.00	98.50	79.20
Zr	64.00	58.00	90.00	65.00

Group	**Ylivieska**	**Ylivieska**	**Ylivieska**	**Ylivieska**
Sample	Ängesneva3	Kiimala1	Kiimala3	Kurula1
Lithology	Intermediate plag porphyrite	Intermediate plag porphyrite	Intermediate plag porphyrite	Qtz-plag schist
AI	31.42	50.13	44.22	37.93
CCPI	68.90	85.08	74.21	59.43
Al_2O_3	19.40	15.50	16.40	15.10
CaO	6.34	7.73	6.32	4.18
Fe_2O_3	9.93	12.20	9.57	5.19
K_2O	1.91	1.69	2.05	1.49
MgO	2.74	7.93	5.48	3.98
MnO	0.08	0.16	0.15	0.07
Na_2O	3.81	1.84	3.18	4.77
P_2O_5	0.28	0.09	0.14	0.17
SiO_2	51.90	47.90	51.80	62.30
TiO_2	0.86	0.49	0.59	0.63
Ag	0.55	1.50	1.60	0.04
As	350.00	320.00	110.00	990.00

Ba	337.00	353.00	480.00	378.00
Cd	0.20	0.20	0.20	0.20
Ce	22.40	20.90	29.50	47.60
Cl	246.00	101.00	67.00	243.00
Co	7.00	34.00	24.00	114.00
Cr	38.00	390.00	120.00	220.00
Cs	6.00	3.00	2.00	5.00
Cu	602.00	408.00	447.00	147.00
Hf	1.60	1.20	1.90	3.60
La	10.60	10.50	15.80	25.80
Mo	1.00	1.00	1.00	3.00
Nb	13.00	12.00	10.00	18.00
Nd	14.20	12.00	15.90	22.70
Ni	22.00	91.00	49.00	70.00
Pb	2.00	2.00	2.00	2.00
Rb	73.00	64.00	64.00	68.00
S	18400.00	12700.00	8490.00	1030.00
Sc	16.60	23.80	21.80	13.00
Sm	3.40	2.30	2.90	4.30
Sn	7.00	8.00	7.00	2.00
Sr	563.00	432.00	283.00	548.00
Ta	1.00	1.00	1.00	1.00
Th	0.80	1.70	3.20	5.80
U	0.30	1.50	0.90	4.10
V	180.00	230.00	230.00	110.00
W	5.00	0.50	2.00	600.00
Y	16.00	10.00	12.00	16.00
Yb	2.00	1.10	1.30	1.60
Zn	57.70	294.00	346.00	65.80
Zr	61.00	60.00	61.00	162.00

Group	**Ylivieska**	**Ylivieska**
Sample	Kurula2	Kurula3
Lithology	Qtz-plag schist	Qtz-plag schist
AI	54.99	42.63
CCPI	71.54	59.08
Al_2O_3	13.10	14.60
CaO	1.62	2.50
Fe_2O_3	7.49	6.23
K_2O	1.58	1.95

MgO	4.10	3.43
MnO	0.04	0.04
Na_2O	3.03	4.74
P_2O_5	0.15	0.16
SiO_2	60.00	63.40
TiO_2	0.53	0.63
Ag	0.16	0.05
As	18000.00	9100.00
Ba	309.00	420.00
Cd	0.20	0.20
Ce	73.30	66.10
Cl	241.00	326.00
Co	1590.00	238.00
Cr	140.00	160.00
Cs	7.00	6.00
Cu	291.00	183.00
Hf	0.00	4.10
La	49.20	34.30
Mo	26.00	5.00
Nb	13.00	17.00
Nd	27.20	27.80
Ni	151.00	60.00
Pb	2.00	2.00
Rb	68.00	96.00
S	9940.00	5360.00
Sc	9.66	12.40
Sm	4.70	4.90
Sn	8.00	7.00
Sr	272.00	349.00
Ta	1.00	1.00
Th	5.40	7.70
U	3.70	3.60
V	110.00	100.00
W	3.00	5.00
Y	12.00	16.00
Yb	1.40	1.80
Zn	57.30	70.40
Zr	124.00	171.00

Group	Pyhäsalmi	Pyhäsalmi	Pyhäsalmi	Pyhäsalmi
Sample	Mafic 1	Mafic 2	Mafic 3	Mafic 4
Lithology	Mafic metalava	Mafic metalava	Mafic metalava	Uraliteporphyry metatuff
AI	44.24	44.52	41.07	35.39
CCPI	93.43	91.95	85.34	88.24
Al_2O_3	15.39	16.07	15.99	17.96
CaO	14.19	12.04	11.52	11.54
Fe_2O_3	10.49	11.42	11.53	12.42
K_2O	0.45	0.86	0.74	0.61
MgO	11.69	9.59	9.26	6.78
MnO	0.17	0.20	0.23	0.21
Na_2O	1.11	0.98	2.83	1.95
P_2O_5	0.02	0.09	0.12	0.19
SiO_2	44.01	45.54	46.97	47.48
TiO_2	0.41	0.50	0.42	0.55
Ag	n.a.	n.a.	n.a.	n.a.
As	n.a.	n.a.	n.a.	n.a.
Ba	100.00	270.00	150.00	200.00
Cd	n.a.	n.a.	n.a.	n.a.
Ce	2.00	n.a.	n.a.	13.10
Cl	n.a.	n.a.	n.a.	n.a.
Co	n.a.	n.a.	n.a.	n.a.
Cr	n.a.	n.a.	n.a.	n.a.
Cs	n.a.	n.a.	n.a.	n.a.
Cu	50.00	60.00	30.00	100.00
Hf	n.a.	n.a.	n.a.	n.a.
La	1.10	n.a.	n.a.	45510.00
Mo	n.a.	n.a.	n.a.	n.a.
Nb	n.a.	n.a.	n.a.	n.a.
Nd	n.a.	n.a.	n.a.	9.80
Ni	150.00	130.00	130.00	50.00
Pb	n.a.	n.a.	n.a.	n.a.
Rb	n.a.	n.a.	n.a.	n.a.
S	720.00	360.00	310.00	190.00
Sc	n.a.	n.a.	n.a.	n.a.
Sm	1.20	n.a.	n.a.	2.60
Sn	n.a.	n.a.	n.a.	n.a.
Sr	270.00	290.00	100.00	460.00
Ta	n.a.	n.a.	n.a.	n.a.

Th	n.a.	n.a.	n.a.	n.a.
U	n.a.	n.a.	n.a.	n.a.
V	250.00	200.00	270.00	260.00
W	n.a.	n.a.	n.a.	n.a.
Y	n.a.	n.a.	n.a.	n.a.
Yb	0.83	n.a.	n.a.	1.30
Zn	50.00	70.00	140.00	90.00
Zr	20.00	30.00	30.00	50.00

Group	**Pyhäsalmi**	**Pyhäsalmi**	**Pyhäsalmi**	**Pyhäsalmi**
Sample	Mafic 5	Mafic 6	Mafic 7	Mafic 8
Lithology	Mafic metavolcanic rock	Mafic metalava	Mafic metalava	Mafic pillow lava
AI	42.93	29.72	32.76	35.41
CCPI	87.66	79.88	82.27	88.11
Al_2O_3	15.95	17.76	17.07	13.92
CaO	12.00	9.52	9.95	12.25
Fe_2O_3	11.85	12.63	10.29	12.27
K_2O	1.73	0.34	0.29	0.30
MgO	8.11	5.47	6.14	7.73
MnO	0.24	0.19	0.17	0.41
Na_2O	1.08	4.22	3.25	2.40
P_2O_5	0.07	0.06	0.08	0.11
SiO_2	48.26	48.75	49.50	49.66
TiO_2	0.46	0.59	0.58	0.51
Ag	n.a.	n.a.	n.a.	n.a.
As	n.a.	n.a.	n.a.	n.a.
Ba	240.00	110.00	130.00	90.00
Cd	n.a.	n.a.	n.a.	n.a.
Ce	n.a.	9.10	n.a.	n.a.
Cl	n.a.	n.a.	n.a.	n.a.
Co	n.a.	n.a.	n.a.	n.a.
Cr	n.a.	n.a.	n.a.	n.a.
Cs	n.a.	n.a.	n.a.	n.a.
Cu	160.00	350.00	10.00	20.00
Hf	n.a.	n.a.	n.a.	n.a.
La	n.a.	3.00	n.a.	n.a.
Mo	n.a.	n.a.	n.a.	n.a.
Nb	n.a.	n.a.	n.a.	n.a.
Nd	n.a.	3.10	n.a.	n.a.

Ni	80.00	30.00	50.00	160.00
Pb	n.a.	n.a.	n.a.	n.a.
Rb	n.a.	n.a.	n.a.	n.a.
S	240.00	3250.00	460.00	30.00
Sc	n.a.	n.a.	n.a.	n.a.
Sm	n.a.	1.50	n.a.	n.a.
Sn	n.a.	n.a.	n.a.	n.a.
Sr	150.00	40.00	230.00	160.00
Ta	n.a.	n.a.	n.a.	n.a.
Th	n.a.	n.a.	n.a.	n.a.
U	n.a.	n.a.	n.a.	n.a.
V	280.00	330.00	300.00	280.00
W	n.a.	n.a.	n.a.	n.a.
Y	n.a.	n.a.	n.a.	n.a.
Yb	n.a.	1.50	n.a.	n.a.
Zn	80.00	100.00	130.00	100.00
Zr	30.00	40.00	40.00	40.00

Group	**Pyhäsalmi**	**Pyhäsalmi**	**Pyhäsalmi**	**Pyhäsalmi**
Sample	Mafic 9	Mafic 10	Mafic 11	Mafic 12
Lithology	Mafic metalava	Mafic metavolcanic rock	Mafic pillow lava	Mafic pillow lava
AI	36.73	57.06	35.09	37.31
CCPI	87.27	91.47	93.41	88.68
Al_2O_3	16.21	11.17	15.32	14.04
CaO	11.08	10.02	12.77	12.70
Fe_2O_3	11.59	12.22	9.99	10.64
K_2O	0.25	1.61	0.17	0.38
MgO	7.67	12.65	7.30	8.40
MnO	0.18	0.21	0.20	0.40
Na_2O	2.56	0.71	1.05	2.05
P_2O_5	0.06	0.28	0.06	0.10
SiO_2	49.70	50.11	50.29	50.31
TiO_2	0.49	0.54	0.48	0.51
Ag	n.a.	n.a.	n.a.	n.a.
As	n.a.	n.a.	n.a.	n.a.
Ba	110.00	460.00	150.00	200.00
Cd	n.a.	n.a.	n.a.	n.a.
Ce	n.a.	21.00	7.10	10.00
Cl	n.a.	n.a.	n.a.	n.a.

Co	n.a.	n.a.	n.a.	n.a.
Cr	n.a.	n.a.	n.a.	n.a.
Cs	n.a.	n.a.	n.a.	n.a.
Cu	20.00	60.00	90.00	10.00
Hf	n.a.	n.a.	n.a.	n.a.
La	n.a.	11.20	3.00	5.30
Mo	n.a.	n.a.	n.a.	n.a.
Nb	n.a.	n.a.	n.a.	n.a.
Nd	n.a.	16.00	n.a.	n.a.
Ni	70.00	290.00	2450.00	180.00
Pb	n.a.	n.a.	n.a.	n.a.
Rb	n.a.	n.a.	n.a.	n.a.
S	30.00	1830.00	4070.00	10.00
Sc	n.a.	n.a.	n.a.	n.a.
Sm	n.a.	3.70	1.30	1.80
Sn	n.a.	n.a.	n.a.	n.a.
Sr	170.00	280.00	80.00	180.00
Ta	n.a.	n.a.	n.a.	n.a.
Th	n.a.	n.a.	n.a.	n.a.
U	n.a.	n.a.	n.a.	n.a.
V	270.00	260.00	250.00	270.00
W	n.a.	n.a.	n.a.	n.a.
Y	n.a.	n.a.	n.a.	n.a.
Yb	n.a.	1.40	1.40	1.30
Zn	80.00	110.00	120.00	90.00
Zr	30.00	70.00	40.00	40.00

Group	**Pyhäsalmi**	**Pyhäsalmi**	**Pyhäsalmi**	**Pyhäsalmi**
Sample	Mafic 13	Mafic 14	Mafic 15	Mafic 16
Lithology	Mafic pillow lava	Mafic pillow lava	Mafic metavolcanic rock	Mafic metavolcanic rock
AI	40.20	36.10	40.88	33.56
CCPI	90.59	87.46	76.12	82.77
Al_2O_3	14.43	14.42	17.14	17.23
CaO	11.18	12.39	7.34	8.21
Fe_2O_3	12.02	10.16	11.20	13.29
K_2O	0.38	0.27	1.83	0.99
MgO	8.30	8.05	5.63	4.53
MnO	0.18	0.35	0.16	0.20
Na_2O	1.73	2.34	3.45	2.72

P_2O_5	0.09	0.09	0.35	0.15
SiO_2	50.32	50.37	51.06	51.11
TiO_2	0.58	0.54	1.52	1.14
Ag	n.a.	n.a.	n.a.	n.a.
As	n.a.	n.a.	n.a.	n.a.
Ba	140.00	130.00	490.00	360.00
Cd	n.a.	n.a.	n.a.	n.a.
Ce	9.90	9.60	n.a.	n.a.
Cl	n.a.	n.a.	n.a.	n.a.
Co	n.a.	n.a.	n.a.	n.a.
Cr	n.a.	n.a.	n.a.	n.a.
Cs	n.a.	n.a.	n.a.	n.a.
Cu	50.00	10.00	20.00	40.00
Hf	n.a.	n.a.	n.a.	n.a.
La	4.60	5.20	n.a.	n.a.
Mo	n.a.	n.a.	n.a.	n.a.
Nb	n.a.	n.a.	n.a.	n.a.
Nd	6.10	7.20	n.a.	n.a.
Ni	80.00	290.00	60.00	30.00
Pb	n.a.	n.a.	n.a.	n.a.
Rb	n.a.	n.a.	n.a.	n.a.
S	270.00	410.00	850.00	770.00
Sc	n.a.	n.a.	n.a.	n.a.
Sm	1.90	1.80	n.a.	n.a.
Sn	n.a.	n.a.	n.a.	n.a.
Sr	150.00	160.00	470.00	180.00
Ta	n.a.	n.a.	n.a.	n.a.
Th	n.a.	n.a.	n.a.	n.a.
U	n.a.	n.a.	n.a.	n.a.
V	270.00	270.00	200.00	390.00
W	n.a.	n.a.	n.a.	n.a.
Y	n.a.	n.a.	n.a.	n.a.
Yb	1.60	1.20	n.a.	n.a.
Zn	80.00	80.00	100.00	120.00
Zr	30.00	50.00	180.00	60.00

Group	Pyhäsalmi	Pyhäsalmi	Pyhäsalmi	Pyhäsalmi
Sample	Mafic 17	Mafic 18	Mafic 19	Mafic 20
Lithology	Mafic pillow lava	Mafic metatuff	Mafic pillow lava	Mafic metavolcanic rock
AI	29.19	28.02	29.95	33.97
CCPI	81.20	81.30	80.41	84.15
Al_2O_3	17.72	17.53	14.66	15.68
CaO	10.26	9.92	12.03	10.78
Fe_2O_3	10.01	11.98	9.93	10.66
K_2O	0.18	1.12	0.18	0.54
MgO	5.45	3.71	6.61	6.38
MnO	0.22	0.18	0.18	0.19
Na_2O	3.40	2.49	3.85	2.67
P_2O_5	0.14	0.25	0.08	0.16
SiO_2	51.43	51.65	51.72	51.95
TiO_2	0.58	0.65	0.44	0.63
Ag	n.a.	n.a.	n.a.	n.a.
As	n.a.	n.a.	n.a.	n.a.
Ba	100.00	360.00	70.00	100.00
Cd	n.a.	n.a.	n.a.	n.a.
Ce	n.a.	n.a.	n.a.	n.a.
Cl	n.a.	n.a.	n.a.	n.a.
Co	n.a.	n.a.	n.a.	n.a.
Cr	n.a.	n.a.	n.a.	n.a.
Cs	n.a.	n.a.	n.a.	n.a.
Cu	320.00	90.00	50.00	60.00
Hf	n.a.	n.a.	n.a.	n.a.
La	n.a.	n.a.	n.a.	n.a.
Mo	n.a.	n.a.	n.a.	n.a.
Nb	n.a.	n.a.	n.a.	n.a.
Nd	n.a.	n.a.	n.a.	n.a.
Ni	210.00	30.00	60.00	60.00
Pb	n.a.	n.a.	n.a.	n.a.
Rb	n.a.	n.a.	n.a.	n.a.
S	610.00	230.00	610.00	720.00
Sc	n.a.	n.a.	n.a.	n.a.
Sm	n.a.	n.a.	n.a.	n.a.
Sn	n.a.	n.a.	n.a.	n.a.
Sr	220.00	580.00	70.00	250.00
Ta	n.a.	n.a.	n.a.	n.a.

Th	n.a.	n.a.	n.a.	n.a.
U	n.a.	n.a.	n.a.	n.a.
V	320.00	280.00	240.00	250.00
W	n.a.	n.a.	n.a.	n.a.
Y	n.a.	n.a.	n.a.	n.a.
Yb	n.a.	n.a.	n.a.	n.a.
Zn	250.00	110.00	60.00	120.00
Zr	40.00	50.00	20.00	60.00

Group	**Pyhäsalmi**	**Pyhäsalmi**	**Pyhäsalmi**	**Pyhäsalmi**
Sample	Mafic 21	Mafic 22	Mafic 23	Mafic 24
Lithology	Uraliteporphyry metatuff	Mafic pillow lava	Mafic pillow lava	Mafic metatuff
AI	39.93	36.18	34.53	34.42
CCPI	85.88	80.89	86.24	82.72
Al_2O_3	16.20	14.89	13.61	17.42
CaO	10.39	9.53	10.79	9.07
Fe_2O_3	9.06	10.53	11.85	10.74
K_2O	0.35	0.18	0.32	0.80
MgO	8.21	7.54	6.77	5.30
MnO	0.20	0.18	0.34	0.19
Na_2O	2.49	4.09	2.65	2.55
P_2O_5	0.12	0.08	0.10	0.15
SiO_2	52.00	52.16	52.57	53.08
TiO_2	0.74	0.45	0.51	0.43
Ag	n.a.	n.a.	n.a.	n.a.
As	n.a.	n.a.	n.a.	n.a.
Ba	100.00	50.00	140.00	170.00
Cd	n.a.	n.a.	n.a.	n.a.
Ce	16.00	7.20	n.a.	n.a.
Cl	n.a.	n.a.	n.a.	n.a.
Co	n.a.	n.a.	n.a.	n.a.
Cr	n.a.	n.a.	n.a.	n.a.
Cs	n.a.	n.a.	n.a.	n.a.
Cu	n.a.	140.00	10.00	210.00
Hf	n.a.	n.a.	n.a.	n.a.
La	8.40	3.30	n.a.	n.a.
Mo	n.a.	n.a.	n.a.	n.a.
Nb	n.a.	n.a.	n.a.	n.a.
Nd	12.10	4.90	n.a.	n.a.

Ni	150.00	60.00	170.00	40.00
Pb	n.a.	n.a.	n.a.	n.a.
Rb	n.a.	n.a.	n.a.	n.a.
S	20.00	570.00	120.00	60.00
Sc	n.a.	n.a.	n.a.	n.a.
Sm	3.00	1.50	n.a.	n.a.
Sn	n.a.	n.a.	n.a.	n.a.
Sr	250.00	110.00	150.00	340.00
Ta	n.a.	n.a.	n.a.	n.a.
Th	n.a.	n.a.	n.a.	n.a.
U	n.a.	n.a.	n.a.	n.a.
V	200.00	230.00	220.00	210.00
W	n.a.	n.a.	n.a.	n.a.
Y	n.a.	n.a.	n.a.	n.a.
Yb	1.80	0.95	n.a.	n.a.
Zn	140.00	80.00	300.00	80.00
Zr	80.00	30.00	40.00	40.00

Group	**Pyhäsalmi**	**Pyhäsalmi**	**Pyhäsalmi**	**Pyhäsalmi**
Sample	Mafic 25	Mafic 26	Mafic 27	Mafic 28
Lithology	Mafic metatuff	Mafic metatuff	Mafic metatuff	Mafic metalava
AI	43.86	34.35	42.75	27.05
CCPI	89.18	74.22	73.51	72.65
Al_2O_3	12.20	18.15	16.32	17.52
CaO	13.82	7.62	5.91	7.76
Fe_2O_3	5.41	10.47	11.20	9.54
K_2O	0.26	2.05	2.05	0.24
MgO	11.98	3.38	5.26	4.51
MnO	0.18	0.18	0.17	0.18
Na_2O	1.85	2.76	3.88	5.05
P_2O_5	0.09	0.19	0.09	0.13
SiO_2	53.81	54.06	54.10	54.26
TiO_2	0.28	0.82	0.53	0.50
Ag	n.a.	n.a.	n.a.	n.a.
As	n.a.	n.a.	n.a.	n.a.
Ba	100.00	750.00	290.00	130.00
Cd	n.a.	n.a.	n.a.	n.a.
Ce	37.00	n.a.	n.a.	n.a.
Cl	n.a.	n.a.	n.a.	n.a.
Co	n.a.	n.a.	n.a.	n.a.

Cr	n.a.	n.a.	n.a.	n.a.
Cs	n.a.	n.a.	n.a.	n.a.
Cu	n.a.	20.00	70.00	10.00
Hf	n.a.	n.a.	n.a.	n.a.
La	18.00	n.a.	n.a.	n.a.
Mo	n.a.	n.a.	n.a.	n.a.
Nb	n.a.	n.a.	n.a.	n.a.
Nd	22.00	n.a.	n.a.	n.a.
Ni	10.00	20.00	30.00	50.00
Pb	n.a.	n.a.	n.a.	n.a.
Rb	n.a.	n.a.	n.a.	n.a.
S	30.00	90.00	2990.00	180.00
Sc	n.a.	n.a.	n.a.	n.a.
Sm	5.10	n.a.	n.a.	n.a.
Sn	n.a.	n.a.	n.a.	n.a.
Sr	270.00	210.00	160.00	70.00
Ta	n.a.	n.a.	n.a.	n.a.
Th	n.a.	n.a.	n.a.	n.a.
U	n.a.	n.a.	n.a.	n.a.
V	40.00	220.00	270.00	290.00
W	n.a.	n.a.	n.a.	n.a.
Y	n.a.	n.a.	n.a.	n.a.
Yb	3.10	n.a.	n.a.	n.a.
Zn	90.00	130.00	110.00	90.00
Zr	160.00	80.00	50.00	20.00

Group	**Pyhäsalmi**	**Pyhäsalmi**	**Pyhäsalmi**	**Pyhäsalmi**
Sample	Mafic 29	Mafic 30	Mafic 31	Mafic 32
Lithology	Mafic pillow lava	Uraliteporphyry metatuff	Mafic metatuff	Mafic pillow lava
AI	39.81	36.77	24.76	30.47
CCPI	84.77	80.74	74.42	71.65
Al_2O_3	14.53	16.00	19.43	16.74
CaO	9.93	8.47	8.88	8.48
Fe_2O_3	9.00	10.54	7.83	7.65
K_2O	0.28	1.31	0.83	0.38
MgO	8.14	5.01	3.05	5.44
MnO	0.11	0.12	0.15	0.09
Na_2O	2.80	2.40	2.91	4.80
P_2O_5	0.07	0.17	0.11	0.11

SiO_2	54.27	54.37	55.08	55.25
TiO_2	0.38	1.19	0.41	0.68
Ag	n.a.	n.a.	n.a.	n.a.
As	n.a.	n.a.	n.a.	n.a.
Ba	230.00	290.00	420.00	160.00
Cd	n.a.	n.a.	n.a.	n.a.
Ce	9.20	n.a.	n.a.	7.20
Cl	n.a.	n.a.	n.a.	n.a.
Co	n.a.	n.a.	n.a.	n.a.
Cr	n.a.	n.a.	n.a.	n.a.
Cs	n.a.	n.a.	n.a.	n.a.
Cu	70.00	70.00	n.a.	30.00
Hf	n.a.	n.a.	n.a.	n.a.
La	3.70	n.a.	n.a.	3.60
Mo	n.a.	n.a.	n.a.	n.a.
Nb	n.a.	n.a.	n.a.	n.a.
Nd	4.70	n.a.	n.a.	5.20
Ni	60.00	60.00	30.00	120.00
Pb	n.a.	n.a.	n.a.	n.a.
Rb	n.a.	n.a.	n.a.	n.a.
S	2070.00	2890.00	50.00	1750.00
Sc	n.a.	n.a.	n.a.	n.a.
Sm	1.60	n.a.	n.a.	1.80
Sn	n.a.	n.a.	n.a.	n.a.
Sr	190.00	350.00	470.00	150.00
Ta	n.a.	n.a.	n.a.	n.a.
Th	n.a.	n.a.	n.a.	n.a.
U	n.a.	n.a.	n.a.	n.a.
V	250.00	220.00	130.00	280.00
W	n.a.	n.a.	n.a.	n.a.
Y	n.a.	n.a.	n.a.	n.a.
Yb	0.77	n.a.	n.a.	1.70
Zn	80.00	90.00	80.00	80.00
Zr	20.00	100.00	50.00	40.00

Group	**Pyhäsalmi**	**Pyhäsalmi**	**Pyhäsalmi**	**Pyhäsalmi**
Sample	Intermediate 1	Intermediate 2	Intermediate 3	Intermediate 4
Lithology	Intermedate metavolcanic rock	Intermediate metatuff	Intermediate metatuff	Intermediate metatuff
AI	34.81	36.62	40.89	34.95
CCPI	80.29	61.22	63.14	62.39
Al_2O_3	18.84	16.50	16.96	16.58
CaO	7.69	5.13	4.65	5.31
Fe_2O_3	9.51	6.81	7.24	6.51
K_2O	2.09	2.39	2.71	2.48
MgO	2.47	2.66	2.61	1.70
MnO	0.21	0.10	0.10	0.12
Na_2O	0.85	3.61	3.04	2.47
P_2O_5	0.21	0.16	0.17	0.18
SiO_2	57.07	61.49	61.66	63.53
TiO_2	0.73	0.63	0.61	0.58
Ag	n.a.	n.a.	n.a.	n.a.
As	n.a.	n.a.	n.a.	n.a.
Ba	750.00	700.00	590.00	620.00
Cd	n.a.	n.a.	n.a.	n.a.
Ce	n.a.	n.a.	46.00	50.00
Cl	n.a.	n.a.	n.a.	n.a.
Co	n.a.	n.a.	n.a.	n.a.
Cr	n.a.	n.a.	n.a.	n.a.
Cs	n.a.	n.a.	n.a.	n.a.
Cu	70.00	20.00	20.00	n.a.
Hf	n.a.	n.a.	n.a.	n.a.
La	n.a.	n.a.	28.00	27.00
Mo	n.a.	n.a.	n.a.	n.a.
Nb	n.a.	n.a.	n.a.	n.a.
Nd	n.a.	n.a.	23.00	22.00
Ni	20.00	20.00	30.00	10.00
Pb	n.a.	n.a.	n.a.	n.a.
Rb	n.a.	n.a.	n.a.	n.a.
S	1350.00	80.00	310.00	50.00
Sc	n.a.	n.a.	n.a.	n.a.
Sm	n.a.	n.a.	4.80	4.90
Sn	n.a.	n.a.	n.a.	n.a.
Sr	180.00	370.00	290.00	320.00
Ta	n.a.	n.a.	n.a.	n.a.

Th	n.a.	n.a.	n.a.	n.a.
U	n.a.	n.a.	n.a.	n.a.
V	190.00	150.00	120.00	110.00
W	n.a.	n.a.	n.a.	n.a.
Y	n.a.	n.a.	n.a.	n.a.
Yb	n.a.	n.a.	1.70	2.20
Zn	200.00	90.00	90.00	90.00
Zr	110.00	140.00	160.00	130.00

Group	**Pyhäsalmi**	**Pyhäsalmi**	**Pyhäsalmi**	**Pyhäsalmi**
Sample	Felsic 1	Felsic 2	Felsic 3	Felsic 6
Lithology	Quartzporphyry	Felsic metavolcanic rock	Felsic metavolcanic rock	Felsic tuffaceous metasediment
AI	51.89	27.59	63.83	38.94
CCPI	44.10	35.70	42.53	26.81
Al_2O_3	13.85	13.51	11.43	12.37
CaO	1.71	1.84	1.59	0.97
Fe_2O_3	3.98	3.52	3.53	1.97
K_2O	3.66	2.20	4.46	2.69
MgO	0.88	0.25	0.80	0.48
MnO	0.11	0.06	0.05	0.03
Na_2O	2.50	4.59	1.39	4.00
P_2O_5	0.02	0.07	0.03	0.03
SiO_2	72.26	73.35	76.04	76.78
TiO_2	0.18	0.32	0.18	0.07
Ag	n.a.	n.a.	n.a.	n.a.
As	n.a.	n.a.	n.a.	n.a.
Ba	770.00	560.00	520.00	1020.00
Cd	n.a.	n.a.	n.a.	n.a.
Ce	31.00	26.00	n.a.	n.a.
Cl	n.a.	n.a.	n.a.	n.a.
Co	n.a.	n.a.	n.a.	n.a.
Cr	n.a.	n.a.	n.a.	n.a.
Cs	n.a.	n.a.	n.a.	n.a.
Cu	n.a.	0.00	20.00	10.00
Hf	n.a.	n.a.	n.a.	n.a.
La	15.00	13.60	n.a.	n.a.
Mo	n.a.	n.a.	n.a.	n.a.
Nb	n.a.	n.a.	n.a.	n.a.
Nd	19.00	13.50	n.a.	n.a.

Ni	10.00	10.00	10.00	20.00
Pb	n.a.	n.a.	n.a.	n.a.
Rb	n.a.	n.a.	n.a.	n.a.
S	40.00	50.00	3910.00	200.00
Sc	n.a.	n.a.	n.a.	n.a.
Sm	5.30	n.a.	2.90	5.10
Sn	n.a.	n.a.	n.a.	n.a.
Sr	80.00	90.00	30.00	70.00
Ta	n.a.	n.a.	n.a.	n.a.
Th	n.a.	n.a.	n.a.	n.a.
U	n.a.	n.a.	n.a.	n.a.
V	n.a.	20.00	10.00	20.00
W	n.a.	n.a.	n.a.	n.a.
Y	n.a.	n.a.	n.a.	n.a.
Yb	5.60	3.20	n.a.	1.60
Zn	150.00	50.00	60.00	20.00
Zr	150.00	310.00	130.00	260.00

Group	**Pyhäsalmi**
Sample	Felsic 7
Lithology	Felsic metatuff
AI	37.62
CCPI	48.21
Al_2O_3	11.75
CaO	0.85
Fe_2O_3	2.69
K_2O	1.02
MgO	1.76
MnO	0.09
Na_2O	3.76
P_2O_5	0.01
SiO_2	76.88
TiO_2	0.16
Ag	n.a.
As	n.a.
Ba	340.00
Cd	n.a.
Ce	n.a.
Cl	n.a.
Co	n.a.

Cr	n.a.
Cs	n.a.
Cu	n.a.
Hf	n.a.
La	n.a.
Mo	n.a.
Nb	n.a.
Nd	n.a.
Ni	20.00
Pb	n.a.
Rb	n.a.
S	1720.00
Sc	n.a.
Sm	n.a.
Sn	n.a.
Sr	60.00
Ta	n.a.
Th	n.a.
U	n.a.
V	10.00
W	n.a.
Y	n.a.
Yb	n.a.
Zn	130.00
Zr	240.00